

University of Alberta

Comparison of Manual Wheelchair Propulsion in “Real-world” and
Computer Simulated Environments

by

Jiajie Wu

A thesis submitted to the Faculty of Graduate Studies and Research in partial
fulfillment of the requirements for the degree of

Master of Science

in

Rehabilitation Science

Faculty of Rehabilitation Medicine

©Jiajie Wu
Spring 2013
Edmonton, Alberta

Permission is hereby granted to the University of Alberta Libraries to reproduce single copies of this thesis and to lend or sell such copies for private, scholarly or scientific research purposes only. Where the thesis is converted to, or otherwise made available in digital form, the University of Alberta will advise potential users of the thesis of these terms.

The author reserves all other publication and other rights in association with the copyright in the thesis and, except as herein before provided, neither the thesis nor any substantial portion thereof may be printed or otherwise reproduced in any material form whatsoever without the author's prior written permission.

Dedication

I am dedicating this thesis to my late grandfather for his unconditional and ever-lasting love. It was he who inspired me to devote myself to research of rehabilitation medicine.

Abstract

Research to help prevent or alleviate the muscle fatigue and injuries prevalent among long-term manual wheelchair users is largely conducted in a laboratory environment. Through laboratory simulations it is possible to focus on a manageable set of variables among the many pertinent ones that characterize daily living; and the closer real-life conditions can be simulated, the more pertinent will be the findings. The goal of this thesis was to test manual wheelchair users' performance on two different real-world surfaces and the transition between them, versus their simulations on a wheelchair ergometer. Two closed-loop models were used to simulate real-world surface propulsion. Surface friction and inertia were simulated through closed-loop steering of ergometer resistance. For one surface, the simulation came very close to real-world parameters, whereas for the other, a considerable deviation needed to be compensated for by calibration. The simulation models were unsuccessful for surface transitions and will need further refinement.

Acknowledgement

The completion of this thesis would not have been possible without the help and guidance of many people, especially the following:

Foremost, I wish to express my sincere gratitude to my supervisor Prof. Martin Ferguson-Pell for his guidance and continuous support throughout my M.Sc. study and research. My sincere thanks also go to Prof. Gregory Kawchuk and Prof. Trish Manns for offering valuable suggestions and ideas for my research and thesis writing.

I would like to thank my fellow students and researchers at the Faculty of Rehabilitation Medicine, University of Alberta, especially my colleagues, Dr. Liping Qi and Dr. Mojtaba A Sohi for their suggestions and support in this study. I would like to thank Dr. Artur Bohnet for proofreading my thesis and his encouragement. I would also like to thank my friends for being supportive in my study and my life.

I would like to acknowledge the generous financial support from the University of Alberta, the Faculty of Rehabilitation Medicine, the Alberta Paraplegic Foundation and the Glenrose Rehabilitation Hospital.

Last but not the least; my special thanks go to my parents for their unconditional and continuous support and for encouraging me to pursue my studies abroad.

Table of Contents

Chapter 1 Introduction	1
1.1 Manual Wheelchair user demographics	1
1.2 Problem statement	2
Chapter 2 Literature Review	5
2.1 Prevalence of upper extremity pain in long term manual wheelchair users..	5
2.2 Factors influencing upper extremity pain.....	6
2.2.1 Propulsion.....	6
2.2.2 Transfer between resting positions	8
2.2.3 Wheelchair design	9
2.2.4 Other factors	10
2.3 Biomechanics of wheelchair propulsion	10
2.3.1 Biomechanics of the upper extremity during wheelchair propulsion...	11
2.3.2 Biomechanics of the trunk during wheelchair propulsion.....	15
2.4 Wheelchair use environment.....	18
2.4.1 Wheelchair-accessible indoor environments	19
2.4.2 Wheelchair accessible outdoor environments	19
2.4.3 Rolling Resistance and its impact on wheelchair propulsion.....	20
2.4.4 Ramps and their impact on wheelchair propulsion	22
2.5 Wheelchair simulation environment	23
2.5.1 Various Types of Simulated environments	24
2.5.2 Visual feedback	27
2.6 Comparison of wheelchair propulsion biomechanics between real-world and laboratory simulated environments	29

Chapter 3 Methods	32
3.1 Statement of objectives	32
3.1.1 Hypothesis 1	32
3.1.2 Hypothesis 2	32
3.1.3 Hypothesis 3	33
3.2 Sample size calculation	33
3.3 Participants	35
3.3.1 Inclusion and exclusion criteria	35
3.4 Measurements and instruments	36
3.4.1 Smart ^{Wheel}	36
3.4.2 Tachyon	38
3.4.3 IMU and calibration.....	39
3.4.4 Real-world settings	43
3.4.5 Roll-down test, rolling resistance and deceleration slope of real-world surfaces	46
3.4.6 Ergometer and calibration	47
3.4.7 Ergometer simulation settings and visual feedback	51
3.5 Biomechanical model for propulsion	54
3.5.1 Model 1- consideration of wheelchair dynamics in the lab ergometer and real-world environments	55
3.4.2 Model 2- correction factor based model.....	62
3.6 Experimental protocol	63
3.7 Data Collection.....	67
3.7.1 Synchronization	67
3.7.2 The Smart ^{Wheel} Data.....	68
3.7.3 The IMU Data	69

3.7.4 The LabVIEW program Data.....	70
3.8 Parameter extraction.....	70
3.8.1 Rolling resistance calculation.....	71
3.8.2 Smart ^{Wheel}	74
3.8.3 IMU.....	76
3.9 Statistical analysis.....	78
Chapter 4 Results.....	81
4.1 Calibration Results.....	81
4.1.1 Inertial Measurement Unit (IMU).....	81
4.1.2 Rolling resistance on real-world surfaces.....	83
4.1.3 Rolling resistance simulation in the Ergometer.....	84
4.2 Participant characteristics.....	85
4.3 Hypothesis 1.....	86
4.4 Hypothesis 2.....	87
4.5 Hypothesis 3.....	89
4.5.1 Peak M_z	90
4.5.2 Peak total force.....	92
4.5.3 Push Length.....	93
4.5.4 Push Frequency.....	94
4.5.5 Average Speed.....	96
4.5.6 Trunk Motion Angle.....	97
4.5.7 Maximum Peak Trunk Angular Velocity.....	98
4.7 Power Analysis.....	100
Chapter 5 Discussion.....	107
5.1 Propulsion kinetics and trunk biomechanics on two surfaces of different rolling resistance existing in a real-world environment.....	107

5.2 Propulsion kinetics and trunk biomechanics on transitions between two surfaces of different resistance in a real-world environment	108
5.3 Comparisons of propulsion kinetics and trunk biomechanics between real-world and ergometer Model 1, and real-world and ergometer Model 2	110
5.3.1 Peak M_z	111
5.3.2 Peak total force	112
5.3.3 Push length	113
5.3.4 Push frequency	113
5.3.5 Average speed.....	114
5.3.6 Trunk motion angle	115
5.3.7 Maximum peak trunk angular velocity.....	115
5.4 Others	115
5.4.1 Weight normalization	115
5.4.2 Visual feedback	116
5.5 Study limitations	117
5.5.1 Selection of subjects	117
5.5.2 Ergometer system	117
5.5.3 Trunk motion measurement.....	117
5.5.4 Transition simulation in ergometer.....	118
5.5.5 Restriction of real-world surface travelled distance	118
5.5.6. Wheelchair configuration	118
5.6 Strength of the study	119
5.7 Clinical interpretation.....	119
5.8 Suggestions to future studies.....	120
Chapter 6 Conclusion.....	122
Appendix 1 References	124

Appendix 2 Real-world and Roller Calibration	133
Appendix 3 Interaction Plots for Hypothesis 3	136

List of Tables

Table 3- 1 One independent variable in hypothesis 1.....	79
Table 3- 2 One independent variable in hypothesis 2.....	79
Table 3- 3 Two independent variables in hypothesis 3.....	80
Table 4- 1 Physical characteristics of 23 participants. Data was reported as Mean \pm SD.....	85
Table 4- 2 Descriptive output and paired t-test results comparing two surfaces in real-world.....	87
Table 4- 3 Descriptive output and paired t-test results comparing transition of two directions in real-world.....	88
Table 4- 4 Descriptive output and pairwise comparison of peak M_z for each treatment condition in real-world and ergometer simulation environment (Model 1 and 2).	90
Table 4- 5 Descriptive output and pairwise comparison of peak total force for each treatment condition in real-world and ergometer (Model 1 and 2).	92
Table 4- 6 Descriptive output and pairwise comparison of push length for each treatment condition in real-world and ergometer (Model 1 and 2).....	94
Table 4- 7 Descriptive output and pairwise comparison of push frequency for each treatment condition in real-world and ergometer (Model 1 and 2).....	95
Table 4- 8 Descriptive output and pairwise comparison of average speed for each treatment condition in real-world and ergometer (Model 1 and 2).....	96
Table 4- 9 Descriptive output and pairwise comparison of trunk motion angle for each treatment condition in real-world and ergometer (Model 1 and 2).	98
Table 4- 10 Descriptive output and pairwise comparison of maximum peak trunk angular velocity for each treatment condition in real-world and ergometer (Model 1 and 2).	99
Table 4- 11 Paired t test power analysis for hypothesis 1 and 2.....	101
Table 4- 12 ANOVA power analysis for hypothesis 3 (ergometer Model 1).....	104
Table 4- 13 ANOVA power analysis for hypothesis 3 (ergometer Model 2).....	105
Table Appendix 2- 1 Deceleration α of real-world surfaces and weight of participants.....	133

Table Appendix 2- 2 Linear equations of individual participant for pressure used by actuators and the deceleration of both rollers. (a and b are the gradient and intercept values of equation respectively)..... 134

List of Figures

Figure 2- 1 Shoulder joint (Google Image, from http://www.chiro.org/LINKS/Shoulder.shtml)	6
Figure 2- 2 Muscles and soft tissues around shoulder (Google Image, from http://www.drugs.com/health-guide/rotator-cuff-injury.html)	7
Figure 2- 3 Semi-circular propulsion trajectory. Black dots show the push phase, while the hands are in contact with the hand rim. The gray dots show the recovery phase, while the hands are off the hand rim [74].	11
Figure 2- 4 Propulsion pattern. Four kinds of propulsive strokes: (A) SC; (B) SLOP; (C) DLOP; (D) ARC [21, 32]	12
Figure 2- 5 Orientation of force and moments [78]	13
Figure 2- 6 Planes in human movement analysis (Google Image, from http://www.brianmac.co.uk/musrom.htm)	16
Figure 2- 7 (A) A motor-driven treadmill with a wheelchair [29]; (B) A dynamometer with a wheelchair [27]; (C) Components of a dynamometer without cover [27]; (D) A diagram of dynamometer [27].	24
Figure 3- 1 Smart ^{Wheel} attached to a Quickie manual wheelchair	37
Figure 3- 2 Tachyon and installation (A) Tachyon (B) Tachyon mounted to the back of a Quickie wheelchair	39
Figure 3- 3 IMU and its orientation (A) IMU device; (B) Six degrees of freedom in three-dimensional space [110]; (C) Participant with IMU attached to chest; (D) IMU six degrees of freedom drawing with the same portrait as in (C).	40
Figure 3- 4 IMU Calibration (A) IMU pendulum model in static position (B) Accel data used in the model	41
Figure 3- 5 Real-world environment including two surfaces: carpet and artificial turf	44
Figure 3- 6 Transition detection system: a RF transmitter (left), a retro-reflective sensor (middle), and a reflector (right).	44
Figure 3- 7 A participant crossing the transition with a wheelchair.	45
Figure 3- 8 The roller ergometer system	47
Figure 3- 9 Control and feedbacks of laboratory ergometer system	48

Figure 3- 10 (A) Friction applying system with two fabric straps; (B) two double-acting pneumatic actuators and (C) a digital pressure controller with a vault.....	49
Figure 3- 11 Two tachometers were used to measure the speed of the two rollers	50
Figure 3- 12 LabVIEW program inputs and real time feedbacks of speed and travelled distance to the program and researchers.	52
Figure 3- 13 Ergometer visual display of carpet and artificial turf compared to real-world.....	53
Figure 3- 14 Schematic of wheel and roller motion during wheelchair push in ergometer environment	55
Figure 3- 15 Free body diagram of wheel and roller in ergometer environment..	56
Figure 3- 16 A wheelchair on carpet.....	57
Figure 3- 17 Free body diagram of one wheel of wheelchair on a real-world environment surface.....	57
Figure 3- 18 A participant sitting on a wheelchair with her hands placed at top center of push rim.	65
Figure 3- 19 Smart ^{Wheel} data moment M_z during propulsion in real-world plotted against time.	68
Figure 3- 20 IMU data angular velocity Roll during propulsion on a real-world surface plotted against time.	69
Figure 3- 21 Signal of the transition between two real-world surfaces.	70
Figure 3- 22 Wheelchair velocity plotted against time in a real-world surface roll down test.	71
Figure 3- 23 Velocity deceleration slope after the last push plotted against time.	72
Figure 3- 24 Linear relationships of actuator pressure and roller deceleration slopes α for the left and for the right roller.....	73
Figure 3- 25 Finding the pressure value C_{RR} to simulate real-world surface rolling resistance.....	73
Figure 3- 26 Smart ^{Wheel} M_z data with transition period plotted against time.	74
Figure 3- 27 Task directions from artificial turf to carpet or reversed.	75

Figure 3- 28 Trunk angular velocity (degrees/s, blue line, RollS) after smoothing, propulsion moment M_z (N*m, magenta line, MzBothS) after smoothing and transition period (s, green line, Transition) plotted against time.	76
Figure 4- 1 Linear regression of $\theta(t)$ reading from XClinometer and $\theta(t)$ value calculated from Accel data.....	81
Figure 4- 2 Angular velocity $\theta(t)$ calculated from Accel data compares to the Gyro data $Roll(t)$	82
Figure 4- 3 Deceleration α on real-world surface for each participant.....	83
Figure 4- 4 Calibration of roller deceleration (linear relation of α and actuator pressure).....	84
Figure Appendix 2- 1 Resistive Torque and Ergometer Actuator Pressure.....	135
Figure Appendix 3- 1 Interaction plot for parameter peak M_z (comparing real-world and ergometer Model 1) of two independent variables: Environment and Surface (with mean and standard error).....	136
Figure Appendix 3- 2 Interaction plot for parameter peak total force (comparing real-world and ergometer Model 1) of two independent variables: Environment and Surface (with mean and standard error).....	136
Figure Appendix 3- 3 Interaction plot for parameter average speed (comparing real-world and ergometer Model 1) of two independent variables: Environment and Surface (with mean and standard error).....	137
Figure Appendix 3- 4 Interaction plot for parameter trunk motion angle (comparing real-world and ergometer Model 2) of two independent variables: Environment and Surface (with mean and standard error).....	137

List of Abbreviations and Symbols

α :	deceleration slope of roll down test
$\dot{\theta}$:	trunk motion angular velocity
A/D:	analog-to-digital
Accel:	accelerometer
ANOVA:	analysis of variance
ARC:	arcing pattern of wheelchair propulsion
DLOP:	double loop-over pattern of wheelchair propulsion
F_r :	force radial to the pushrim of a wheelchair wheel
F_t :	force tangential to the pushrim of a wheelchair wheel
F_x :	force along the x (longitudinal) axis of a wheelchair wheel
F_y :	force along the y (vertical) axis of a wheelchair wheel
F_z :	force along the z (lateral) axis of a wheelchair wheel
IMU:	inertial measurement unit
LCD:	liquid crystal display
M_x :	moment around the x (longitudinal) axis of a wheelchair wheel
M_y :	moment around the y (vertical) axis of a wheelchair wheel
M_z :	moment around the z (lateral) axis of a wheelchair wheel
RF:	radio frequency
SC:	semicircular pattern of wheelchair propulsion
SCI:	spinal cord injury
SD:	secure digital (memory card)
SLOP:	single loop-over pattern of wheelchair propulsion

TTL: transistor-transistor logic

θ : trunk motion angle or displacement

Chapter 1 Introduction

1.1 Manual Wheelchair user demographics

There are about 65 million people (approximately 1% of the global population) who need to use a wheelchair in their everyday life [1]. In 2000 to 2001, 0.6% of Canadian domestic population, i.e., about 155,000 people needed a wheelchair, and about 80 percent of those used a manual wheelchair [2]. It is estimated that 1.5 million Americans (0.58% of the population) and 3.3 million Europeans are manual wheelchair users[3]. Approximately 66% of manual wheelchair users in the UK propel their wheelchair themselves, rather than being pushed by a helper [4].

The proportion of the population using manual wheelchairs in the United States increases sharply with age: 88,000 people or 0.1% of the nation's population are under 18 years of age, around 600,000, or 0.4%, are working-age adults, and about 900,000, or 2.9%, are aged 65 or older. A significant majority (60%) of manual wheelchair users are women, comprising 0.7% of the nation's female population, men accounting for 40%, or 0.5% of the total male population [3].

Manual wheelchair users can be divided into three main categories: people disabled through a spinal cord injury (SCI), people who have suffered a stroke, and some whose mobility is affected by old age. Other manual wheelchair users are individuals with spina bifida (a developmental congenital disorder),

amputation, cerebral palsy (a group of brain and nervous system function disorders) and multiple sclerosis (MS) (an autoimmune disease that affects the brain and spinal cord) [5].

According to the Rick Hansen Institute's "Incidence and Prevalence Report" [6] there are currently 85,556 persons living with SCI in Canada. Almost half of the new traumatic injuries in Canada occur in the population aged between the ages 15 to 39 (mostly male) because of motor vehicle accidents, sporting accidents and other trauma-related causes. Due to this relatively early occurrence of SCI, many people with SCI spend most of their normal life expectancy in a wheelchair.

1.2 Problem statement

Extensive researches on wheelchair propulsion have been done in the laboratory. However, more clear evidence are needed to clarify that laboratory is closely related to the real-world in which manual wheelchair users live.

Wheelchair propulsion uses the shoulder and wrist structures of the upper extremities. Long-term use of a manual wheelchair carries the risk of secondary injuries in the upper extremities and around the shoulder [7-13].

A major concern for wheelchair users is the type of surface on which they have to move [8, 14-19]. Thus, there are various studies investigating wheelchair propulsion on different surfaces such as tile, linoleum, carpet, artificial turf, either on level ground or on a slope [14-16, 20-23]. Some surfaces are harder to

negotiate than others, and so are transitions between two different types of ground, with suddenly increased or diminished rolling resistance [3, 20, 23]. Therefore, the effects of the transitions between two surfaces of different rolling resistance have been incorporated in this study. The degree of difficulty also depends on clinical factors such as level of injury, and/or completeness of motor and sensory loss.

Most wheelchair studies have been done in a laboratory setting, using different types of simulators such as treadmills, rollers, ergometers and dynamometers [21, 24-29]. Laboratory simulations will continue to be useful and necessary, because without a controlled environment, studies are easily hampered by a lack of equipment operability and sensitivity as well as the immense variability of spatial and other conditions. The question remains how effectively a simulated environment replicates real-world conditions, and thus how much the findings can actually be used to represent a real-world environment for experimental and training purposes.

Overuse injuries are thought to be closely related to the number of pushes per unit of time (cadence or push frequency) and incorrect or inefficient propulsion [3]. The Smart^{Wheel} (a customized wheel with instrumentation) has been used in many studies to collect pushrim biomechanics information [20, 22, 30-35]. In order to avoid fatigue or injury in different scenarios, it is important to optimize propulsion performance, i.e. forces, moments, speed and cadence. Another factor influencing propulsion is trunk movement [26, 28, 36-38]. In

particular, for wheelchair users with SCI, paradoxical trunk movement (trunk moving in the opposite direction to the arms during force production) can severely affect push performance [11, 39-41]. Therefore, both propulsion and trunk movement need to be incorporated in this study.

What is clear is that the considerable incidence of wheelchair-related injuries requires studies to guide clinical support and training programs and the development of wheelchair technology.

Chapter 2 Literature Review

2.1 Prevalence of upper extremity pain in long term manual wheelchair users

Manual wheelchair users rely on their upper extremities, including shoulder, wrist, hand and elbow, for their daily activities. The upper extremities are needed for locomotion, for movements to achieve pressure relief or to transfer in and out of the wheelchair. Pain and injuries in these areas affect a manual wheelchair user's daily activities, ability to function, independence and quality of life; they may increase the level of disability [6, 42, 43].

A large proportion (63%) of wheelchair users report upper extremity pain, and 32% of the patients have pain in more than one region [44]. Much of the research in this field has been conducted with people with SCI. This is because nearly all use wheelchairs and they are usually otherwise healthy and relatively young and have the potential to benefit substantially from research to reduce wheelchair use injuries. Within the group of people with SCI, shoulder pain is the most commonly reported (71%), followed by wrist pain (53%), hand pain (43%) and elbow pain (35%) [45]. In a national survey of 610 full-time manual wheelchair users with SCI, 62% of paraplegics and 74% of tetraplegics reported pain in the shoulder [46]. Carpal tunnel syndrome, a very common dysfunction within the group of people who perform repetitive motions of the hand and wrist, was found in 49% to 73% of the population with SCI [44, 47-50].

2.2 Factors influencing upper extremity pain

Most individuals with SCI use wheelchairs at home, school and work. They experience pain during wheelchair propulsion, transfers, dressing and other activities of daily living [45, 51, 52]. All of these activities place unusually high demands because of repetitive loads and the considerable forces placed on joints, soft tissues and bones of the upper extremities [9]. Many studies attribute upper extremity pain to repetitive use injuries among manual wheelchair users, especially wheelchair athletes [9, 10, 44, 51]. Since the methods of propulsion or transfer as well as wheelchair setup are found to be key factors in upper body injuries [45, 51, 52], these factors are explored in detail next.

2.2.1 Propulsion

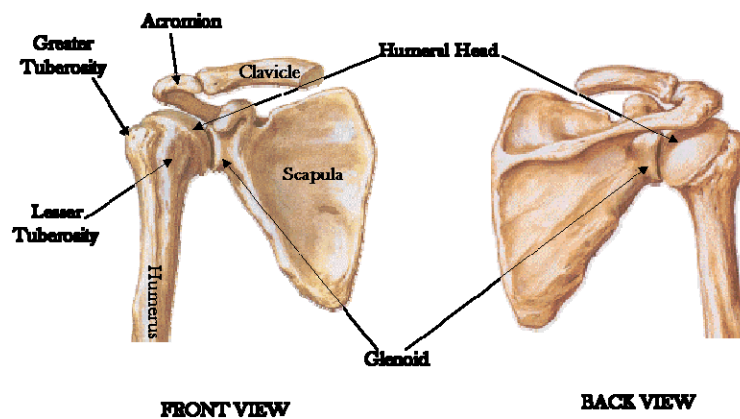


Figure 2- 1 Shoulder joint (Google Image, from <http://www.chiro.org/LINKS/Shoulder.shtml>)

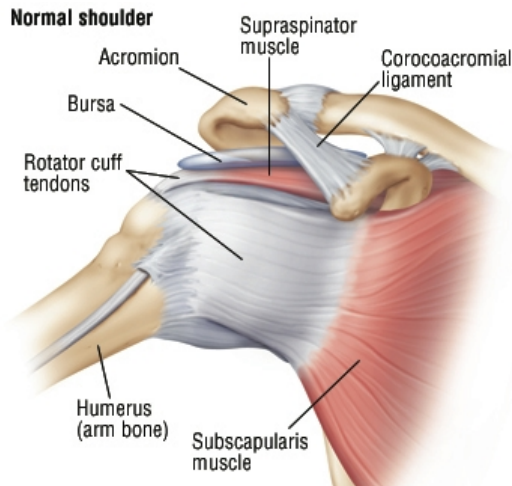


Figure 2- 2 Muscles and soft tissues around shoulder (Google Image, from <http://www.drugs.com/health-guide/rotator-cuff-injury.html>)

Manual wheelchair users are reported to push their wheelchair for 2000 to 3000 times, more than 10 hours every day, in the course of daily activities [53-55]. The highly repetitive nature of wheelchair propulsion frequently stresses the shoulder area, as shown in Figure 2-1. The human shoulder, a very loosely connected joint, consists of muscles, ligaments, tendons and bones (Figure 2-2). It requires the soft tissue structures to retain the balance of the joint, keeping the humeral head in contact with the acromion and the glenoid during functional activities. The rotator cuff (Figure 2-1), containing a group of muscles and tendons, plays a very important part in stabilizing the glenohumeral joint [56].

Several muscles connected to the shoulder joint are active during wheelchair propulsion. On the wheelchair, a push cycle consists of two phases: the push phase – while the hand is in contact with the wheelchair hand rim, and the recovery phase – when the hand is off the hand rim. A group of muscles including anterior deltoid, pectoralis major and biceps brachii is dominating the push phase while the middle and the posterior deltoid are recruited mainly in the

recovery phase [33, 57, 58]. Muscles which are active in the push phase become stronger, and those active in the recovery phase remain at the same level of strength. This difference of strength causes an imbalance in opposing muscles surrounding the shoulder joint, and as a result they are not able to provide the balanced amount of force necessary to secure the shoulder joint in its center position [33, 58]. Abnormal stresses applied to the sub-acromial area and high demands placed on shoulder muscles during wheelchair propulsion may also lead to shoulder pain [9, 59].

The repetitive nature of wheelchair propulsion [60], muscular imbalance and rotator cuff impingement due to overuse [11, 60] are possible factors causing upper-extremity pain and injury. In addition to self-propelled travel, wheelchair users need to perform transfers and fold and stow their wheelchair, for example in a car.

2.2.2 Transfer between resting positions

Transfer between a wheelchair and various resting surfaces e.g. the bed, chair, tub, car, or commode is required in the course of daily life. Studies have estimated that wheelchair users have to execute transfers 14 to 21 times a day [61-64] and do many weight-relief raises [64]. In preparation for a transfer, the arms are used to lift the body off the seat and so the weight of the body shifts from buttocks to hands. In order to complete a transfer, wrist and shoulder perform an internal rotation at the same time as they may be subject to excessive loads. High-strength requirements during downward pushing and abnormal stresses applied to

muscles and joints in wrist and shoulder areas during transfers are often required and contribute to the high rate of shoulder problems [9, 34, 59, 64, 65].

2.2.3 Wheelchair design

The basic framework of manual wheelchair design over the last 100 years has consisted of a seat, a backrest, two armrests, two rear wheels and two front wheels. In the last decade, researchers, designers and manufacturers have turned their attention to ways of improving the design so that wheelchairs can be used more efficiently for the various situations in everyday life, in sports and recreation. Some key design factors are weight, axle position, the type of frame (rigid, folding, adjustable), rear wheel camber, seat and backrest height and angle. Researchers have found that wheelchair configuration has an impact on pushing patterns, propulsion force and shoulder movements. Wheelchair users perform better in light, adjustable wheelchairs with a low, horizontal seat and the axle relatively forward [23, 46, 66, 67].

Only a few studies have focused on wheelchair designs as affecting upper extremity pain. In a study with 610 participants, a higher proportion of folding-frame wheelchair users with SCI reported severe pain when pushing for more than 10 minutes on a level surface travelling up a ramp, compared to rigid frame users [46]. An ergonomic hand rim (Natural-Fit) with twice the conventional rim width is reported to significantly reduce hand and wrist pain [68]. More improvements to reduce upper extremity pain are constantly being sought.

2.2.4 Other factors

Several studies have focused on the relation between upper extremity pain and the characteristics of manual wheelchair users such as gender, age, height, weight, duration after onset of injury, as well as working and living environment. Through questionnaires, physical examinations, the analysis of shoulder kinematics and kinetics, several factors could be correlated with shoulder pain, positive trends showing in increased age, years after injury, and weight [48, 51, 69, 70].

Collinger et al. [70] suggested that neither gender nor height were factors in the prevalence of shoulder pain; they were not significant demographic predictors for excessive loads to the shoulder during any speed of manual wheelchair propulsion among 61 paraplegics. Due to the inappropriate design of working [71] and living environments [72], manual wheelchair users in many situations have to raise their arms above shoulder height to perform functional activities, which increases shoulder pain when injury has occurred.

From the above review, it is obvious that long-term use of a wheelchair can lead to pain or injury for manual wheelchair users and that this affects their daily life. Factors influencing the onset of pain or injury include inappropriate or inefficient pushing styles.

2.3 Biomechanics of wheelchair propulsion

Human movement is explored through biomechanics (including kinematics and kinetics). Kinematics is concerned with the details of movement

itself while kinetics is focused on the cause of movement [73]. Both kinematics and kinetics have been used in the study of manual wheelchair propulsion, and particularly to estimate upper-extremity overuse and injuries. The upper extremity, when considered together with the trunk is referred to as the *upper body*. The study of upper body biomechanics can be divided into two categories: biomechanics of the upper extremities and biomechanics of the trunk.

2.3.1 Biomechanics of the upper extremity during wheelchair propulsion

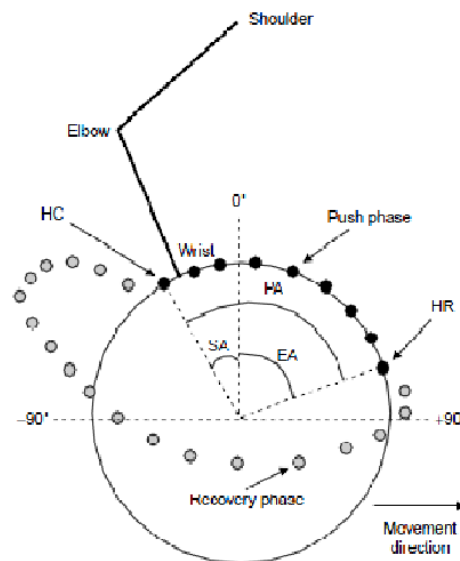
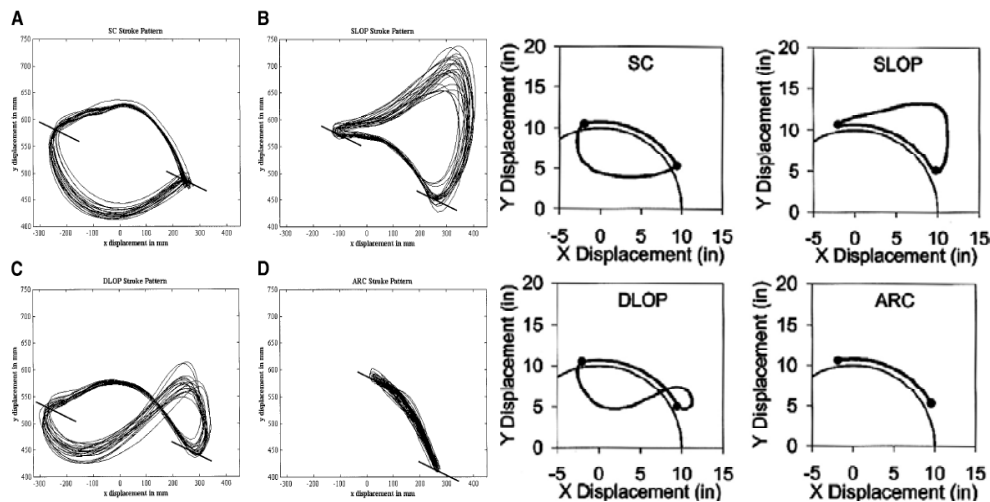


Figure 2- 3 Semi-circular propulsion trajectory. Black dots show the push phase, while the hands are in contact with the hand rim. The gray dots show the recovery phase, while the hands are off the hand rim [74].

Wheelchair propulsion is achieved by repeated pushes. Every push cycle can be divided into push phase and recovery phase (Figure 2-3) [74]. During the push phase, the wheelchair occupant contacts the wheelchair hand rims with his hands, applies force to grip them and to push forward. The rolling friction of the wheels being smaller than the force applied to the rims, the wheelchair accelerates. In the recovery phase, the hands leave the hand rims and so prepare

for the next cycle, as soon as no more force is applied to the hand rims, the rolling friction makes the wheelchair decelerate. The hands, in swinging back, can follow different paths. These recovery phase trajectories together with the push phase trajectory along the path of the rim have been described and placed into four categories [21, 32, 67, 75, 76]. These propulsion patterns are called semicircular (SC), single loop-over-propulsion (SLOP), double loop-over propulsion (DLOP), and arcing (ARC) (see Figure 2-4). In one study[32], it was found that SLOP (45%) was the most common pattern used by individuals with paraplegia who pushed on a dynamometer at a required target speed, followed by DLOP (25%), SC (16%) and ARC (14%). The SC pattern was found to be associated with a larger contact angle (also called “push length”) on the hand rim.



Notes: The dark bars in every sub figures represent the beginning and the end of a propulsive stroke, and the end and beginning of recovery.

Figure 2- 4 Propulsion pattern. Four kinds of propulsive strokes: (A) SC; (B) SLOP; (C) DLOP; (D) ARC [21, 32]

Vanlandewijck, Theisen et al. [74] found that the majority of subjects propelled with the same pattern on both sides at test speeds of 0.9m/s and 1.8m/s. However, they did not determine how subjects changed patterns gradually for

different speeds since they only designed the study with two levels of steady-state speed. The study could be improved by adding more speeds in the protocol design, as did Veeger et al. [77]. Richter et al. [21] studied different stroke patterns selected by individuals with SCI on a treadmill with different inclinations (0° or level, 3° uphill and 6° uphill) at a self-selected speed. The results showed that ARC was the most popular pattern in all situations (with 42% of participants on a level surface to 73% going up a 6° slope). On level ground, SLOP was found to be prevalent in 31% participants compared to DLOP with 27%, while SC was not found here or in any uphill conditions. These results are not consistent with previous findings by Boninger et al. [32, 67]. However, the study of Richter et al. [21] was based on self-selected speed, which appears to reveal the most natural propulsion patterns.

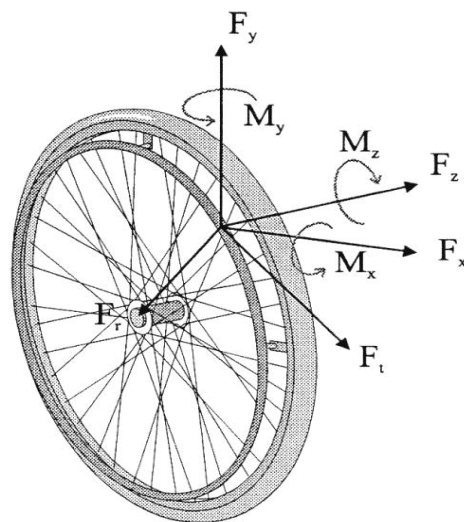


Figure 2- 5 Orientation of force and moments [78]

Smart^{Wheel} is a customized device widely used to collect kinetic data (detailed description in section 3.4.1) to investigate how the hand applies force during its contact with the pushrim. It measures component forces (F_x along

longitudinal/x axis, F_y along vertical/y axis and F_z along lateral/z axis) and moments (M_x around longitudinal/x axis, M_y around vertical/y axis and M_z around lateral/z axis) in three dimensions (Figure 2-5). Further processing results in F_t , a force tangential to the pushrim and F_r , a force radial to the pushrim. F_t and F_r are calculated on the basics of F_x and F_y , whereas F_z , the radial/axial force, is read directly at the rim. It is the force vertical to the plane of the pushrim. The total force F is calculated by F_t , F_r and F_z (Equation 2-1).

$$\frac{F_z^2}{F^2} + \frac{F_r^2}{F^2} + \frac{F_t^2}{F^2} = 1 \quad \text{Equation 2- 1}$$

Although the total force applied to the pushrim is seen as moving the wheelchair forward, it is only the tangential component, F_t , that causes the rotation of the wheel [58, 79]. F_r and F_z create the friction necessary to apply F_t . Many wheelchair users grip the rims too strongly, which results in insufficient F_r and F_z . People with SCI with high injury levels have difficulty generating enough grip force with their hands. As a result, they apply downward force in order to create friction, only part of which contributes to F_r . In all cases, gloves allow decreasing the grip force while still maintaining the necessary friction.

Push frequency is the number of times per second a wheelchair user pushes the hand rim. It is a key factor in the occurrence of upper extremity injuries. Wheelchair propulsion is of a repetitive nature, and the higher the push frequency the more repetitive it becomes. Therefore, it stands to reasons that repetitive movement injuries can be reduced by minimizing the push frequency

[3]. Push length is the length of rim pushed forward in one stroke. It is measured as the angle between the points at which the hand touches and then leaves the rim. A shorter push length is usually associated with more frequent pushes, thus increasing repetitiveness [20, 22, 23]. Participation in community life requires certain minimum speeds. For example, wheelchair users have to achieve a functional speed of 1.06 m/s in order to clear a pedestrian crossing in the time allotted to walking people (Hoxie et al. [80]). Speed, push frequency/cadence, and push length are all interrelated [17, 18, 23, 54, 78, 79] and thus have been studied in this thesis.

2.3.2 Biomechanics of the trunk during wheelchair propulsion

During wheelchair propulsion, not only the upper extremity but also the trunk is involved. Trunk movements during wheelchair propulsion are mostly in the sagittal plane, which is a vertical plane dividing the body into right and left sections and passing from front to rear (Figure 2-6). Flexion and extension are the forward and backward movement of the trunk.

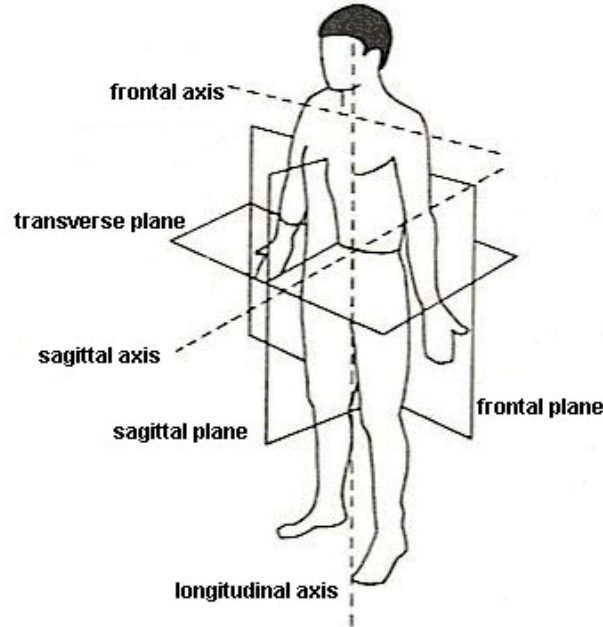


Figure 2- 6 Planes in human movement analysis (Google Image, from <http://www.brianmac.co.uk/musrom.htm>)

With able-bodied participants, Hwang et al. [38] found that trunk flexion and momentum were largely increased with increased resistance on the dynamometer, but there was no significant increase in shoulder, elbow or wrist movement. Participants had almost no trunk excursion when the system was loaded with a 5kg resistance and a 22 and 27 degrees of excursion with 10 and 15kg load respectively. The trunk reached a maximum flexion after hands reached the ending point of contact with rim. It is possible that additional momentum from trunk movement is necessary in accelerating the wheelchair, maintaining speed under difficult environments and a supplement to the energy loss of whole wheelchair-user system due to high resistance.

However, due to injury or disease, individuals who have trunk impairment might have little or no control of their torso muscles [81]. People with the cervical level of SCI have to use strategies to stabilize their trunk during propulsion

because of their limited trunk controls. People with thoracic level of injuries might have partial or complete trunk control and they can involve their trunk in wheelchair propulsion [82]. Often manual wheelchair users don't straighten their back while they are sitting in a wheelchair [11] and individuals with SCI may have kyphotic posture due to lack of trunk control [83]. Rice and Koontz found that there were paradoxical trunk movements in SCI wheelchair users while pushing, which means that when the propulsion force was generated the trunk moved in the opposite direction of the arms (i.e. backwards). This may be due to impaired trunk stability associated with paralysis of the back and abdominal core muscles. Koontz et al. [41] studied the paradoxical trunk movements and their relationship with mechanical efficiency during steady-state wheelchair propulsion on a simulator. According to this study, reactive forces send the trunk backward when the subject pushes the rim forward and abdominal musculature acts to oppose these forces and even enable leaning forward during the "push phase" of propulsion. As wheelchair speed increased from 0.9m/s to 1.8m/s, both unimpaired individuals and paraplegic group increased their trunk excursion (includes flexion and extension), respectively from 15.7mm to 30.4mm (with 93.6% rise) and whereas the tetraplegic group's excursion only changed from 25.35mm to 27mm (with 6.5% rise). However, the measurement of trunk excursion using linear measurement is complicated because some subjects are taller than the others. Hence, the trunk displacement angle would be a better option to measure trunk movement.

Later Worobey et al. [40] studied paradoxical movement with manual wheelchair users on a more natural range of surfaces such as carpet, linoleum, as well as on a ramp and found that paradoxical movements became more pronounced as the surface resistance to propulsion increased and pushing became less efficient. The question of whether there exist certain limits of trunk excursion with respect to efficient wheelchair propulsion has yet to be explored. Therefore, more specific studies on how the trunk is involved in wheelchair propulsion and how people with or without trunk impairment can improve their performance and propulsion efficiency by engaging the trunk is required. Angular displacements or excursions of the trunk are important in characterizing the wheelchair users' performance and are closely linked with the functions of other parts of the body.

In the above review, it has been shown that researchers have studied different biomechanical parameters for wheelchair propulsion in real-world environments as well as simulated environments. In the following sections, a comparison of these two environments is provided.

2.4 Wheelchair use environment

Most buildings, parks, and community facilities have been designed or modified to accommodate manual wheelchair users according to the disability accessibility regulations of their local community. In spite of all improvements, a manual wheelchair users' environment is still not always predictable. Short walk lights, buildings without elevators, high curb stones, uneven or snow-covered

sidewalks can be sudden impediments to locomotion when it is absolutely necessary to get from one place to another.

2.4.1 Wheelchair-accessible indoor environments

Depending on the surface condition and its type, different indoor environments can be easy or hard to access using a wheelchair. Ordinary indoor floorings including linoleum, hardwood, tile, and low-pile carpet are wheelchair accessible. Medium-, high-pile carpet and wet floors may be comparatively challenging for manual wheelchair users [14]. Automatic side sliding doors with level thresholds are helpful to wheelchair users, but they are not commonly seen in a regular house. Elevators are required in multiple-floor buildings, and wheelchair platform lifts are mandatory for height differences not exceeding 1980mm [84].

2.4.2 Wheelchair accessible outdoor environments

Wheelchair users experience all kinds of surfaces in their normal outdoor life. Wheelchair users report that outdoor environments such as uneven ground, ramps/hills, high rolling resistance surfaces such as gravel, sand, mud, grass, are challenging [14]. Sidewalks are often uneven and difficult for wheelchair locomotion and they often involve side slopes that require constant steering [18]. In addition, concrete sidewalks with different patterns of surface transmit vibration to wheelchair users. Studies with powered wheelchairs have found that long-term exposure of the body to vibrations on sidewalks is significant and may lead to secondary injuries and fatigue; this is even true for manual wheelchair

users [7, 8]. Pedestrian crossings with traffic lights are challenging for manual wheelchair users because the crossing time is based on the requirements of able-bodied pedestrians, or a walking speed of 1.2m/s. In most parts of Canada, many surfaces including sidewalks are covered with ice or snow for several months of the year [17] [19]. Wheelchair users with SCI in Japan reported that rear wheels or casters can become very slippery, and that casters are easily buried in snow and that pushrim is very cold with a risk for frost-bite [85]. Wheelchair users have to constantly assess their environment, such as the rolling resistance, possible soft surfaces that might catch casters and make steering difficult, or an unstable surface. Researchers [86] have studied the accessibility of the national parks in the USA and developed international standards for exterior terrain wheelchair accessibility.

2.4.3 Rolling Resistance and its impact on wheelchair propulsion

A frictional force, called *rolling resistance* applies in the direction opposite to the wheelchair motion when a wheelchair tire rolls on a surface. This force is determined by the material of the tire and the type of ground. Resistance means a loss of energy to wheelchair propulsion and it affects the efficiency of pushing.

Pneumatic tires (made of reinforced rubber and filled with compressed air) are widely used. It was found that rolling resistance increased as the tire pressure decreased [87-89]. According to a study by Sawatzky et al.[89], high tire pressure

(>75%) is recommended to achieve reduced energy expenditure by the wheelchair user and better rolling performance.

Several studies [15, 16, 20, 23, 90] focused on the effects of rolling resistance or roughness of different surfaces on the wheelchair propulsion kinetics. The roughness of the surface ranges from those involving aggregate materials to smooth surfaces, for instance, from gravel to grass, concrete, and carpet to tile. As resistance increases, the effort expended in crossing the surface and the number of pushes per unit of time (push frequency) will increase, and the risk of inducing upper extremity pain or injury might be higher [15, 16, 20, 23, 90]. These studies have helped define the effects of surface conditions on propulsion biomechanics and provide consistent findings for improving our understanding of wheelchair users' everyday experiences. However, all of the previous studies are focused on the user propelling on one particular surface type at a time. They did not consider transitions from one surface to another. In real life, the wheelchair user has to move frequently from one surface to another. Therefore, it would be useful to understand how transitions between different surface types affect propulsion. Surface properties are an important factor in the study of wheelchair propulsion biomechanics. Additionally some studies have focused on wheelchair propulsion along inclined surfaces (ramps). In the following section, the effect of slopes on wheelchair propulsion is summarized.

2.4.4 Ramps and their impact on wheelchair propulsion

Ramps are designed to connect surfaces of different levels, such as a transition between sidewalks and pavement roads or from floor to stage. It is common to have slopes at the entrance of a building, with an inclination between 1:20 and 1:12 [84, 91]. Studies have found that compared to level ground propulsion, uphill propulsion demands more effort and is more challenging for the participants, even when they push at their self-selected speed (the speed with which they are the most comfortable) [16, 22, 23, 28]. The effect of a slope on wheelchair propulsion biomechanics has been studied on ramps outside of buildings [16, 22, 23], on a treadmill [21], or on inclined adjustable wooden ramps [28]. In the two latter situations, stationary equipment is used to control and adjust for ramp research. Wheelchair users may use different propulsion techniques on level ground compared to slopes of varied inclination. Apart from the additional effort of working against gravity, the wheelchair user also has to ensure that the wheelchair does not tip. Tipping can occur simply due to the setup of the wheelchair, where the center of gravity of the user starts to fall behind the axle. The risk of tipping during the propulsion stroke may be overcome by leaning forward, if the user has trunk control. They may have to limit the intensity of the propulsion stroke to conserve stability. Chow et al. [28] found their participants increased forward leaning of their trunk as slope angles increased from 0 degrees to 12 degrees. There were major adjustments in stroking kinematics as well (decrease of stroking speed, push angle and recovery time, increased stroke frequency). It was also found that a significant increase took place in muscle

activity at slope between 4 degrees to 10 degrees. Wheelchair users adopt different stroke patterns to accommodate environments and most of them (73%) adopt an arcing stroke pattern (discussed in detail in section 2.5) as they push uphill [21]. Cowan et al. [22] also found that wheelchair users push slower on a smooth ramp compared to level carpet or tile. However, since they used different surfaces for the ramp and the level ground, they were not able to establish a difference between push frequency and stroke length in these two environments.

In summary, several factors influence wheelchair propulsion in real-world environments. Experiments may be influenced by the constraints of budget, space, or operating condition. Therefore, to mimic the real-world environment, researchers have generated different types of simulated environments to conduct these studies. A discussion about the use of different simulated environments is given next.

2.5 Wheelchair simulation environment

Simulated environments and the use of virtual reality are designed to mimic real-world conditions, tasks and environments. Researchers have investigated how human subjects react to and interact with external factors [92, 93]. A simulated environment is usually a stationary system with controls and feedback, combining computation, mechanics and electronic sensors functioning together. With simulated environments, experimental parameters can be controlled and the performance of participants can be measured and recorded.

The following sections will focus on manual wheelchair simulation environments that have been widely used by researchers.

2.5.1 Various Types of Simulated environments

Primarily 4 types of stationary devices are used to explore manual wheelchair propulsion study in a lab environment: a) motor-driven treadmill, b) custom-made or commercially available roller system, c) custom-made ergometer with wheelchair or simulated wheelchair, and d) custom-made dynamometer with wheelchair or simulated wheelchair [24, 27, 29, 77, 94].

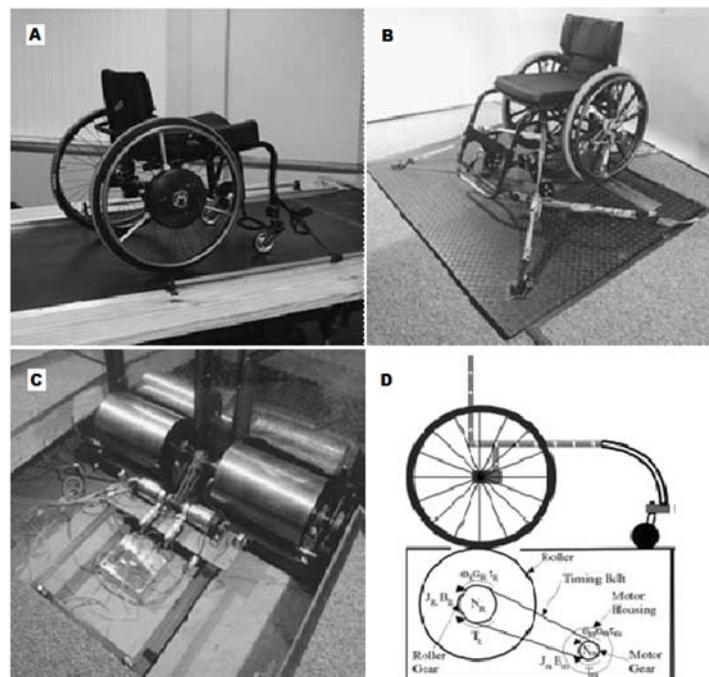


Figure 2- 7 (A) A motor-driven treadmill with a wheelchair [29]; (B) A dynamometer with a wheelchair [27]; (C) Components of a dynamometer without cover [27]; (D) A diagram of dynamometer [27].

A motor-driven treadmill (Figure 2-7(A)) is a moving platform which is driven by a belt through an electric motor. In this system, the output of wheelchair propulsion is converted into the traveled distance. This is similar to a real-world

situation. Wheelchair users push it at a controlled speed with the wheelchair attached to the system. Treadmills can provide different levels of workload for participants by increasing the speed [29], changing the inclination degree of the platform [26, 29, 95, 96], and adding a pulley system working against the motion [26]. Controlled speed and power are widely used in athletic training, and inclination is a mimic of uphill pushing in users' everyday life. However, wheelchair users push at their self-selected speed or in a comfortable way instead of keeping up a certain speed in their everyday life. One of the limitations of these studies [26, 29, 95, 96] using treadmills is that rolling resistance cannot be simulated.

It can be difficult to control the rolling resistance on a roller system as well. However, to control the rolling resistance, an ergometer equipped with a dynamometer can be used. All roller systems, ergometers and dynamometers share a common design characteristics: a pair of parallel steel rollers (Figure 2-7(C)). As the wheelchair user rotates the wheelchair wheel, the motion and force are transferred to rotate the two rollers. This is different from a treadmill and real-world propulsion. Several factors influence the resistance to motion of the wheelchair wheel experienced by the user. The wheelchair, itself, has some friction and the wheelchair wheel has its own moment of inertia that resists rotational acceleration. The selection of rollers used in the ergometer can simulate part of the inertia resistance that the users normally encounter in unconstrained propulsion. The mass, diameter and construction of the rollers influence their moment of inertia. Finally, the resistance to rotation of the rollers

may be due to either friction in the bearings or through a deliberate application. In all three laboratory systems, the wheelchair frame has to be mounted and fixed, with the two wheels contacting the top of the two rollers. A simple roller system can measure the speed of the wheels only and has not been widely used because of its limitation. An ergometer can measure speed, work and power of propulsion. A dynamometer is a device which can measure torque (with torque sensors installed on the axles of roller) and add or subtract power to the system in addition to all the functions of the ergometer [27]. With a computer-controlled function in the ergometer and dynamometer, resistance can be adjusted in order to increase the resistance to pushing. Dynamometers can simulate and mimic real-world surfaces with different levels of friction, such as carpet and concrete pavement. Participants are able to push at their comfortable speed and make changes dynamically according to their preference, or in response to other aspects of the simulated propulsion task. Besides being widely adopted in wheelchair propulsion biomechanics research [34, 97-100], ergometer and dynamometer can also be used in the training of daily wheelchair users for gaining strength and improving upper extremity resistance [101, 102] and for training athletes [103]. However, the rollers' rotation design of ergometer/dynamometer cannot fully translate wheelchair travel on a real-world ground. Another important consideration is the influence of inertial factors associated with the participant and the wheelchair (due to their mass) and the acceleration being generated during propulsion. Inertial effects are usually accommodated when using treadmill-based simulators as long as the wheelchair user is not being constrained by safety

devices. There are two types of treadmills employed in wheelchair studies. The first one [29] is an open loop system, with the belt set at a fixed speed and wheelchair users have to keep up. The other [26] is a closed-loop treadmill. Wheelchair users push on the treadmill, the speed of the treadmill has to be controlled so that the wheelchair-user system is in the middle of the treadmill during propulsion. However, for ergometer and dynamometer used in above studies reported in the literature to date, they did not include a means to simulate inertial factors. Hence, we need to study the incorporation of mass on the wheelchair-participant system, moments of inertia on system components and the acceleration being generated by the user in these simulated environments.

While performing simulated experiments, it is necessary for participants to receive feedback about their push so that, if necessary, they can increase or decrease the applied force to mimic the real environment. Visual feedback systems can be used for this purpose. In the following section visual feedback systems and related literature are reviewed.

2.5.2 Visual feedback

In a simulation environment, visual feedback is usually required to engage the participants and give them information so that they can adapt their effort according to the task being simulated. There are different types of visual feedback systems. These include non-immersive systems, semi-immersive systems or fully immersive head-mounted display systems. A detailed report on different types of immersive systems is available in the report [104]. Of these, non-immersive

systems are widely used because of their low cost and no need for a high level of graphic performance. Non-immersive systems include desktop systems using a high-resolution monitor. Interaction with the virtual environment can occur by conventional means such as keyboard, mouse and trackball. The virtual environment is viewed through a portal or window by utilizing a standard high-resolution monitor. For example, this approach is widely used for simple motor vehicle simulation training and assessment.

In earlier non-immersive studies, feedback was available for a limited number of parameters and not as a complete biomechanical environment [18, 35, 105]. In a study of mechanical efficiency, Goosey-Tolfrey et al. [106] used average propulsion speed as feedback. However, the participant was not able to feel the resistance of the environment in which the pushing was performed. Similarly, Qi et al. [58] investigated muscle activity during wheelchair propulsion and used average propulsion speed as a feedback parameter.

Studies to date have not provided virtual-reality environments where participants are able to “feel” the environment of wheelchair propulsion. Therefore, their responses are based on the parameter values only. A more realistic response will be obtained if participants “feel” the environment and react accordingly. It is necessary to design a non-immersive system that can simulate the environment plus allows the participant to “feel” to task and respond in real time.

To experiment in the simulated lab environment, it is necessary for participants to perform tasks that are as close as possible to the real-world conditions [18, 21, 26, 29, 34]. To attain this, a feedback system is required. Most feedback systems used in studies of wheelchair propulsion, used a parameter such as speed or force as feedback to the participant [22, 23, 35, 58, 105, 106]. The reaction of the participant depends on the value of the parameter. It is important that the participant sense a real-world-like environment condition while performing on the simulators. To accomplish this, a system was designed in this study which provides feedback to the participants by not only letting them feel the resistance of the real-world environment but also providing a visual representation akin to real-world condition.

2.6 Comparison of wheelchair propulsion biomechanics between real-world and laboratory simulated environments

Real-world or over ground conditions represent the most realistic environment for wheelchair propulsion studies. However, due to the limitations of space, weather and inconvenience of research data collection, it is difficult to undertake comprehensive biomechanical studies in the real-world. Researchers have employed laboratory simulated environments and explored possible ways to closely simulate real-world environments. Stephens and Engsberg [107] studied stroke pattern differences between real-world and treadmill and found that the differences were significant. Later a study by Kwarciak et al. [29] compared manual wheelchair propulsion on treadmill and an over-ground surface which comprised a low pile carpet at self-selected speed. They found that data

distribution within a push cycle of all hand rim biomechanics (including contact angle, peak force, average force and peak axle moment) were similar and highly correlated. However, there were slight differences in power output and cadence. In order to provide a similar challenge of carpet on the treadmill, they adjusted the inclination grade of the platform, which may not be a correct representation of the carpet environment. It is possible that increasing the power output of the treadmill by elevation would affect the trunk motion as the neutral position of the trunk is changed and participants have to balance their body on the tilted floor.

In another study, Koontz et al. [34] compared wheelchair propulsion for individuals with SCI on a level tile surface to that on a dynamometer at self-selected speed. It was found that the correlation in parameters of push length, push frequency and total force were consistent between these two conditions. They found that the rolling resistance of the tile surface could not be represented by the dynamometer. They also neglected the subject's inertia during the simulation. No visual feedbacks were provided to the participants during the dynamometer propulsion.

These studies come to different conclusions about the representation of the real-world in the lab environment. More studies are required for the comparison of manual wheelchair propulsion performance in the laboratory and real-world environments. An ergometer may also be used to check whether a real-world environment can be simulated in the lab environment. So far, no comparison has

been undertaken for comparison between ergometers and a real-world environment.

Upper-extremity pain and injury affect and restrict a manual wheelchair users' everyday life in the real-world. Researchers and clinicians offer recommendations on improving upper extremity health based on many studies conducted in a laboratory environment. However, whether lab system can represent the real-world is still not sure and would be valuable to investigate.

Chapter 3 Methods

3.1 Statement of objectives

This study included three different objectives. First, it focuses on how rolling resistance affects performance of able-bodied subjects. Second, how the transition between surfaces of different rolling resistance affects the users' performance. Last, our aim was to compare performance in two environments (real-world vs. ergometer-simulated environment). We intended to establish whether the lab environment is representative of the real-world environment and identify factors that significantly influence any differences that may exist. To conduct the study and meet the objectives, three hypotheses were considered as follows.

3.1.1 Hypothesis 1

In a real-world environment, there is no significant difference in the biomechanics of wheelchair propulsion and trunk motion of able-bodied subjects at a self-selected speed between two surfaces with different resistance.

3.1.2 Hypothesis 2

In a real-world environment, the biomechanics of wheelchair propulsion and trunk motion of able-bodied subjects' do not change significantly when the direction of transition between two different surfaces at a self-selected speed is reversed.

3.1.3 Hypothesis 3

The biomechanics of wheelchair propulsion and trunk motion of able-bodied subjects at a self-selected speed show no significant difference between a real-world environment and the corresponding laboratory ergometer environment, regardless of the type of surface.

Real-world experimental conditions included two surfaces with different rolling resistance: medium pile carpet (carpet), artificial turf (turf), and the transition between these surfaces. Laboratory roller ergometer experimental conditions included a simulation of these surfaces. Two models were used to adjust the resistance to motion on the ergometer, simulating inertial effects and the rolling resistance of the surfaces. Details of both models can be found in Section 3.5. Hereafter we will mention these models as Model 1 and Model 2, respectively.

3.2 Sample size calculation

A power analysis was conducted to calculate the minimum sample size for statistical test with a 90% confidence level. From previous studies [57, 79], mean and standard deviation of propulsion moment (of push force along a hub axis) data were taken, for subjects pushing on a linoleum (lino) surface and on a ergometer for 3 repeated tests.

The sample size was determined using the steady-state push data of moment values. μ_0 and μ_1 are the mean values of moments collected from

linoleum and ergometer. Equation 3-1 is used to calculate the sample size ‘ n ’ [108].

$$n = \frac{(u + v)^2 (\sigma_1^2 + \sigma_0^2)}{(\mu_1 - \mu_0)^2} \quad \text{Equation 3- 1}$$

where, σ_0 and σ_1 are the standard deviations of moment values from lino and ergometer, respectively. u and v denote the constants associated with the power of the study (two-sided and 90% in this case) and their values are: $u=1.29$, $v=1.96$. The following standard deviation values were used in the previous study: σ_1 = standard deviation of moment values when pushing on lino = 1.6, σ_0 =standard deviation of moment values when pushing on ergometer = 1.6. The difference of the mean of moments ($\mu_1 - \mu_0$) the effect size of the experiment was chosen to be 1.6 (one standard deviation). Applying these values in Equation 3-1 we get;

$$n = \frac{(1.29 + 1.96)^2 (1.6^2 + 1.6^2)}{1.6^2} = 21.12 \quad \text{Equation 3- 2}$$

hence, the minimum sample size value is 21. It is good practice to conduct experiments with the more participants than the minimal sample size value. In this study, 25 participants are included. The participants and their inclusion and exclusion criteria are described as follows.

3.3 Participants

The study took place at the Wheelchair Biomechanics Laboratory, Faculty of Rehabilitation Medicine, University of Alberta, Edmonton, AB. Participants were recruited through various ways including posters, group emails to students in the Faculty of Rehabilitation Medicine, and friends. Individuals interested in participating in the study answered questions by email or telephones to screen them for the study inclusion and exclusion criteria (listed below). Those who met all the criteria, read the information letter and signed the study consent form became participants.

The ethics approval for this study was an amendment to an established protocol used by the lab “Shoulder muscle function during wheelchair propulsion, comparing performance in real-world and laboratory settings”, and was approved by the Human Research Ethics Review Process (HERO), University of Alberta. Subjects’ data were coded without personal information and were kept confidentially.

3.3.1 Inclusion and exclusion criteria

Individuals were excluded if they presented upper-body orthopedic disorders or neuromuscular conditions (e.g. multiple sclerosis, motor neuron disease) that limited upper body exercise performance and those with pre-existing pain or injury during exertion in upper extremities as stated in the physical activity readiness questionnaire (PAR-Q). Individuals who had used a manual wheelchair for primary mobility in the past were excluded, so that the sample would be sufficiently uniform, for a study mainly focused on a comparison of

research environments. No gender or hand dominance preference factors were considered. Subjects who were able bodied, with body weight between 40kg and 100kg and whose age was between 18 and 40 were selected, because the study had to follow the inclusion criteria in a larger project.

3.4 Measurements and instruments

In this thesis, hand rim biomechanics including parameters such as peak total propulsion force, peak moment M_z , push length, push frequency and average speed, recorded with the Smart^{Wheel}, were selected to study upper extremity wheelchair propulsion. Trunk motion was measured in terms of the trunk's angular displacement $\theta(t)$ and peak angular velocity. Trunk motion data, measured by an IMU (Inertial Measurement Unit), were collected with Tachyon, a data logging system developed by the Ferguson-Pell laboratory for wheelchair propulsion.

3.4.1 Smart^{Wheel}

Smart^{Wheel} (Three Rivers Inc., Mesa, AZ, USA), an instrumented wheelchair wheel, can measure the hand rim biomechanics of wheelchair propulsion and can be mounted to most manual wheelchairs (Figure 3-1). Hand rim biomechanical parameters include but are not limited to speed, force, moment, contact angle/ push length, push frequency. Two Smart^{Wheel}s were used to collect biomechanical data from both the left and the right side. Smart^{Wheel} detects force applied with multiple transducers, records data with a microprocessor, and transmits data to computer wirelessly through Wi-Fi. As

mentioned in section 2.5.1, parameters such as total force, M_z , push frequency, push length and speed are very important in describing the performance of wheelchair users.

In this study, a rigid frame, lightweight wheelchair (Quickie GP, Sunrise Medical, Longmont, CO, USA) was used with two Smart^{Wheel}s attached.



Figure 3- 1 Smart^{Wheel} attached to a Quickie manual wheelchair

The following measurements were used to represent hand rim propulsion biomechanics:

- Peak Moment M_z : It is the peak propulsion moment that the participant applies to the hand rim of Smart^{Wheel} during each push, which results in rotation of the wheel. M_z is plotted against time and the highest value of M_z of each push is recorded as peak M_z value.

- Average Speed: It can be used as an index of functionality. The average walking speed is $1.4m/s$ and the functional speed (speed of crossing a traffic light) is $1.2m/s$.
- Push Length: It is the angle travelled by the hand on the push rim from the point of contact to the point of release, units in degree.
- Push Frequency: This is defined as on average number of pushes a participant conducted during a period of one second.

All measurements from the left and the right wheel were combined and averaged. A mean value was calculated throughout each trial for each measurement.

3.4.2 Tachyon

Tachyon (Figure 3-2) is a data logger that can measure the real-world “day-to-day” propulsion activity data for extended periods about 5-6 days [109]. It is capable of recording parameters of the environment and the wheelchair user, including individual wheel velocity, roll and pitch of the wheelchair frame, compass heading, temperature and humidity, wind speed and user heart rate. Additionally, it can interface wirelessly with an external Inertial Moment Unit (IMU) (sampling at 50 Hz) and record its data. Wheel velocity is sampled at 50 Hz and other parameters at 1 Hz . All data was stored using an onboard SD card and streamed wirelessly to a computer using ZigBee protocol. In this thesis, Tachyon was used as a data collector for IMU data.

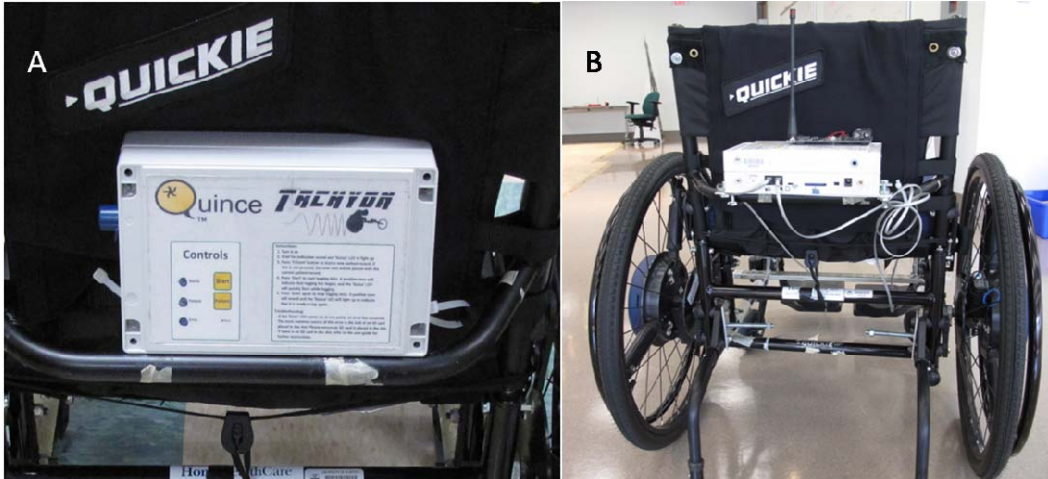


Figure 3- 2 Tachyon and installation (A) Tachyon (B) Tachyon mounted to the back of a Quickie wheelchair

3.4.3 IMU and calibration

An IMU (Sparkfun™ Electronics, Boulder, CO, USA) (Figure 3-3A), an external device to Tachyon, can detect the motion of an object in six degrees of freedom by using gyroscopic and accelerometer sensors. Six degrees of freedom (Figure 3-3B(Up Right)) include left/right (X -axis), forward/backward (Y -axis), up/down (Z -axis), and three rotations (Pitch, Roll and Yaw) about these three axes. They are used to describe the freedom of movement of a rigid body in a three-dimensional space. Accelerometers (Accel) incorporated in the IMU measure linear acceleration values along three axes (X , Y and Z) as a function of time they are defined as $A_x(t)$, $A_y(t)$ and $A_z(t)$, in units of $m \cdot s^{-2}$. Readings from the IMU's gyroscopes (gyros) describe the rotation around the system's three axes and the angular velocity is referred to as $Pitch(t)$, $Roll(t)$ and $Yaw(t)$, in units of $Degree \cdot s^{-1}$. The IMU was attached to the chest of the participant with a length-adjustable strap (Figure 3-3C). Located in this way the IMU's Y -axis is

associated with left/right, Z-axis associated with forward/backward, X-axis associated with up/down (Figure 3-3(D)). When a participant pushes a wheelchair, the trunk performs translational movements forward and backward, and at the same time rotates around the hip. IMU accelerates in both X-axis and Z-axis and has rotational velocity around Y-axis, which is Roll. IMU was sampled at a frequency of 50Hz.

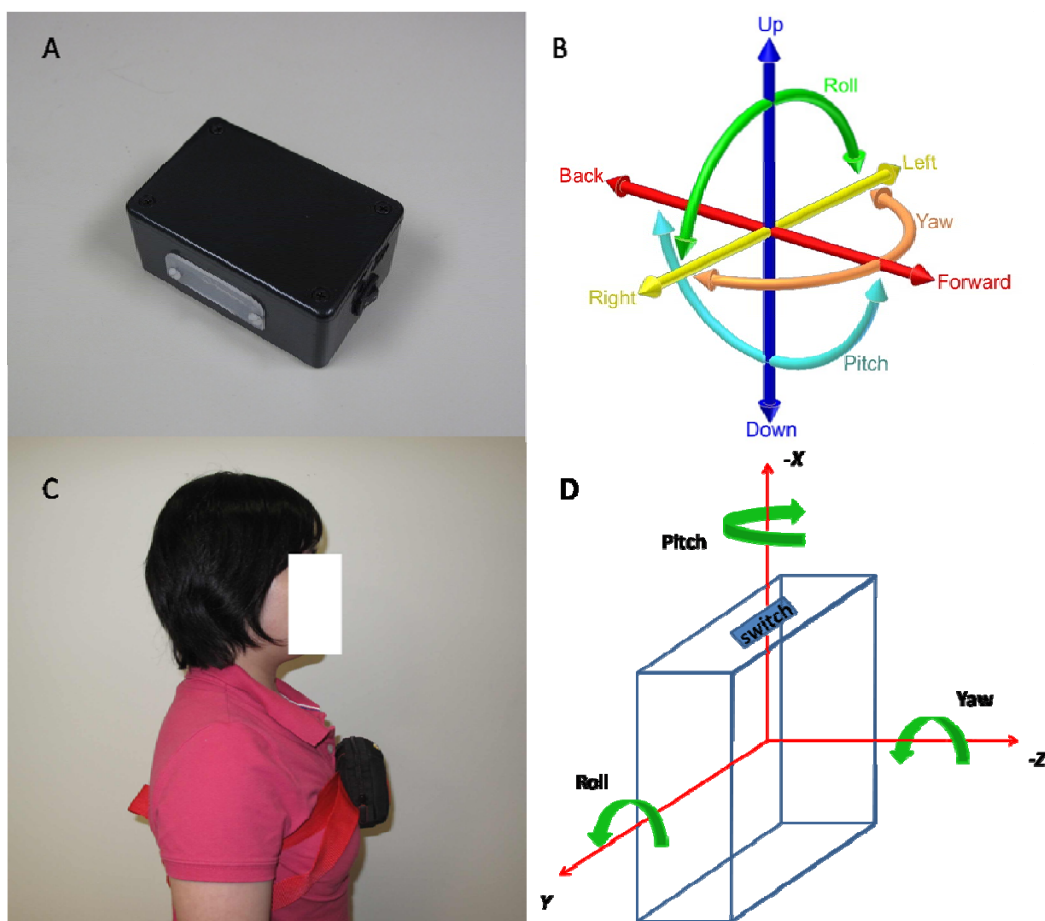


Figure 3- 3 IMU and its orientation (A) IMU device; (B) Six degrees of freedom in three-dimensional space [110]; (C) Participant with IMU attached to chest; (D) IMU six degrees of freedom drawing with the same portrait as in (C).

The calibration of IMU includes two parts: calibration of Accel data and calibration of Gyro data using Accel data. Since the readings of Accel and Gyro

are highly correlated, the readings of Accel were used to validate the Gyro data in the second part.

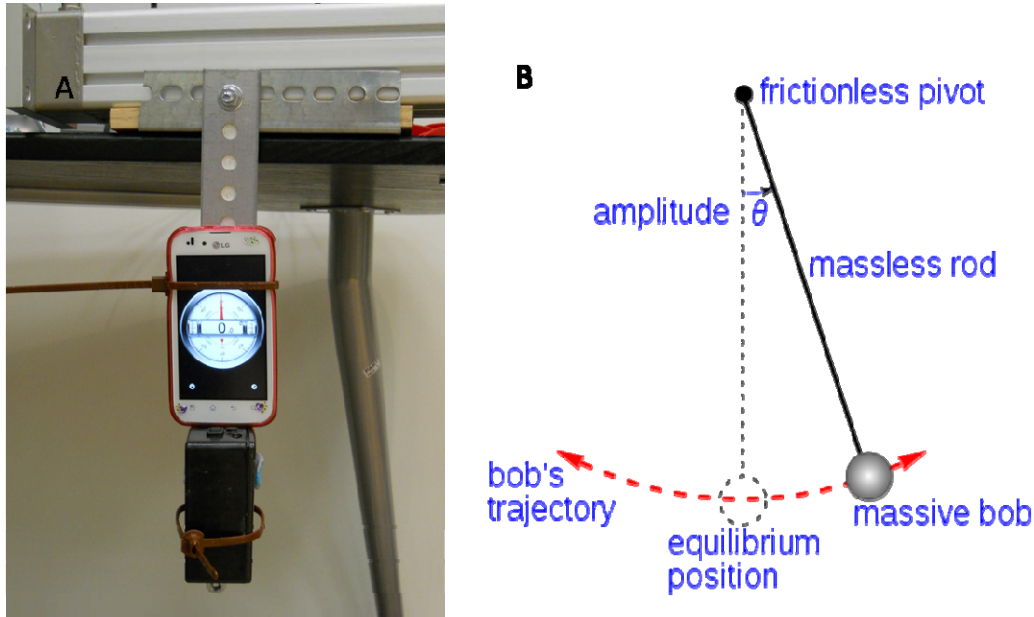


Figure 3- 4 IMU Calibration (A) IMU pendulum model in static position (B) Accel data used in the model

To calibrate Accel data, a simple IMU calibration model was built according to the theory of a simple pendulum (Figure 3-4A)). In this model, the movement of IMU is similar to the movement of the trunk during wheelchair pushing, rotating around one fixed point/axis. The top end of a metal rod was attached to the platform allowing the IMU at the other end to swing back and forth like a pendulum. The coordination of IMU was the same as that in Figure 3-3C and D. Figure 3-4B shows that, in a/the static position, the metal rod is vertical to the ground and the only acceleration applied to IMU is gravity (g). When the IMU swung away from the static position, the width of swing was described with amplitude or angle $\theta(t)$. At this stage, gravity can be divided into accelerations in X -axis and Z -axis. In order to measure the value of $\theta(t)$, a smart phone with the

application ‘XClinometer’ (Plaincode™ Software Solution) was attached to the rod and displayed the angle at the start of the swing (Figure 3-4A). The XClinometer application also samples the swing amplitude or angle $\theta(t)$ in real time, and the readings are stored at a URL and can be accessed after the test as a text file. This XClinometer sampled the swing angle at 20 Hz and was used to compare with the value of $\theta(t)$ calculated from Accel data. The Tangential value of $\theta(t)$ is the result of the acceleration in the X-axis ($A_x(t)$) divided into the acceleration in the Z-axis ($A_z(t)$).

$$\text{Tan}[\theta(t)] = \left(\frac{A_z(t)}{A_x(t)} \right) \quad \text{Equation 3- 3}$$

The value of swing angle $\theta(t)$ calculated from Accel readings is:

$$\theta(t) = \text{Tan}^{-1} \left(\frac{A_z(t)}{A_x(t)} \right) \quad \text{Equation 3- 4}$$

Nine different angles, from -55 degrees to 40 degrees, with about 10 degrees interval of each were collected. The calibration results of Accel in the next chapter show that there is a linear relationship between the swing angle $\theta(t)$ and the angle calculated from Accel data.

The second part was to calibrate Gyro data with the Accel reading. The swing angle $\theta(t)$ is the rotation angle around Y -axis. Angular velocity $\dot{\theta}(t)$ is equal to the differentiation of $\theta(t)$ to time t :

$$\dot{\theta}(t) = \frac{d(\theta)}{d(t)} \quad \text{Equation 3- 5}$$

According to the afore-mentioned equation, angular velocity:

$$\dot{\theta}(t) = \frac{d(\theta)}{d(t)} = \frac{d\left\{ \text{Tan}^{-1}\left(\frac{A_z(t)}{A_x(t)}\right) \right\}}{d(t)} \quad \text{Equation 3- 6}$$

A participant pushed a wheelchair with IMU attached to his chest and finished a few tests. A linear relationship between angular velocity $\dot{\theta}(t)$ and $Roll(t)$ was found and results are shown in next chapter.

3.4.4 Real-world settings

Real-world experimental conditions included two surfaces with different rolling resistance: 8 meters of medium pile carpet (carpet) and 8 meters of artificial turf (Figure 3-5). These two surfaces were joined with carpet tape and the transition (or conjunction) between these two surfaces was studied as well. This arrangement represents what happens when a wheelchair user encounters a

sudden change in rolling resistance. In order to know how subjects perform on the transition from a surface of lower resistance to a surface of higher resistance and vice versa, the real-world experiments included travelling in both directions - from carpet to artificial turf and from artificial turf to carpet. It is also shown in section 3.8.2 Figure 3-27.



Figure 3- 5 Real-world environment including two surfaces: carpet and artificial turf

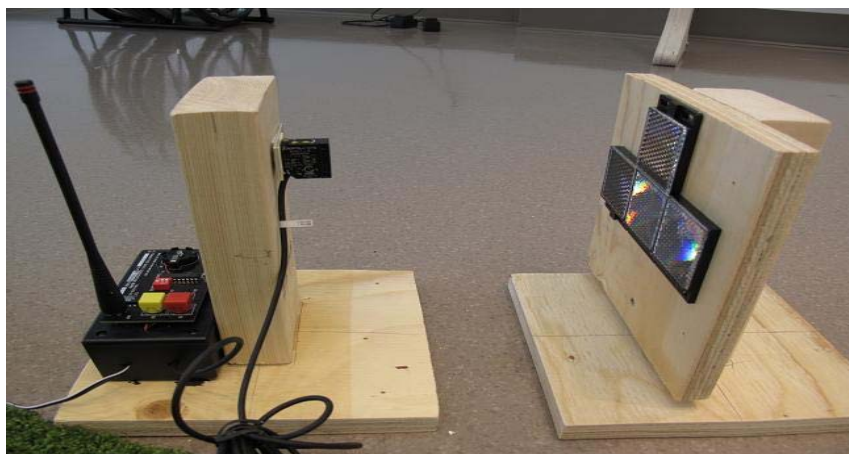


Figure 3- 6 Transition detection system: a RF transmitter (left), a retro-reflective sensor (middle), and a reflector (right).

On either side of the transition between artificial turf and carpet, there was a retro-reflective sensor (PEPPERL+FUCHS Inc., Mannheim, Germany) and a reflector, for the use of transition detection (Figure 3-6). If any object crossed the transition (Figure 3-7), the light beam sent out from retro-reflective sensor would be interrupted and a switching signal was sent through a pair of RF module (LINX Technology Inc., Merlin, OR, US) wirelessly to the desktop. A LabVIEW (Version 8.5, National Instrument Inc., US) program was designed to record the transition-switching signal along with a timestamp.



Figure 3- 7 A participant crossing the transition with a wheelchair.

3.4.5 Roll-down test, rolling resistance and deceleration slope of real-world surfaces

Rolling resistance is the main force acting on wheelchair deceleration. It is related to the mass of the wheelchair and its user and to the deceleration. In Equation 3-7, F_{rr} is the deceleration force (rolling resistance), M is mass of wheelchair and user together and α is the deceleration slope.

$$F_{rr} = M \times \alpha$$

Equation 3- 7

In everyday life, the wheelchair occupant has to generate propulsion forces that overcome rolling resistance and inertia associated with the mass of the user and wheelchair. Rolling resistance is relatively insensitive to the speed of propulsion but is sensitive to the mass of the wheelchair and its occupant [111]. As a result, each participant had to conduct several roll down tests before the experiments so that the α values of these two surfaces associated with their own weight could be ascertained and used in the ergometer simulation. Results in chapter 4 show that artificial turf has a higher rolling resistance than carpet, which was also the same to feedback from participants.

Roll-down (or coast down) tests are widely used for checking the rolling resistance [111, 112]. During a test, the occupant accelerates the wheelchair with several continuous pushes, and holds his upper body steady and hands away from hand rim until the wheelchair deceleration has stopped. The speed of both wheels during deceleration are recorded using the Smart^{Wheel} and the slopes of deceleration versus time (α) were calculated and defined as the rolling resistance

of this surface. Since α described the deceleration, its value was negative. The higher rolling resistance of the surface is, the higher the absolute value of α will be.

3.4.6 Ergometer and calibration

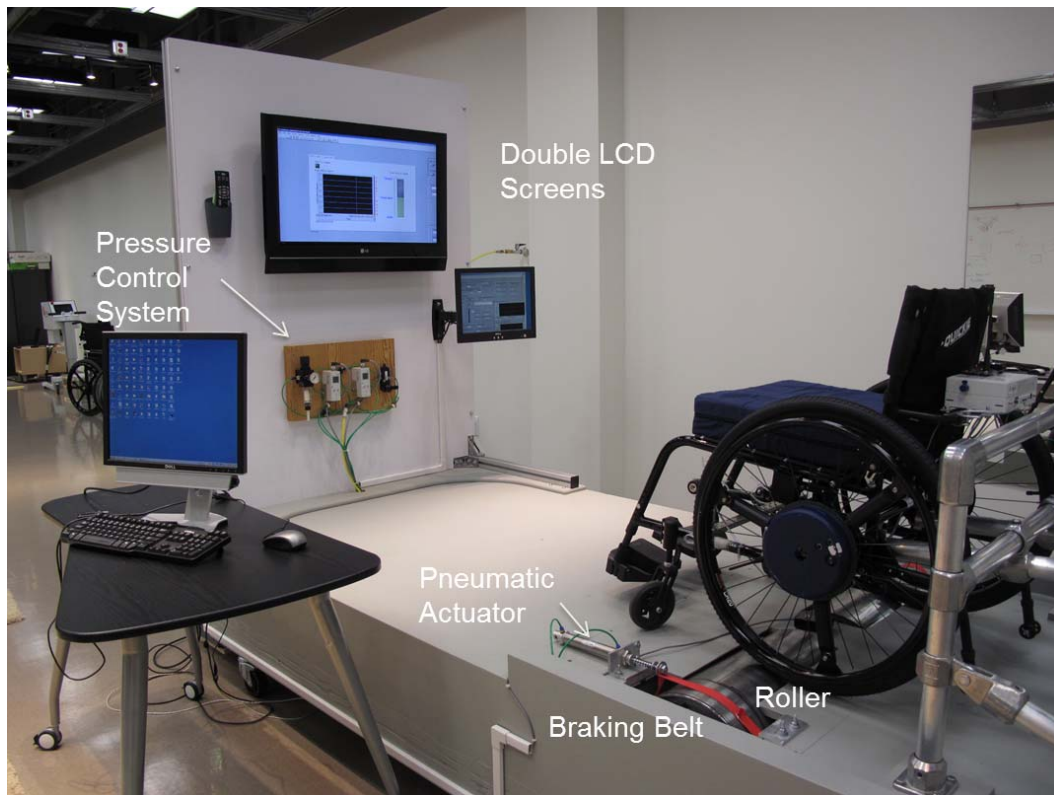


Figure 3- 8 The roller ergometer system.

A double-roller ergometer system (Figure 3-8) was constructed and incorporated with two rollers, a friction applying system, an analog-to-digital (A/D) converter (DT304, Data Translation Inc., Marlboro, MA, USA), a desktop (Dell) with Microsoft Windows XP system and a double liquid crystal display (LCD) screens. A wheelchair was settled on the ergometer, with its frame fixed to the metal bars behind. Once either of the wheelchair wheels moves, the associated

roller will move at the same time. As followed, Figure 3-9, is a schematic of the control and feedbacks in laboratory ergometer system.

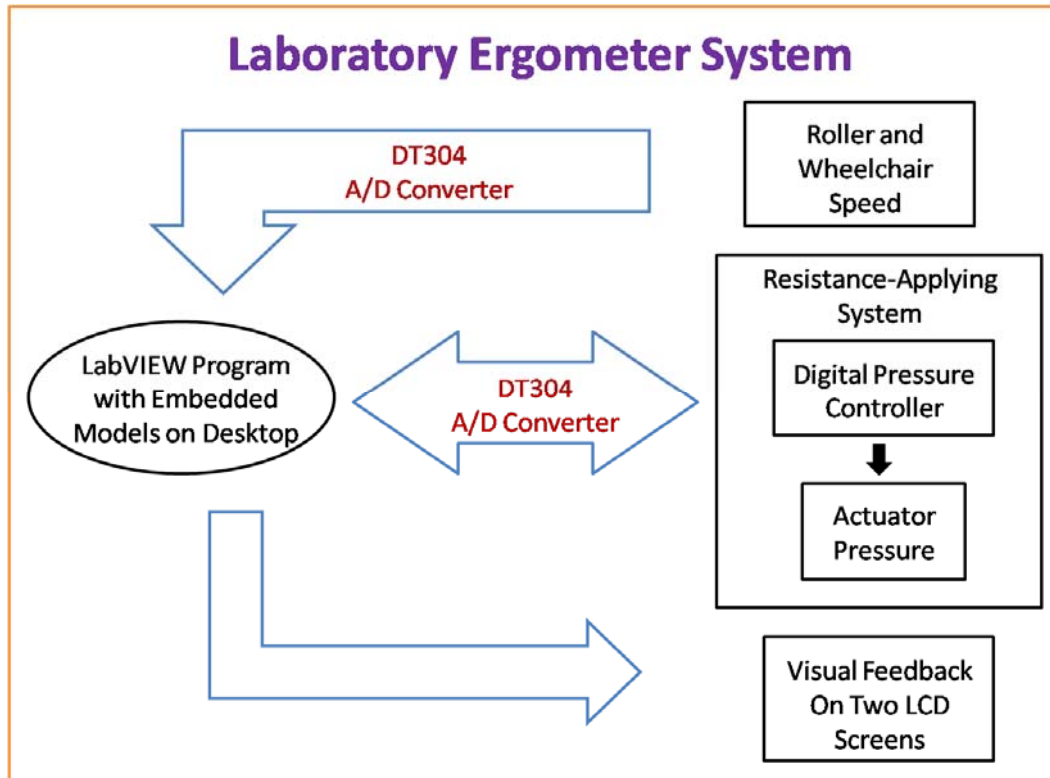


Figure 3- 9 Control and feedbacks of laboratory ergometer system

A friction-applying system was designed to act on both rollers (Figure 3-10), in order to simulate the rolling resistance of different surfaces. This system includes: a pressurized-air supply, a digital pressure controller (FESTO, Esslingen am Neckar, Germany) with a proportional valve – to regulate the pressure of air delivered to the pneumatic actuators and read the actual pressure inside both actuators, two double-acting pneumatic actuators (SMC Pneumatics, Oakville, ON, Canada), and two fabric straps – to apply friction on the surface of both rollers.

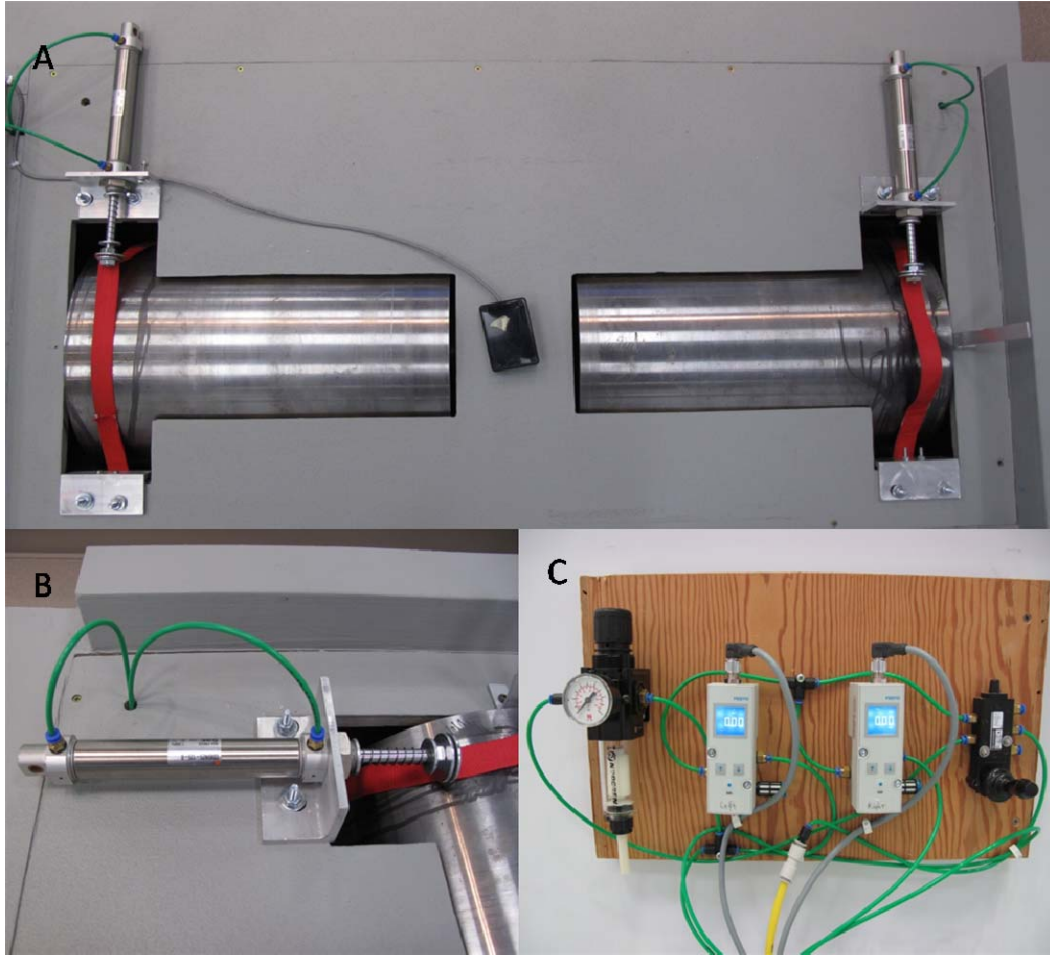


Figure 3- 10 (A) Friction applying system with two fabric straps; (B) two double-acting pneumatic actuators and (C) a digital pressure controller with a vault.

The pneumatic actuators applied an axial force to the straps which were designed to apply a varying friction force to the rollers.

A customized LabVIEW (Version 8.5, National Instrument Inc., US) program was designed to control the pressure value, read the actual pressure feedback, and measure the velocity of both rollers. In order to measure the speed of two rollers, two tachometers (Figure 3-11) were connected to the surface of both rollers as they rotate at the same linear speed of both rollers. The A/D converter was an interface between the hardware (e.g. digital pressure controller and tachometers) and LabVIEW program.

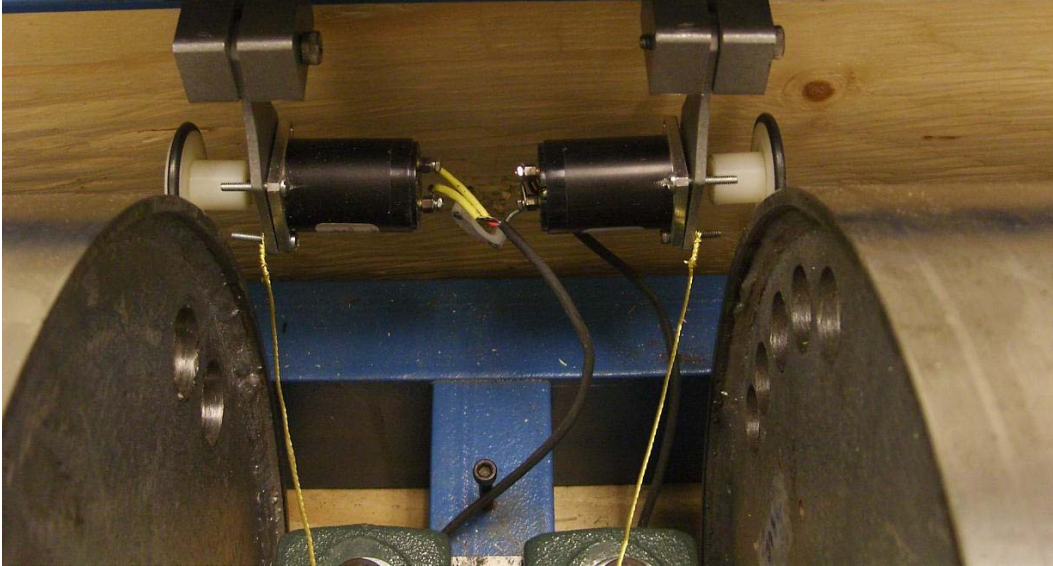


Figure 3- 11 Two tachometers were used to measure the speed of the two rollers

A calibration of the air pressure (units: bar) used by the actuators and the deceleration slope (α) of roller was conducted for both sides using roll-down test. The force applied to a strap can be represented by the amount of air pressure used to activate an actuator. The deceleration slope of the rollers determined the rolling resistance simulated by ergometer. A LabVIEW program was written for this test to change the air pressure values and to record the angular speed of both rollers with respect to time. Since the deceleration of the ergometer rollers was sensitive to the weight of a wheelchair participant, several participants with different weights were recruited to conduct the test. Deceleration data of both rollers with air pressure changing from 0 to 4 bar were collected. During the test, the wheelchair occupants accelerated both wheels to a self-selected speed and allowed both rollers to slow down naturally. It was found that when the actuators' air pressure increases, the deceleration slope (α) of both rollers increases and this linear relationship is sensitive to the weight of a wheelchair occupant. As a result, another calibration for every participant was completed during the experiment so

that the resistance and friction simulated by the ergometer were tailor-made for the participant's weight. It is likely that the α was sensitive to different participant weights because the bearings used for the rollers experienced higher friction under high loading. These calibration results and linear equations (two variables: both actuators' pressure and α of both rollers) associated with different weights are shown in the next chapter.

3.4.7 Ergometer simulation settings and visual feedback

The ergometer simulation system comprised the combination of both hardware and software. A LabVIEW software program (Figure 3-12) was written to dynamically control the friction applied to the rollers. A biomechanical model developed by several members of the laboratory team, including this author, is outlined in the next section. Several variables were used as input to the model, including weight of the participant, rollers' angular acceleration, and α values of both actual medium pile carpet and artificial turf surfaces. According to the aforementioned linear equations for actuator pressure and α of both rollers, the α of real-world surfaces and additional friction related to our model can be simulated by simply controlling the actuator air pressure using the LabVIEW program. Variables such as wheelchair wheels' speed and travelled distances were calculated using rollers' speed detected by two tachometers and used as feedback to the program, participant and researchers.

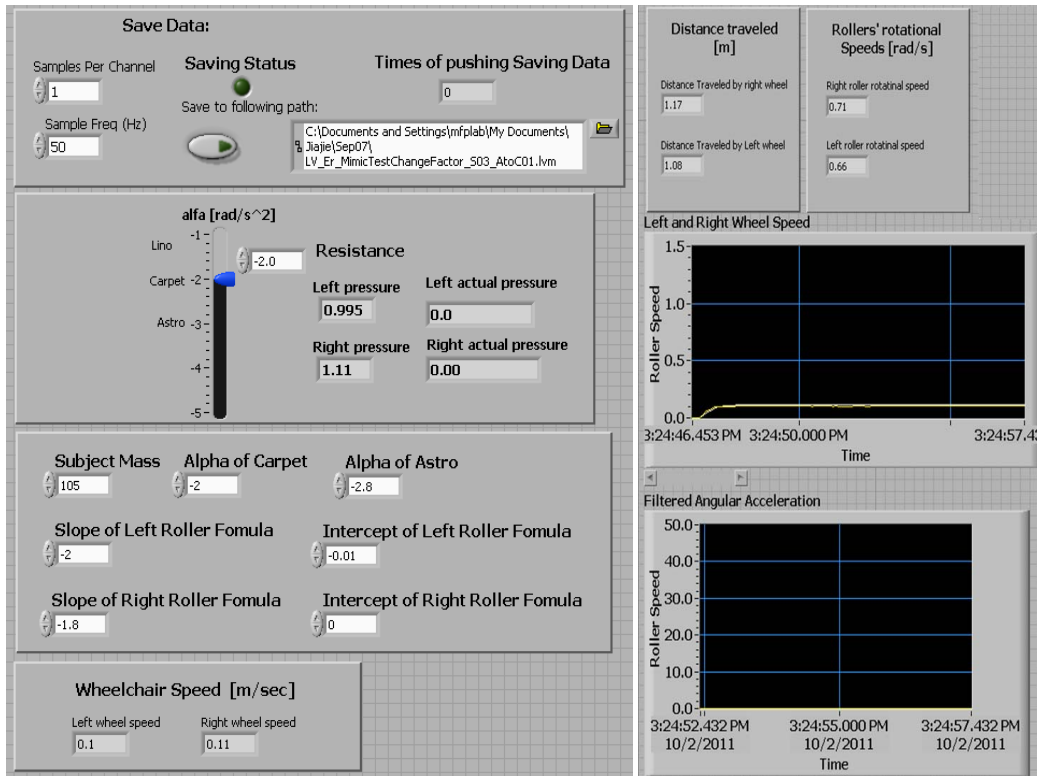


Figure 3- 12 LabVIEW program inputs and real time feedbacks of speed and travelled distance to the program and researchers.

Two LCD screens were placed in the front of the ergometer system to provide visual feedback (Figure 3-13) to wheelchair occupants to capture the feeling of pushing in the real-world situation. The displays showed both carpet and artificial turf surfaces and the transition in between. The visual feedback of surfaces sequence including from carpet to artificial turf and from artificial turf to carpet could be changed. A yellow color progressing bar indicated the distance travelled by the participant.



Figure 3- 13 Ergometer visual display of carpet and artificial turf compared to real-world.

To represent what subjects experienced in the real-world, resistance applied to the rollers was associated with visual feedback. If the test direction was from carpet to artificial turf, a primary α value of carpet was chosen for the participant from the result of roll-down test in real-world. When the participant pushed the test wheelchair on the ergometer, once the accumulated travelled distance reached a threshold value of 8 meters, the participant would cross the transition between carpet and artificial turf, experiencing a sudden change of α to artificial turf. The participant by watching the progressing bar from visual feedback could see when the destination had been reached. The settings would be similar for the opposite direction, from artificial turf to carpet.

3.5 Biomechanical model for propulsion

It is very important to understand the differences in the mechanics of motion for a wheelchair when it is free to move and inertial effects occur, compared to a wheelchair constrained on an ergometer, where there are no inertial effects other than the rotation of the wheels and the rollers. In the real-world, the wheelchair occupant has to generate propulsion forces that overcome rolling resistance of the surface and inertia associated with the mass of the user and wheelchair. Rolling resistance is relatively insensitive to the speed of propulsion. However the forces needed to overcome inertia are proportional to the acceleration of the wheelchair and its occupant. On a roller ergometer, the participant has to overcome the rotational inertia of two rollers and friction from bearings and the actuator system. “Static” mechanisms have been used to represent rolling resistance for typical propulsion surfaces on roller ergometers, but a method to simulate the inertial component has not been reported.

By dynamically adjusting resistance applied to the rollers, a laboratory ergometer can represent the inertial effects as well as the rolling resistance of a real-world task, at least for straight-line wheelchair propulsion. In the following biomechanics model, for simplification of the system, only half of the wheelchair and its rear wheels were considered. In the following section, a relationship is derived considering the dynamic behavior on the wheelchair in the real-world and lab ergometer environments. This relationship is defined as Model 1.

3.5.1 Model 1- consideration of wheelchair dynamics in the lab ergometer and real-world environments

When using the ergometer, a participant has to push the wheelchair on a stationary platform, and both rollers move at the same linear velocity as the wheelchair wheels. The roller is attached to a strap which offers resistance to its rotation, and this is controlled by how much pressure is applied by a pneumatic actuator. The goal is to find a formula for this actuator pressure so that the real-world surface can be simulated in the lab ergometer environment.

3.4.1.1 Dynamics of wheelchair on ergometer

The direction of motion of the wheel and the roller in the lab ergometer environment is shown in the Figure 3-14.

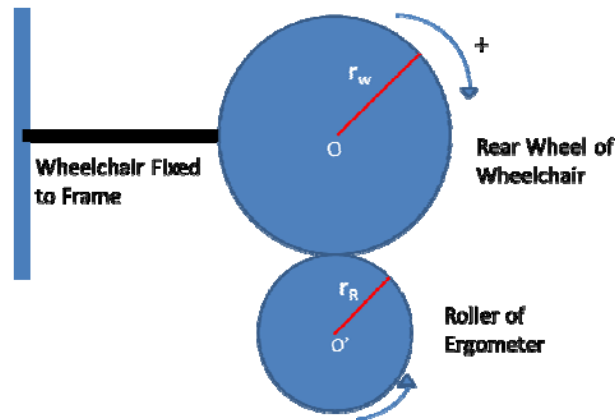


Figure 3- 14 Schematic of wheel and roller motion during wheelchair push in ergometer environment

The free body diagram of wheel and roller can be drawn separately as shown in the Figure 3-15.

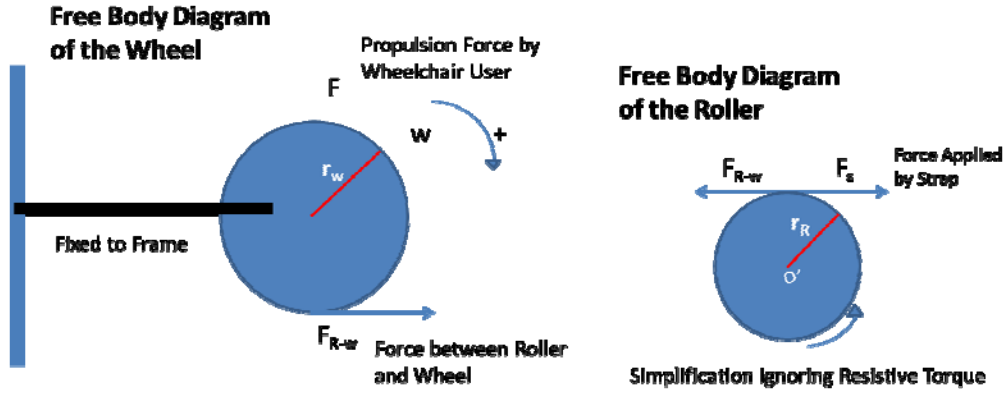


Figure 3- 15 Free body diagram of wheel and roller in ergometer environment.

The mass of the participant and wheelchair used in this study are constant and therefore the force associated with their weight will be canceled out by a reaction at the point of contact between the roller and the wheel, hence not included in the Figure 3-14. After balancing the torque in the clockwise and anticlockwise directions in Figure 3-14A and B respectively, we get:

$$(F - F_{R-W}) \times r_W = I_W \gamma_W \quad \text{Equation 3- 8}$$

$$(F_S - F_{R-W}) \times r_R = I_R \gamma_R \quad \text{Equation 3- 9}$$

In the above equations, F is the force applied to the hand rim of wheelchair by occupant, F_S is the force applied by strap, F_{R-W} is the force between roller and wheel, r_W and r_R are radius of wheel and the roller, I_W and I_R are the moment of inertia, γ_W and γ_R are the angular acceleration of the wheel and the roller.

From equation (Equation 3-8) and (Equation 3-9), we get,

$$F - F_S = \frac{I_W \gamma_W}{r_W} - \frac{I_R \gamma_R}{r_R} \quad \text{Equation 3- 10}$$

3.4.1.2 Dynamics of wheelchair on real-world surface

The direction of motion of the wheelchair wheels on the real-world environment is shown in the Figure 3-16.

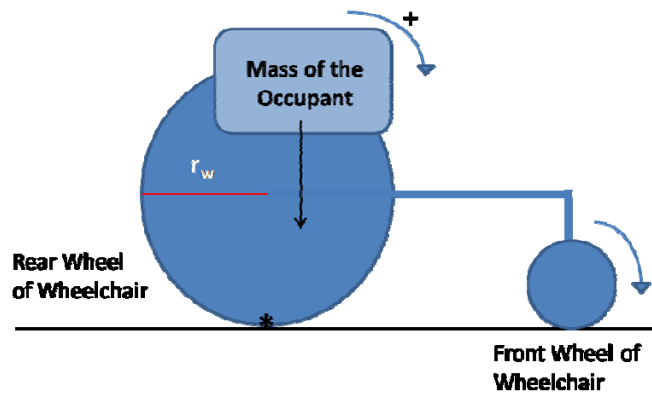


Figure 3- 16 A wheelchair on carpet.

The mass of the participant will be equally distributed on both sides of the wheelchair, and the loading on the castor wheels is neglected. Hence, for the free body diagram, half of the wheelchair and half of participant’s mass are considered.

Free Body Diagram of the Wheel on a Surface

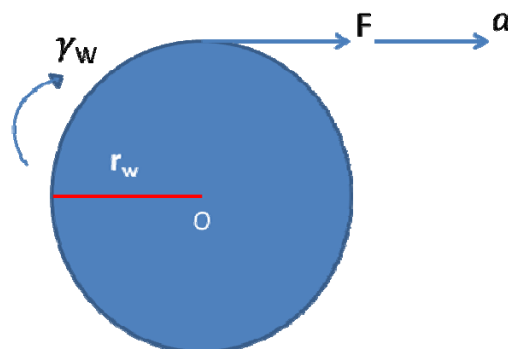


Figure 3- 17 Free body diagram of one wheel of wheelchair on a real-world environment surface.

From the free body diagram shown in Figure 3-17, after balancing the rotational and linear forces, we get:

$$F \cdot 2r_W - F_{axle} \cdot r_W = I_W \cdot \gamma_W \quad \text{Equation 3- 11}$$

$$(F_{axle} - F) = \frac{M}{2} \cdot \alpha \quad \text{Equation 3- 12}$$

In above equation F_{axle} is the force acting on the axle of the wheel, and α is due to the linear acceleration of the wheel.

It should be noted that linear acceleration of the roller and the wheel are the same, hence we can write that:

$$\alpha = r_W \cdot \gamma_W = r_R \cdot \gamma_R \quad \text{Equation 3- 13}$$

From equation (Equation 3-12) and (Equation 3-13) we get:

$$(F_{axle} - F) = \frac{M}{2} \cdot r_W \cdot \gamma_W \quad \text{Equation 3- 14}$$

From equation (Equation 3-11) and (Equation 3-14), we obtain:

$$F = \frac{I_W \gamma_W}{r_W} + \frac{M}{2} \cdot r_W \cdot \gamma_W$$

Equation 3- 15

The propulsion force F applied by the participant is the same for both real-world and ergometer situation. By putting the value of F from Equation 3-15 to Equation 3-10, we get:

$$F_S = \frac{I_R \gamma_R}{r_R} + \frac{M}{2} \cdot r_W \cdot \gamma_W$$

Equation 3- 16

Now in Equation 3-16, replacing $\gamma_W = \frac{r_R \cdot \gamma_R}{r_W}$ from Equation 3-13, we get:

$$\begin{aligned} F_S &= \frac{I_R \gamma_R}{r_R} + \frac{M}{2} \cdot r_R \cdot \gamma_R \\ &= \frac{\gamma_R}{r_R} \left[I_R + \frac{M}{2} \cdot r_R^2 \right] \end{aligned}$$

Equation 3- 17

Or, we can write,

$$F_S \cdot r_R = \gamma_R \left[I_R + \frac{M}{2} \cdot r_R^2 \right]$$

Equation 3- 18

In the above equation, $F_S \cdot r_R$ is the resistive torque applied to the roller by the strap, which can be measured at the moment of the wheelchair wheel starts

rotating. For different values of pressure (P) applied by the actuator, there will be the corresponding torque $F_S \cdot r_R$.

To determine it experimentally, we have measured values of $F_S \cdot r_R$ by using the Smart^{Wheel} as a torque transducer for different values of P . The scatter plot (see Figure Appendix 2-1) obtained was a good linear fit. In this way, $F_S \cdot r_R$ can be represented by a fitted line given by $k_1 \cdot P + k_2$, where k_1 is the slope of the line, k_2 is the Y-intercept which represents friction of the roller bearings (sensitive to user mass). If we assume (experiment bears this out) k_2 is relatively small, we can set it equal to 0. Therefore:

$$P = \frac{F_S \cdot r_R}{k_1} \quad \text{Equation 3- 19}$$

$$\therefore P = \frac{\gamma_R}{k_1} \left[I_R + \frac{M}{2} \cdot r_R^2 \right] \quad \text{Equation 3- 20}$$

In the above Equation 3-20, the ergometer setting of P is determined based on the roller angular acceleration γ_R , moment of inertia of the roller I_R , its radius r_R and mass of the wheelchair and its participant M . It is therefore possible to control the roller resistance in response to the instantaneous roller acceleration generated by the occupant so that the force that has to be generated is comparable to that in an unconstrained ‘real-world’ wheelchair. However, the “static” force

used to represent rolling resistance on typical propulsion surfaces has not been included in Equation 3-20.

For example, if a participant with a mass of 85kg pushes the test wheelchair (weight 20kg with both Smart^{Wheel}s attached) on the ergometer with the roller rotating at an angular acceleration of $0.3\text{rad}\cdot\text{s}^{-2}$. Inertia of a roller I_R is $0.66\text{kg}\cdot\text{m}^2$, and radius of a roller is 0.158m , the value of k_I is $1.746\text{N}\cdot\text{m}/\text{bar}$, the pressure used to simulate inertia would be 0.339 bars .

In section 3.4.5, rolling resistance is relatively insensitive to the speed of propulsion but is a function of the mass of the wheelchair and its occupant. By using a roll-down test, a deceleration slope (α) can be calculated and used to describe the rolling resistance of the surface for the wheelchair and occupant. The same deceleration slope can be represented on the ergometer by adjusting the actuator pressure. As a result, to represent the rolling resistance of a surface on the ergometer for a particular participant, a constant C_{RR} is used. The resistance for both rollers is therefore the combination of: roller inertia, the simulated inertia of the wheelchair occupant and wheelchair calculated in real time and known rolling resistances of a real-world scenario. It can be described using the following equation:

$$P = \frac{\gamma_R}{k_I} \left[I_R + \frac{M}{2} \cdot r_R^2 \right] + C_{RR} \quad \text{Equation 3- 21}$$

Equation 3-21 represents ‘Model 1’ in the current study.

Some technical difficulties were experienced due to delays in the response of the control system. By altering the value of k_1 for different participants it was possible to make sure through subjective feedback that the resistance on the ergometer felt similar to the real-world experience. To verify this, several participants were asked to experience both of the environments one after another. They pushed the wheelchair on the real-world surface first, and experienced the lab ergometer environment with parameter settings using Model 1 for each of the simulated surfaces.

In order to determine the value of C_{RR} , every participant conducted roll-down tests on both real-world surfaces and on ergometer, and the processing of this parameter is shown in Section 3.8.1.

Participants' feedback about the similarity between different real-world and simulated lab ergometer environments required a correction factor to be introduced for the model. This correction factor represents the intuitive change required in the model based on the response of the participants, and these changes are referred to as 'Model 2'.

3.4.2 Model 2- correction factor based model

It is found that artificial turf surface was well represented by the ergometer environment; however, when using a real-world carpet environment, participants experience much higher resistance in the corresponding ergometer environment. Only after reducing the actuator pressure applied to the strap in the lab ergometer, did all participants report an experience similar to the carpet environment. It was

observed that, for most of the participants, the reduction of pressure this change in k_1 produced is about one third of the pressure used to simulate the inertia calculated using Model 1. With the above variations, it is concluded that Model 1 needs modification to accommodate the real-world carpet environment in the lab roller ergometer condition. Hence, a modified model with a correction factor is used in Model 2 as given below:

$$P = q \cdot \frac{\gamma_R}{k_1} \left[I_R + \frac{M}{2} \cdot r_R^2 \right] + C_{RR} \quad \text{Equation 3- 22}$$

In Equation 3-22, q represents the correction factor introduced to adjust the Model 1, based on the feedback obtained from the participants. Here, $q=1/3$ in the case of carpet experiments performed on the ergometer, and $q=1$ in the case of artificial turf experiments performed on the ergometer. Further exploration of biomechanical mapping between the real-world and ergometer environments is not included in this study and remains a challenge for future. Nevertheless, since ‘Model 1’ works well with artificial turf conditions and with modification, ‘Model 2’ covers both types of real-world environment, we have investigated both of the models in details and found the consequences the probable variation.

3.6 Experimental protocol

All participants used the same test wheelchair. During the experiments, subjects were asked to sit on a lightweight rigid wheelchair (Quickie) with one Smart^{Wheel} attached to each side, Tachyon was attached to the back of the

wheelchair and the IMU (trunk motion sensor) to the chest of the subject. The real-world environment was set up in a hallway.

Each subject was asked to complete a wheelchair propulsion practice on a linoleum surface in a hallway for around 20mins before the experiments so that they were familiar with basic wheelchair pushing techniques. Long and smooth strokes which are an ideal way of pushing at self-selected speed on different surfaces were taught to the participants. They also practice wheelchair propulsion on the lab ergometer for about 5 minutes.

Stage One: Maximum Capacity Measurement

Each participant placed both of hands at the top center of each pushrim and pushed forward at his maximum effort while the test wheelchair was braked (Figure 3-18). Measurements of M_z were recorded and the maximal values were chose as the participants' maximum capacity.



Figure 3- 18 A participant sitting on a wheelchair with her hands placed at top center of push rim.

Stage Two: Roll Down Test on Carpet and Artificial Turf Surfaces

As the rolling resistance of real-world surfaces is sensitive to the weight of wheelchair participant, each participant was required to perform three roll-down tests on both surfaces. The average values of measurements for each surface of the individual were used as C_{RR} value for the ergometer simulated surface setting in the same participant experiment.

Stage Three: Performance on Real-World surfaces

A random sequence of starting tests in directions either from carpet to artificial turf or from artificial turf to carpet was established before the experiment. A total of six runs were conducted, three runs in each direction, as well a three-minute rest in between. Participants pushed the wheelchair in the

real-world environment which included a stretch of medium pile carpet with a sudden transition to a stretch of artificial turf. Participants pushed the test wheelchair at their self-selected speed once the researcher asked them to start. Data collected at this stage were for both hypothesis 1 and 2.

Stage Four: Calibration of Roller Ergometer

To determine the linear relationship between actuator pressure and roller deceleration slope (α) for both sides of the ergometer, participants repeated the roll-down test on the ergometer with six different levels of pressure applied by the actuators. The associated simulation for the α value of both real-world carpet and artificial turf can then be found by the linear relationship equation.

Stage Five: Performance on Roller Ergometer with Model 1 Setting

Participants repeated the tests on the ergometer at self-selected speed following the same test sequence in Stage Three. At this time, they were looking at the LCD screen for visual feedback. The resistance applied on the roller was determined from the previously described Model 1.

Stage Six: Performance on Roller Ergometer with Model 2 Setting

Participants repeated the test with resistance simulation according to Model 2 similar to Stage Five.

Data collected at both Stage Five and Six were for hypothesis 3.

3.7 Data Collection

Data of wheelchair propulsion performance including moment (M_z), push length, push frequency and velocity were collected using the Smart^{Wheel}. Parameters such as trunk motion angle ($\theta(t)$) and trunk angular velocity were collected by IMU – which is the trunk motion sensor of Tachyon. Both Smart^{Wheel} and IMU were working wirelessly to transmit data to their logging systems.

3.7.1 Synchronization

A pair of radio frequency (RF) modules (LINX Technology Inc., Merlin, OR, US) including a transmitter (model TXM-433-LR-S) and two receivers (model RXM-433-LR-S) were used to start and stop the data collection by Smart^{Wheel}, IMU and LabVIEW program at the same time. These RF modules communicate wirelessly at a frequency of 433Hz. One receiver was connected to the parallel port of a desktop computer and an analog input of the A/D converter. When a transistor-transistor logic (TTL) level voltage was sent through the parallel port, software Smart^{Wheel} 2008 and the LabVIEW program detected the signal and read it as a trigger to record data. Smart^{Wheel} and LabVIEW recorded data with a frequency of 240Hz and 40 Hz respectively. The other RF receiver was connected to Tachyon - the data logging system of IMU. IMU streamed data to Tachyon at a frequency of 50 Hz. The transmitter sends out signals to both receivers at the same time to start data recording in three systems and send out another signal to end it.

3.7.2 The Smart^{Wheel} Data

The hand rim propulsion data collected by the Smart^{Wheel} were both stored in a SD memory card and transmitted to a desktop wirelessly. Data for four parameters including moment M_z , speed, push length and push frequency were selected and analyzed using the Smart^{Wheel} Data Analyzer 1.6.0 (Three Rivers) and the MATLAB program. For example, Figure 3-19 showed the M_z value against time during one test on a real-world surface. Each spike represents the push phase of one push cycle, with the adjoining smooth part showing the recovery phase. It is thus possible to identify the beginning and end of each push. The peak value of each spike was recorded as one of our outcome measurement, peak M_z . Data of left and right wheel are similar, which is also close to the findings of previous studies [75, 107].

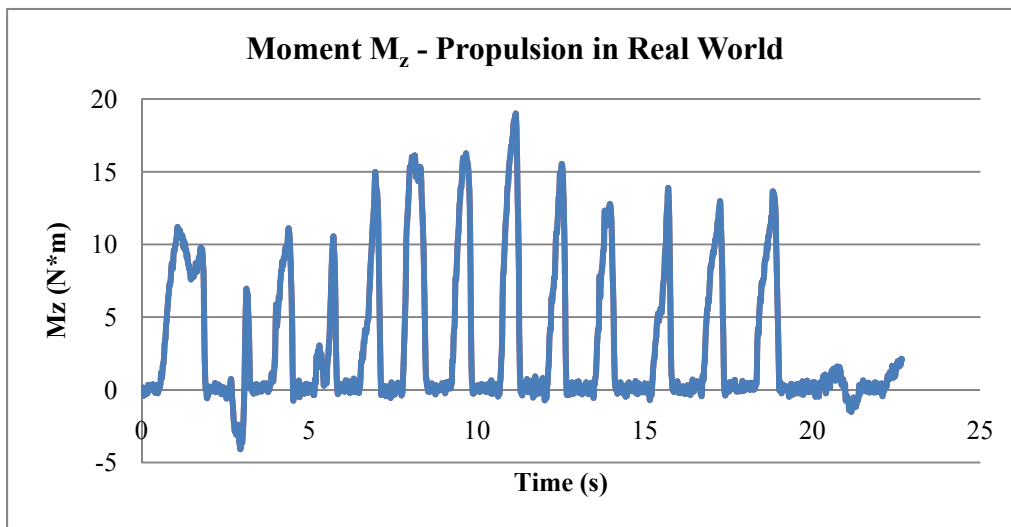


Figure 3- 19 Smart^{Wheel} data moment M_z during propulsion in real-world plotted against time.

3.7.3 The IMU Data

The trunk movement data collected by IMU were transmitted wirelessly to Tachyon and recorded in a SD memory card. Angular velocity in the anterior/posterior plane (Roll) was selected to represent the movement of the trunk during wheelchair propulsion. Figure 3-20 shows one example of the trunk angular velocity data and its noise was eliminated during data extraction for further processing.

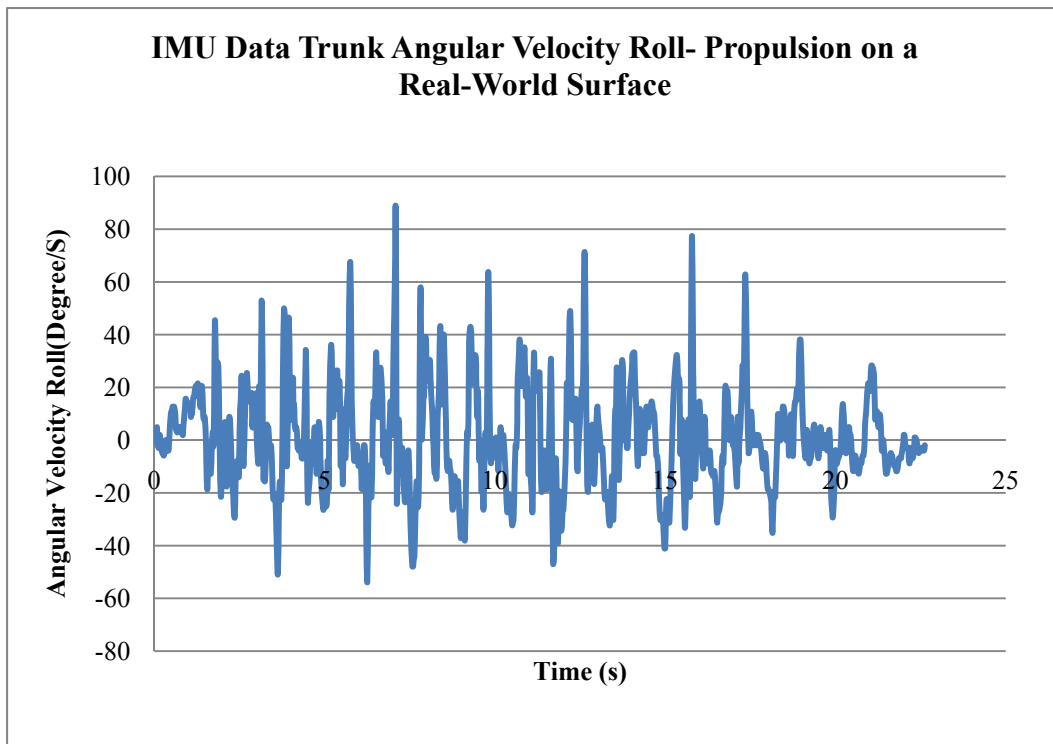


Figure 3- 20 IMU data angular velocity Roll during propulsion on a real-world surface plotted against time.

3.7.4 The LabVIEW program Data

Signals from the detector at the transition between the two surface types were recorded by a LabVIEW program and stored in EXCEL files. As is shown in Figure 3-7, when the test wheelchair crossed the transition, the front wheel and then the rear wheel blocked the light beam sent from the retro-reflective sensor, and so the duration of the transition was captured. As shown in Figure 3-21, the transition happens from the 12th to the 13th second.

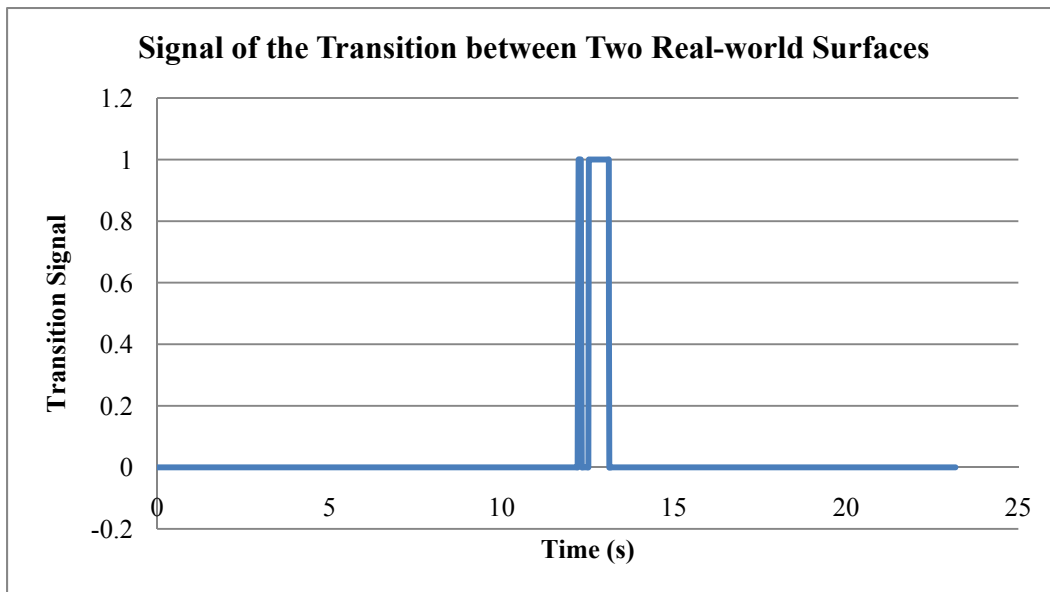


Figure 3- 21 Signal of the transition between two real-world surfaces.

3.8 Parameter extraction

Several MATLAB (MathWorks, Natick, MA, US) programs were written to extract key outcome measurements from data collected by Smart^{Wheel} and IMU, and α on real-world surfaces and on the ergometer.

3.8.1 Rolling resistance calculation

The rolling resistance of the real-world surfaces, carpet and artificial turf, were measured using the roll-down test and represented by the deceleration slope (α). The velocity of the wheelchair accelerating and decelerating during the roll-down test was recorded (Figure 3-22). The MATLAB program first extracted the part of data after the last push until velocity decreased to zero. Then the closest linear curve was found to fit these data and used to define the α value (Figure 3-23). An average value of deceleration of three roll-down tests on the surface was calculated and used as the α of the given surface, carpet or artificial turf.

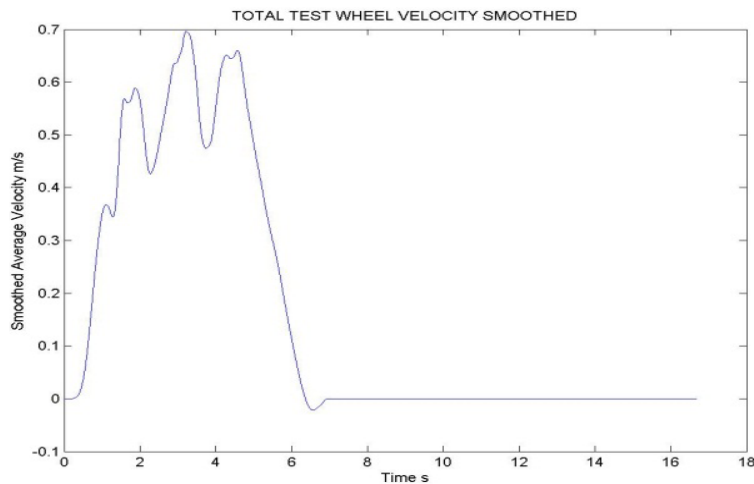


Figure 3- 22 Wheelchair velocity plotted against time in a real-world surface roll down test.

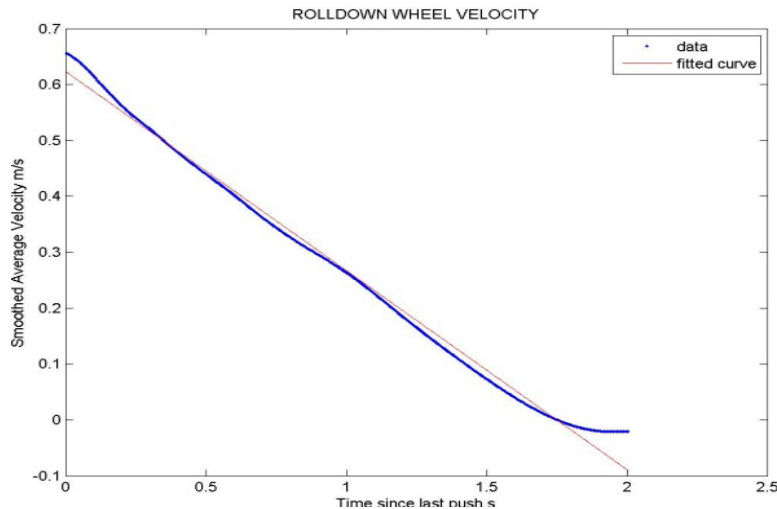


Figure 3- 23 Velocity deceleration slope after the last push plotted against time.

The roll-down test was repeated on both ergometer rollers with six different levels of pressure (from 0.5 to 2.5 bars) applied by actuators, and α were calculated in the same way as for the real-world surfaces. When the actuator increased the pressure of the strap, the roller decelerated with a steeper slope and this linear relationship was shown in section 4.1.3 of roller calibration. The closest linear curve for each roller was calculated using a MATLAB program (Figure 3-24). By using these two linear relations, the rolling resistance constant of a surface for each participant can be simulated by setting the actuator pressure to a certain value (Figure 3-25). This is the rolling resistance constant C_{RR} mentioned in the biomechanics model for simulating the deceleration slopes on carpet and artificial turf.

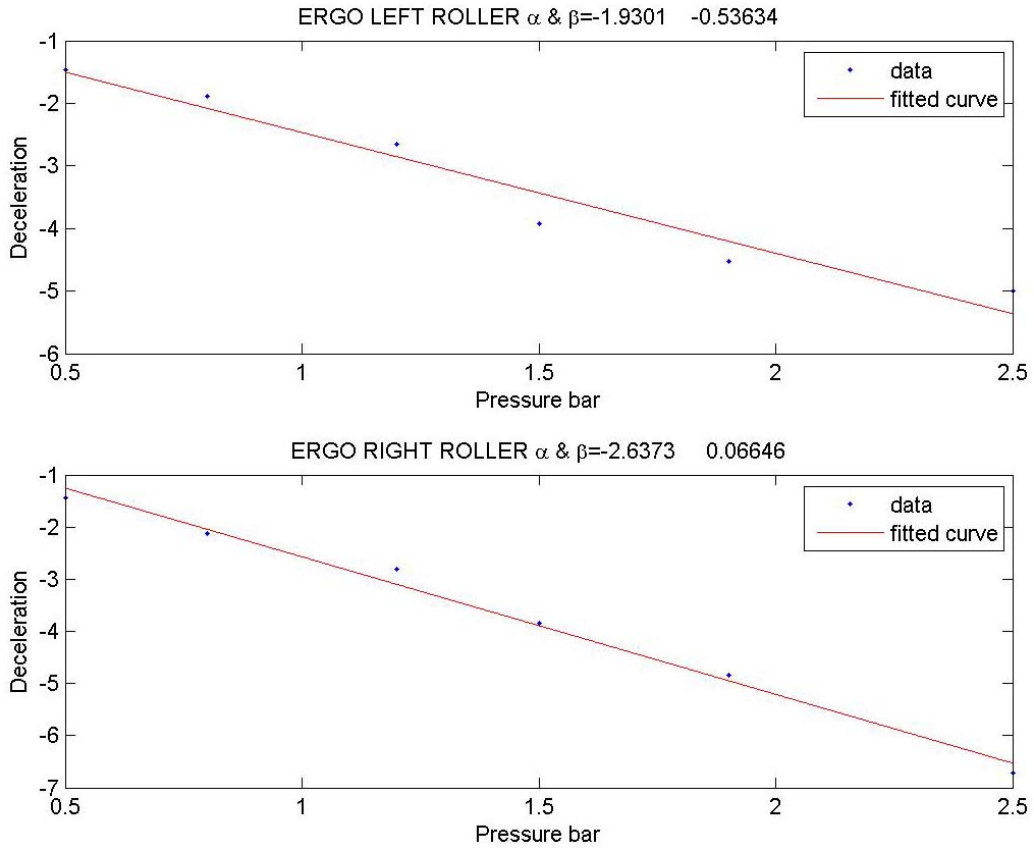


Figure 3- 24 Linear relationships of actuator pressure and roller deceleration slopes α for the left and for the right roller.

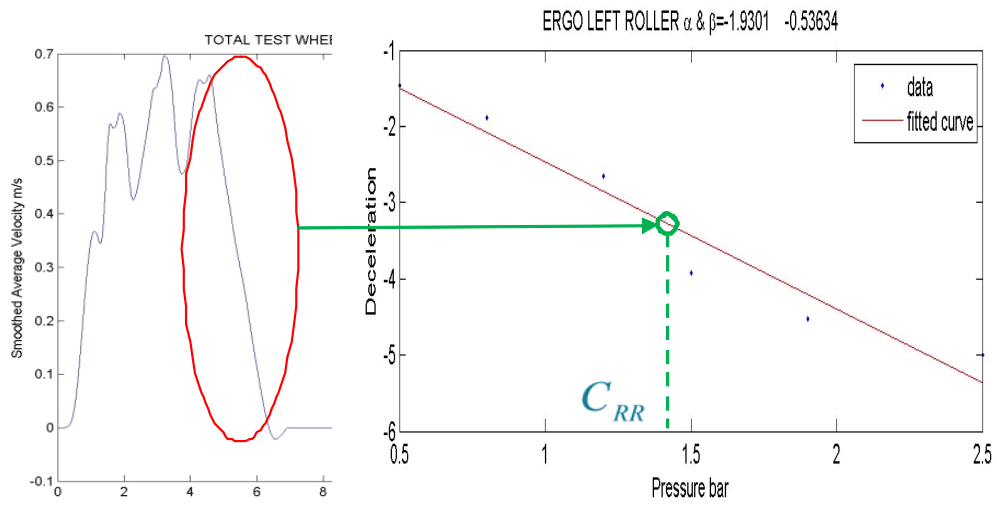


Figure 3- 25 Finding the pressure value C_{RR} to simulate real-world surface rolling resistance.

3.8.2 Smart^{Wheel}

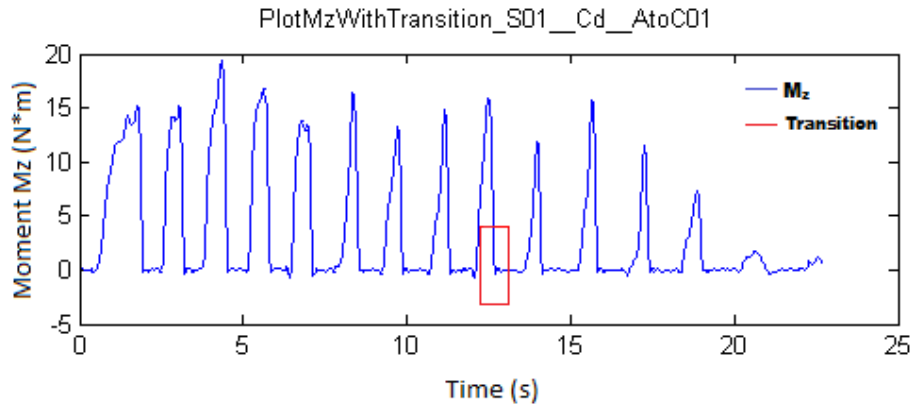


Figure 3- 26 Smart^{Wheel} M_z data with transition period plotted against time.

A MATLAB program used the data for M_z (Figure 3-26) to identify the beginning and end of each push as well as the total number of pushes. When the participant is contacting the hand rim of the wheel and pushing forward, M_z values will be higher than zero; when the participant's hands are recovering from propulsion and are away from the hand rims, M_z values will be close or equal to zero. During wheelchair propulsion on a given surface, pushes can be distinguished as different categories including start-up, steady-state, and the end (Figure 3-27). Start-up pushes refer to the first three pushes and the steady-state pushes are from the fourth push to the one before the end. Together with the information for the transition period, pushes in related categories were classified for further processing.

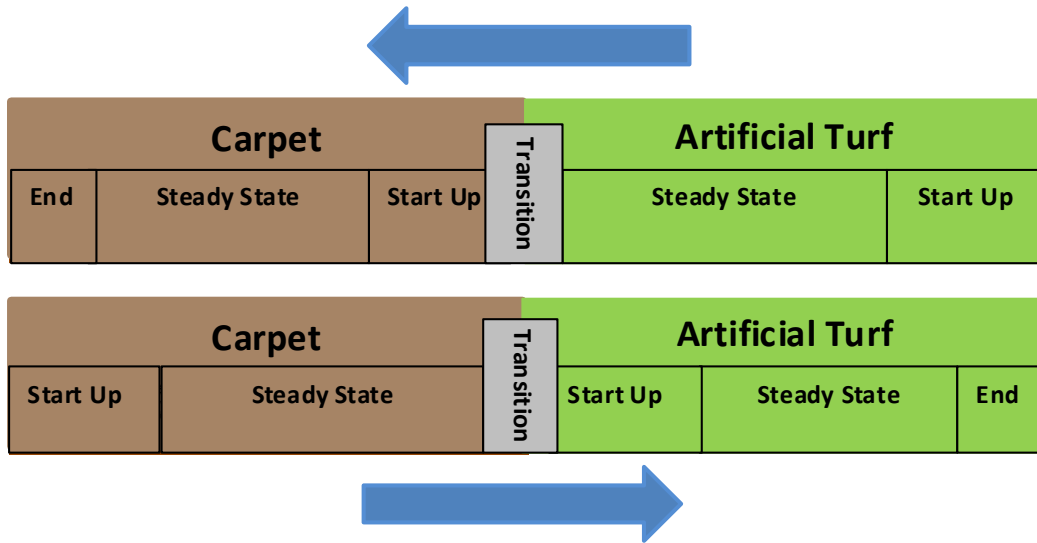


Figure 3- 27 Task directions from artificial turf to carpet or reversed.

In both the real-world and simulation environments, only the data during steady-state pushes on carpet and artificial turf surfaces and pushes at the transition were considered. The Smart^{Wheel} Data Analyzer 1.6.0 software was used to analyze and organize data for Peak M_z , Average Velocity, Push Length and Push Frequency for each push.

3.8.3 IMU

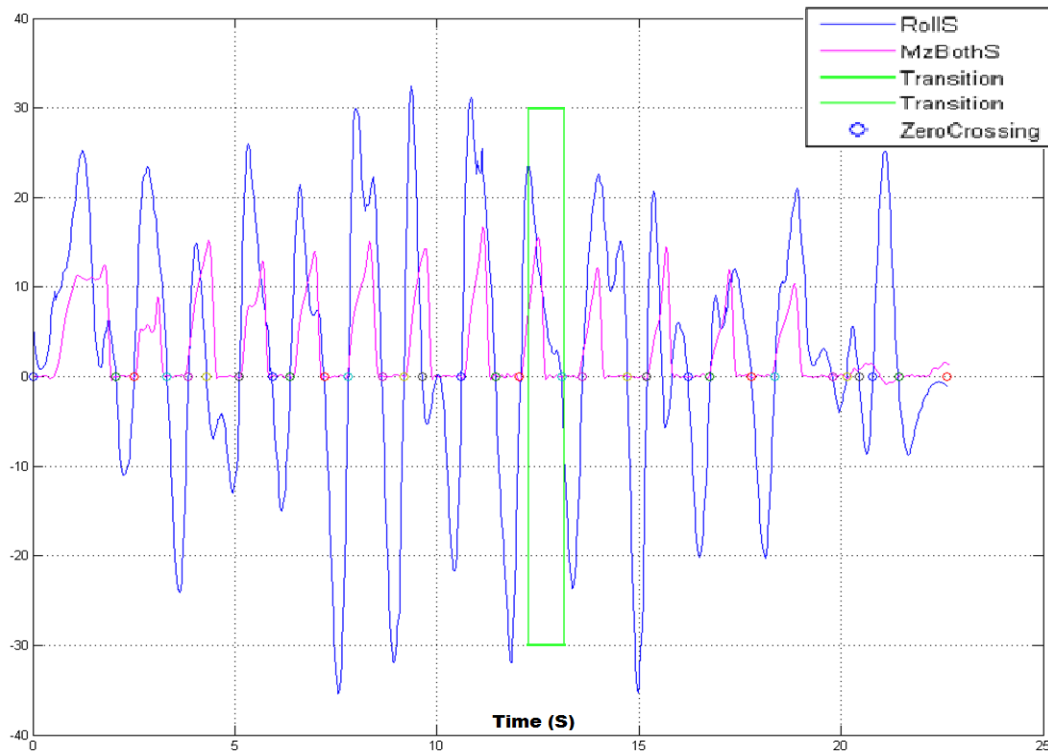


Figure 3- 28 Trunk angular velocity (degrees/s, blue line, RollS) after smoothing, propulsion moment Mz (N*m, magenta line, MzBothS) after smoothing and transition period (s, green line, Transition) plotted against time.

Figure 3-28 is a plot for the data of trunk angular velocity Roll collected by IMU and smoothed. Method of 'rloess' (local regression using weighted linear least squares and 2nd degree polynomial model; zero weight is assigned to data outside six mean absolute deviations) in MATLAB program and a moving window with an average of 50 points were used to smooth the data. A method was used to detect when the data crossed the zero amplitude axis. Each major zero crossing defines the start and end of a major trunk movement. When Roll values are positive, the trunk is moving forward, negative values show the trunk moving backward. If a participant pushes forward, the trunk starts to move and the Roll value crosses the zero axis. When the participant reaches the maximum forward position of the trunk, it stops, creating a zero angular velocity and its plot crosses

the zero amplitude axis and then the trunk in the opposite. The program first found the peaks of all major spikes, then traced to the closest zero crossing points and marked down the timestamps for the most forward and backward position of the trunk.

A simple integration of the angular velocity Roll with time was performed to estimate the angular displacement of the trunk. The angular displacements of the trunk moving forward and backward during the same push were equal. The program identified the positive Roll values as the trunk moving forward and integrated them with time. Hence, the measurement of the Trunk Angular Motion (Displacement) was used to describe the movement of trunk. The peak value of angular velocity during each push was recorded and used as another parameter. The trunk movement data were categorized into different push states just as the M_z data. Associated with the transition period timestamp, data of steady-state and transition were distinguished.

The following two parameters were used to describe trunk movement:

- Trunk Motion Angle $\theta(t)$: It is the range of trunk movement from back to front or vice versa during one push, units in degrees.
- Maximum Peak Trunk Angular Velocity $\dot{\theta}(t)$: Participant accelerates and decelerates trunk movement during one push. Peak velocity happens after acceleration but before slowing down. The maximum peak trunk angular

velocity is defined as the maximum value among these peak velocity of each push, units in degrees per second.

3.9 Statistical analysis

Excel (Microsoft, Redmond, WA, USA) and SPSS V19.0 (IBM, Armonk, NY, USA) were used to analyze the data. There were 23 participants completed both the real-world and the ergometer Model 1 test, 13 of them completed the ergometer Model 2 test. A paired t-test was used to determine whether there was a significant difference in propulsion and trunk movement on the two different real-world surfaces for hypothesis 1. Data of steady-state pushes on different surfaces were of main interest. Another paired t-test was used to determine whether there were any significant differences in propulsion and trunk movement at the transition in either direction in hypothesis 2. Data at transition propulsion between different surfaces was studied. Repeated measures Analysis of Variance (ANOVA) were performed to detect whether there were significant differences between performance on the two different real-world surfaces in both directions, between the real-world surface and ergometer Model 1, and between the real-world surface and ergometer Model 2. Eight performance parameters were tested with ANOVA separately and results are presented one by one.

Because multiple statistical comparisons were done on the same data pool in the analysis of both hypothesis 1 and three, a correction factor is given to the value of significance level. Therefore, according to the correction suggestion, dividing the significant level value by the numbers of hypotheses, the adjusted

significance value is 0.025 for both the first and the third hypothesis. In hypothesis 2, a set of data different from hypothesis 1 and three was used, therefore, the significance level value remains at 0.05.

There are three independent variables, namely Environment (2 levels: real-world surfaces and ergometer roller); Resistance or Surface (2 levels: medium pile carpet and artificial-turf surface); Direction (2 levels: from carpet to artificial turf or from artificial turf to carpet). In the analysis of performance on two actual surfaces, hypothesis 1, surface type was considered as an independent variable, see Table 3-1. The analysis of the transition between actual surfaces, hypothesis 2, direction was considered as an independent variable, see Table 3-2. Table 3-3 shows that two independent variables, environment and surface, in hypothesis 3, i.e. the comparison between real-world and laboratory environment.

Table 3- 1 One independent variable in hypothesis 1.

Independent Variable: Surface (or Resistance)	
On Artificial Turf	On Carpet

Table 3- 2 One independent variable in hypothesis 2.

Independent Variable: Direction	
From Artificial Turf to Carpet	From Carpet to Artificial Turf

Table 3- 3 Two independent variables in hypothesis 3.

		Independent Variable: Environment		
		Real-world	Ergometer Model 1	Ergometer Model 2
Independent Variable: Surface (or Resistance)	Artificial Turf			
	Carpet			

Smart^{Wheel} data for the left and right side were averaged. Since the trial order was randomized, it was assumed that there was no learning effect between trials. Smart^{Wheel} and trunk movement data for three repeated trials under the same experiment condition were averaged for statistics analysis.

Significance p value, r value, η^2 value and observed power in section 4.7 were calculated in SPSS analysis. The required number of subjects were found in table of sample size calculation with given power and significance level.

Chapter 4 Results

4.1 Calibration Results

Before the experiment, calibration of the inertial measurement unit (IMU) device, both ergometer rollers, deceleration and the deceleration of test wheelchair with the participant on two real-world surfaces were undertaken.

4.1.1 Inertial Measurement Unit (IMU)

The first part of the calibration was to validate the accelerometer readings (Accel). After collecting nine different angles (from -55 degrees to 40 degrees, with about 10 degrees interval of each), a linear regression of $y = 1.1x + 0.95$ between actual swing angle value $\theta(t)$ (read from XClinometer), as x , and $\theta(t)$ value calculated from Accel readings, as y , see in Figure 4-1.

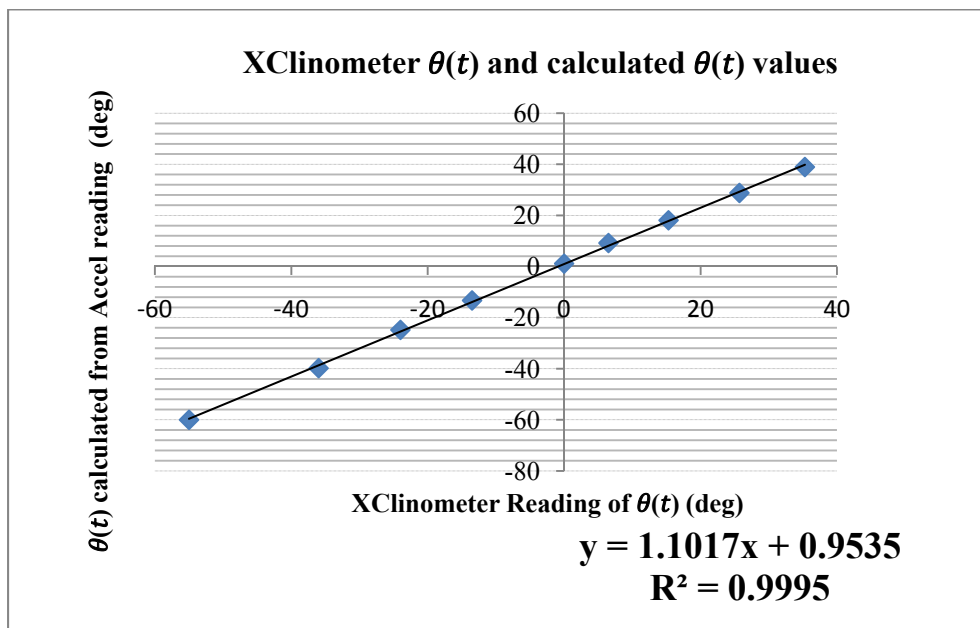


Figure 4- 1 Linear regression of $\theta(t)$ reading from XClinometer and $\theta(t)$ value calculated from Accel data.

The equation can be revised to

$$x = 0.91y - 0.87 \quad \text{Equation 4-1}$$

The Accel data of IMU was calibrated and the actual swing angle $\theta(t)$ can be calculated from the acceleration data by:

$$\theta(t) = 0.91 * \text{Tan}^{-1} \left(\frac{A_z(t)}{A_x(t)} \right) - 0.87 \quad \text{Equation 4-2}$$

The second part was to calibrate Gyro data with the Accel reading. A series of tests in which a participant pushed a wheelchair with IMU attached were conducted. Since one of the Gyro data $Roll(t)$ also describes the angular velocity around the Y -axis, $Roll(t)$ was compared to the angular velocity $\dot{\theta}(t)$ calculated from Accel data, as shown in Figure 4-2. There were differences of amplitude between $\dot{\theta}(t)$ and $Roll(t)$.

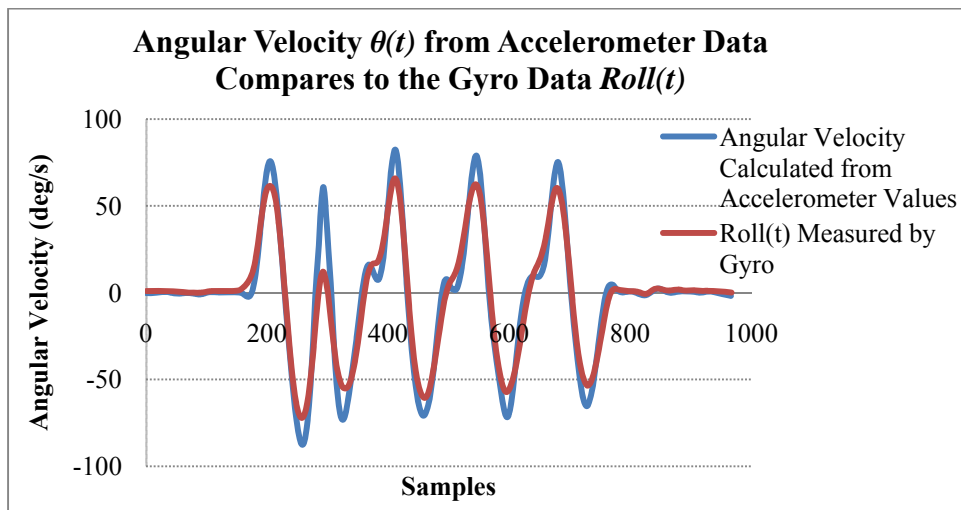


Figure 4-2 Angular velocity $\dot{\theta}(t)$ calculated from Accel data compares to the Gyro data $Roll(t)$.

After comparison of several test results, the angular velocity $\dot{\theta}(t)$ and $Roll(t)$ has a linear relationship of:

$$\dot{\theta}(t) = 1.25 * [Roll(t) + 2.71] \quad \text{Equation 4-3}$$

Hence, the data $Roll(t)$ of Gyro was calibrated.

4.1.2 Rolling resistance on real-world surfaces

Deceleration slope (α) of linear velocity of wheelchair wheel on a certain surface was used to describe the rolling resistance of the surface. In Appendix 2, α on artificial turf and carpet surfaces and weight of each participant are reported. No linear relation exists between the weight of the participant and the α of the surface (data distribution in Figure 4-3).

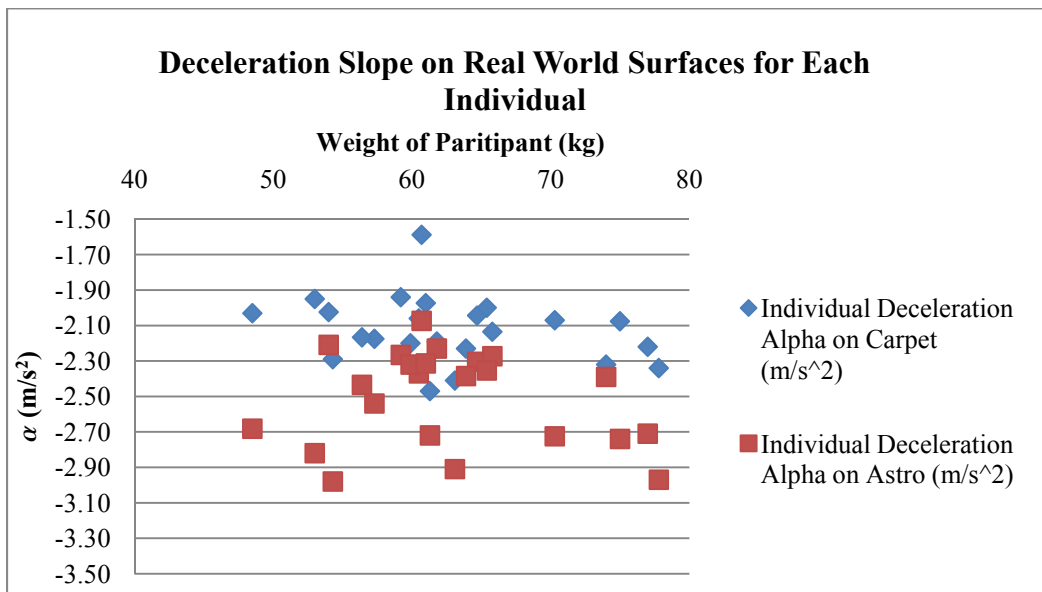


Figure 4-3 Deceleration α on real-world surface for each participant

4.1.3 Rolling resistance simulation in the Ergometer

Deceleration slope (α) of linear velocity of wheelchair wheel on ergometer roller was used to describe the simulated rolling resistance, while the linear velocity of the wheelchair wheel and ergometer roller are equal. Figure 4-4 shows the calibration results of the pressure applied by actuators and the α of both rollers. Three participants with different weights (60, 75 and 83kg) performed roll-down tests on the rollers as pressure increased from 0bar to 3.5bar with 0.5bar increments. It was found that the deceleration slopes (α) of both rollers with different friction applied by the straps are sensitive to the weight of the participant. As a result, a calibration of rollers test has to be performed by each participant in order to get the equation of the relationship, as shown in Appendix 2.

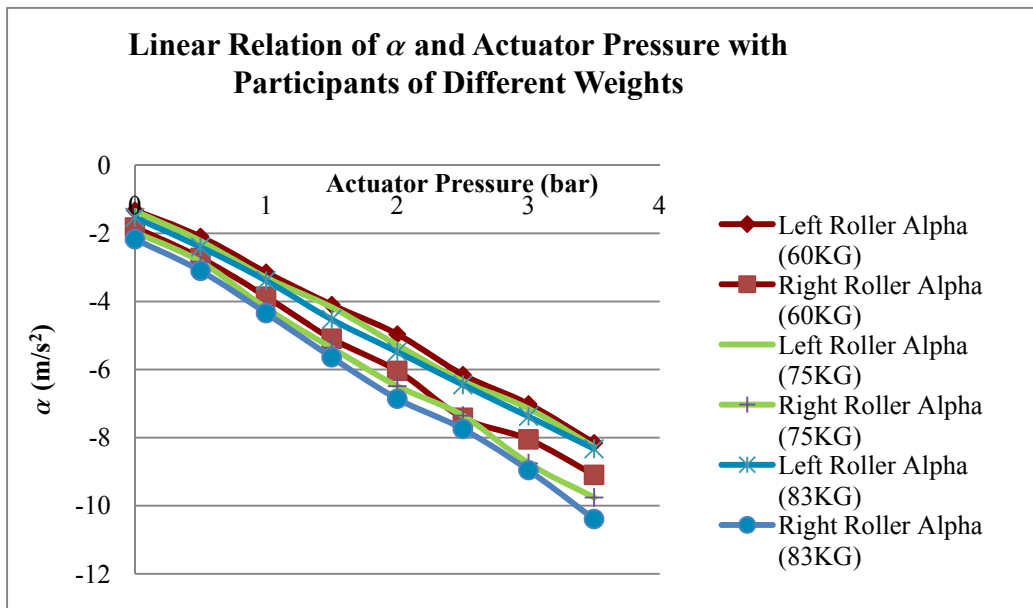


Figure 4- 4 Calibration of roller deceleration (linear relation of α and actuator pressure).

The weight sensitivity of the ergometer was considered and this information was included in the algorithm for inertia simulation and the actuator pressure control software program.

4.2 Participant characteristics

A total of 25 people participated in the study, however, two of them (Subject No. 17 and 19) felt fatigue during the experiments and withdrew from the study. In Table 4-1, 23 participants' characteristics are shown (13 males and 10 females with a mean age of 26 ± 4 , a mean body mass of 62.82 ± 7.80).

Table 4- 1 Physical characteristics of 23 participants. Data was reported as Mean \pm SD.

Subject No.	Gender	Age	Body Mass (kg)
1	F	26	54
2	M	26	77
3	M	30	64.7
4	M	26	74
5	F	28	53
6	M	26	57.3
7	F	24	61.3
8	M	24	54.3
9	F	23	60.5
10	M	22	77.8
11	F	26	56.4
12	M	26	70.3
13	F	20	59.2
14	M	27	75
15	M	24	59.9
16	M	30	61.8
18	M	40	63.1
20	F	31	60.7
21	F	22	48.5
22	M	26	63.9
23	F	24	65.8
24	M	25	61
25	F	24	65.4
Mean \pm SD	N/A	26 ± 4	62.82 ± 7.80

All 23 participants accomplished the first two experiments including wheelchair propulsion on the real-world surfaces, and on ergometer Model 1. However, a subset of the whole group including 12 subjects finished the experiments on ergometer Model 2. As a result, the sample size was $n=23$ in hypothesis 1, two and the first part of hypothesis 3; $n=12$ in part two of hypothesis 3.

4.3 Hypothesis 1

H_0 : In a real-world environment, there is no significant difference in the biomechanics of wheelchair propulsion and trunk motion of able-bodied subjects at a self-selected speed between two surfaces with different resistance.

Paired t-test was used to test the hypothesis and a significant level of 0.025) was used. The value of r shown in this table was used for power calculation, in table 4-11. The results are shown in Table 4-2.

Table 4- 2 Descriptive output and paired t-test results comparing two surfaces in real-world.

Surface	Artificial turf	Carpet	Paired T-test Comparisons		
			Parameter	Mean ± SD	Mean ± SD
Peak M_z ($N \cdot m$)	14.97±3.00	13.07±2.81	7.631	0.000	0.85
Peak Total Force (N)	68.39±14.35	59.33±11.80	7.110	0.000	0.83
Push Length (deg)	69.39±8.82	69.53±9.74	-0.195	0.847	0.04
Push Frequency (s^{-1})	0.86±0.13	0.84±0.15	2.224	0.037	0.43
Average Speed ($m \cdot s^{-1}$)	0.76±0.14	0.83±0.17	-7.062	0.000	0.83
Trunk Motion Angle (deg)	8.74±4.67	8.62±3.80	0.261	0.796	0.06
Max. Peak Trunk Angular Velocity ($deg \cdot s^{-1}$)	33.98±13.34	32.24±12.04	1.288	0.211	0.26

NOTE. n=23 and $df=22$.

+ Significant difference between comparison ($p \leq 0.025$).

- No significant difference.

It can be seen in Table 4-2 that, on average, participants applied significantly higher (14%) peak value of M_z and total force to both rims of the test wheelchair on artificial turf than on carpet. They pushed faster on the carpet than on artificial turf with a significant (8%) difference. Push frequency on trunk angular velocity were slightly higher on artificial turf than on carpet. Participants pushed with similar push length and trunk motion angle on both surfaces.

4.4 Hypothesis 2

H_0 : In a real-world environment, the biomechanics of wheelchair propulsion and trunk motion of able-bodied subjects' do not change significantly when the direction of transition between two different surfaces at a self-selected speed is reversed.

Paired t-test was used to test the hypothesis. In hypothesis 2, data at transition propulsion between different surfaces was studied. Since this is a different set of data compared with hypothesis 1 and 3, therefore, the significance level value remains at 0.05. The value of r shown in this table was used for power calculation, in table 4-11. The results are provided in Table 4-3.

Table 4- 3 Descriptive output and paired t-test results comparing transition of two directions in real-world.

Transition	Artificial turf to Carpet	Carpet to Artificial turf	Paired T-test Comparisons		
			t	p	r
Parameter	Mean \pm SD	Mean \pm SD			
Peak M_z ($N \cdot m$)	14.28 \pm 3.20	15.45 \pm 3.16	-2.966	0.007	0.53
Peak Total Force (N)	63.70 \pm 12.88	68.21 \pm 14.53	-2.531	0.019	0.47
Push Length (deg)	71.94 \pm 10.63	72.47 \pm 10.49	-0.365	0.718	0.08
Push Frequency (s^{-1})	0.86 \pm 0.15	0.88 \pm 0.14	-1.444	0.163	0.29
Average Speed ($m \cdot s^{-1}$)	0.85 \pm 0.16	0.79 \pm 0.16	7.137	0.000	0.84
Trunk Motion Angle (deg)	8.67 \pm 5.66	9.35 \pm 5.37	-0.809	0.427	0.12

NOTE. $n=23$ and $df=22$.

r value is effect size.

+ Significant difference between comparison ($p \leq 0.05$).

- No significant difference.

It is apparent from Table 4-3 that participants in the real-world applied significantly (8%) lower peak value of M_z and significantly (7%) lower peak total force to both rims of the test wheelchair at significantly (7%) higher speed on transition from artificial turf to carpet (“A to C”) than on transition from carpet to artificial turf (“C to A”). Participants used higher total force, longer push length and greater trunk movement at the transition from C to A, but the difference is not

significant. It was found that almost the same push frequency was applied at transitions in both directions.

4.5 Hypothesis 3

H_0 : The biomechanics of wheelchair propulsion and trunk motion of able-bodied subjects at a self-selected speed show no significant difference between a real-world environment and the corresponding laboratory ergometer environment, regardless of the type of surface.

In hypothesis 3, data during steady-state propulsion on different surfaces were used. There are two settings for the simulated ergometer: Model 1 and Model 2 and their results were compared to real-world environment respectively. ANOVA was used for data analysis. Eight performance parameters were tested with ANOVA separately and results are presented one by one. Significance level value is 0.025 due to correction for family wise error.

4.5.1 Peak M_z

The mean and standard deviation of peak M_z for all treatment conditions are shown in Table 4-4. The two factor ANOVA analysis for comparison between real-world and ergometer Model 1 showed a significant main effect for environment, $F(1,22) = 35.21, p < 0.001, r = 0.78$; a significant main effect for surface, $F(1,22) = 64.35, p < 0.001, r = 0.78$; and a significant interaction between environment and surface, $F(1,22) = 10.87, p = 0.003, r = 0.58$. An interaction plot is shown in Appendix 3.

For the comparison between real-world and ergometer Model 2, the two factor ANOVA showed a significant main effect for environment, $F(1,11) = 13.06, p = 0.004, r = 0.74$; a significant main effect for surface, $F(1,11) = 55.01, p < 0.001, r = 0.91$; and no significant interaction between environment and surface, $F(1,11) = 2.79, p > 0.0125, r = 0.45$.

Table 4- 4 Descriptive output and pairwise comparison of peak M_z for each treatment condition in real-world and ergometer simulation environment (Model 1 and 2).

Peak M_z ($N \cdot m$)		Independent Variable: Environment			Comparison Between Two Environments on the Same Surface	
		Real-world (a) Mean(SD)	Ergometer Model 1(b) Mean(SD)	Ergometer Model 2(c) Mean(SD)	Mean Difference (a-b)	Mean Difference (a-c)
Independent Variable: Surface	Artificial Turf (d) Mean(SD)	14.97(3.00)	17.81(3.85)	19.09(4.7)	-2.84 (+) 17.3%	-3.15 (+) 18.0%
	Carpet (e) Mean(SD)	13.07(2.81)	16.89(4.18)	15.93(4.34)	-3.82 (+) 25.5%	-1.95 (-)
Comparison Between Two Surfaces in the Same Environment	Mean Difference (d-e)	1.90 (+) 13.6%	0.92 (+) 5.3%	3.16 (+) 18%		

NOTE. n=23 for real-world (a) and ergometer Model 1(b); n=12 for ergometer Model 2(c).

+ Significant difference within a comparison ($p \leq 0.025$).

- No significant difference.

Details of pairwise comparisons between treatment conditions are also provided. Participants applied 14% higher peak M_z on artificial turf than on carpet in real-world environment. A substantially noticeable difference of 5% between simulated artificial surface and simulated carpet exists in ergometer Model 1. There is a 17% difference between real-world artificial turf and ergometer Model 1 simulated artificial turf, and a 26% difference between real-world carpet and ergometer Model 1 simulated carpet.

A substantially noticeable difference of 18% between simulated artificial surface and simulated carpet exists in Model 2. There is a 18% difference between real-world artificial turf and Model 2 simulated artificial turf, and no significant difference between real-world carpet and ergometer Model 2 simulated carpet is spotted.

4.5.2 Peak total force

The mean and standard deviation of peak total force for all treatment conditions are shown in Table 4-5. The two factor ANOVA for comparison between real-world and ergometer Model 1 showed a significant main effect for environment, $F(1,22) = 15.20, p = 0.001, r = 0.64$; a significant main effect for surface, $F(1,22) = 47.50, p < 0.001, r = 0.83$; and a significant interaction between environment and surface, $F(1,22) = 18.40, p < 0.001, r = 0.67$. An interaction plot is shown in Appendix 3.

For the comparison between real-world and ergometer Model 2, the two factor ANOVA showed no significant main effect for environment, $F(1,11) = 4.92, p > 0.0125, r = 0.56$; a significant main effect for surface, $F(1,11) = 49.94, p < 0.001, r = 0.91$; and no significant interaction between environment and surface, $F(1,11) = 0.95, p > 0.0125, r = 0.28$.

Table 4- 5 Descriptive output and pairwise comparison of peak total force for each treatment condition in real-world and ergometer (Model 1 and 2).

Peak Total Force (<i>N</i>)		Independent Variable: Environment			Comparison Between Two Environments on the Same Surface	
		Real-world (a) Mean(SD)	Ergometer Model 1(b) Mean(SD)	Ergometer Model 2(c) Mean(SD)	Mean Difference (a-b)	Mean Difference (a-c)
Independent Variable: Surface	Artificial Turf (d) Mean(SD)	68.39(14.35)	76.68(16.44)	81.32(22.84)	-8.29 (+) 11.4%	-11.11 (-)
	Carpet (e) Mean(SD)	59.33(11.80)	73.52(17.37)	69.95(21.6)	-14.19 (+) 21.4%	-8.51 (-)
Comparison Between Two Surfaces in the Same Environment	Mean Difference (d-e)	9.06 (+) 14.2%	3.16 (+) 4.2%	11.38 (+) 15%		

NOTE. n=23 for real-world (a) and ergometer Model 1(b); n=12 for ergometer Model 2(c).

+ Significant difference within a comparison ($p \leq 0.025$).

- No significant difference.

Details of pairwise comparisons between treatment conditions are also provided. Participants applied 14% higher peak total force on artificial turf than on carpet in real-world environment. A substantially noticeable difference of 4% between simulated artificial turf surface and simulated carpet exists in ergometer Model 1. There is a 11% difference between real-world artificial turf and Model 1 simulated artificial turf; and a 21% difference between real-world carpet and ergometer Model 1 simulated carpet and.

A substantially noticeable difference of 15% between simulated artificial turf surface and simulated carpet exists in Model 2. The ergometer simulation in Model 2 is similar to real-world for both artificial turf and carpet surfaces.

4.5.3 Push Length

The mean and standard deviation of push length for all treatment conditions are shown in Table 4-6. The two factor ANOVA for comparison between real-world and ergometer Model 1 showed no significant main effect for environment, $F(1,22) = 7.31, p = 0.0129, r = 0.50$; no significant main effect for surface, $F(1,22) = 0.00, p > 0.0125, r = 0.00$; and no significant interaction between environment and surface, $F(1,22) = 0.12, p > 0.0125, r = 0.07$.

For comparison between real-world and ergometer Model 2, the two factor ANOVA showed no significant main effect for environment, $F(1,11) = 0.35, p > 0.0125, r = 0.18$; no significant main effect for surface, $F(1,11) = 2.61, p > 0.0125, r = 0.44$; and no significant interaction between environment and surface, $F(1,11) = 2.85, p > 0.0125, r = 0.45$.

Table 4- 6 Descriptive output and pairwise comparison of push length for each treatment condition in real-world and ergometer (Model 1 and 2).

Push Length (deg)		Independent Variable: Environment			Comparison Between Two Environments on the Same Surface	
		Real-world (a) Mean(SD)	Ergometer Model 1(b) Mean(SD)	Ergometer Model 2(c) Mean(SD)	Mean Difference (a-b)	Mean Difference (a-c)
Independent Variable: Surface	Artificial Turf (d) Mean(SD)	69.39(8.82)	72.62(11.03)	68.85(13.43)	-3.23 (-)	-2.67 (-)
	Carpet (e) Mean(SD)	69.53(9.74)	72.47(10.84)	66.31(11.55)	-2.94 (+) 4.1%	0.32 (-)
Comparison Between Two Surfaces in the Same Environment	Mean Difference (d-e)	-0.14 (-)	0.15 (-)	2.54 (-)		

NOTE. n=23 for real-world (a) and ergometer Model 1(b); n=12 for ergometer Model 2(c).

+ Significant difference within a comparison ($p \leq 0.025$).

- No significant difference.

In pairwise comparisons between real-world carpet and Model 1 simulated carpet, participants applied 4% bigger push length on ergometer environment.

4.5.4 Push Frequency

The mean and standard deviation of push frequency for all treatment conditions are shown in Table 4-7. The two factor ANOVA showed a significant main effect for environment, $F(1,22) = 16.15$, $p = 0.001$, $r = 0.65$; no significant main effect for surface, $F(1,22) = 3.40$, $p > 0.0125$, $r = 0.37$; and no significant interaction between environment and surface, $F(1,22) = 5.37$, $p > 0.0125$, $r = 0.44$ for the comparison between real-world and ergometer Model 1. The two factor ANOVA comparison between real-world and ergometer Model 2 showed a significant main effect for environment, $F(1,11) = 11.54$, $p = 0.006$, $r = 0.72$; no significant main effect for surface, $F(1,11) = 0.87$, $p > 0.0125$, $r = 0.27$; and no

significant interaction between environment and surface, $F(1,11) = 5.17$, $p > 0.0125$, $r = 0.57$.

Table 4- 7 Descriptive output and pairwise comparison of push frequency for each treatment condition in real-world and ergometer (Model 1 and 2).

Push Frequency (s^{-1})		Independent Variable: Environment			Comparison Between Two Environments on the Same Surface	
		Real-world (a) Mean(SD)	Ergometer Model 1(b) Mean(SD)	Ergometer Model 2(c) Mean(SD)	Mean Difference (a-b)	Mean Differenc e (a-c)
Independent Variable: Surface	Artificial Turf (d) Mean(SD)	0.86(0.13)	0.74(0.16)	0.77(0.14)	0.12 (+) 15%	0.15 (+) 17.9%
	Carpet (e) Mean(SD)	0.84 (0.15)	0.74 (0.17)	0.80 (0.15)	0.10 (+) 12.7%	0.10 (-)
Comparison Between Two Surfaces in the Same Environment	Mean Difference (d-e)	0.02 (-)	0.00 (-)	-0.03 (+) 3.8%		

NOTE. n=23 for real-world (a) and ergometer Model 1(b); n=12 for ergometer Model 2(c).

+ Significant difference within a comparison ($p \leq 0.025$).

- No significant difference.

Details of pairwise comparison between treatment conditions are also provided. There is a 15% difference between real-world artificial turf and Model 1 simulated artificial turf, and a 13% difference between real-world carpet and ergometer Model 1 simulated carpet in terms of the push frequency participants used. An 18% difference between real-world artificial turf and Model 2 simulated artificial turf is observed.

4.5.5 Average Speed

The mean and standard deviation of average speed for all treatment conditions are shown in Table 4-8. The two factor ANOVA showed a significant main effect for environment, $F(1,22) = 49.93, p < 0.001, r = 0.83$; a significant main effect for surface, $F(1,22) = 57.83, p < 0.001, r = 0.85$; and a significant interaction between environment and surface, $F(1,22) = 13.37, p = 0.001, r = 0.61$ for the comparison between real-world and ergometer Model 1. An interaction plot is shown in Appendix 3.

The two factor ANOVA showed a significant main effect for environment, $F(1,11) = 13.95, p = 0.003, r = 0.75$; a significant main effect for surface, $F(1,11) = 28.61, p < 0.001, r = 0.85$; and no significant interaction between environment and surface, $F(1,11) = 6.01, p = 0.03 > 0.0125, r = 0.59$ for comparison between real-world and ergometer Model 2.

Table 4- 8 Descriptive output and pairwise comparison of average speed for each treatment condition in real-world and ergometer (Model 1 and 2).

Average Speed ($m \cdot s^{-1}$)		Independent Variable: Environment			Comparison Between Two Environments on the Same Surface	
		Real-world (a) Mean(SD)	Ergometer Model 1(b) Mean(SD)	Ergometer Model 2(c) Mean(SD)	Mean Difference (a-b)	Mean Difference (a-c)
Independent Variable: Surface	Artificial Turf (d) Mean(SD)	0.76(0.14)	0.60(0.14)	0.60(0.19)	0.16 (+) 23.5%	0.18 (+) 26.1%
	Carpet (e) Mean(SD)	0.83(0.17)	0.63(0.16)	0.73(0.23)	0.20 (+) 27.4%	0.13 (+) 16.5%
Comparison Between Two Surfaces in the Same Environment	Mean Difference (d-e)	-0.07 (+) 8.9%	-0.03 (+) 4.9%	-0.13 (+) 19.7%		

NOTE. n=23 for real-world (a) and ergometer Model 1(b); n=12 for ergometer Model 2(c).

+ Significant difference within a comparison ($p \leq 0.025$).

- No significant difference.

Details of pairwise comparison between treatment conditions are as follows. Participants pushed 9% slower on artificial turf than on carpet in real-world environment. A substantially noticeable difference of 5% between Model 1 simulated artificial turf surface and simulated carpet exists. The speed on real-world artificial turf is 24% faster than on Model 1 simulated artificial turf, and is 27% faster on real-world carpet than on ergometer Model 1 simulated carpet.

Participants pushed 26% slower on Model 2 simulated artificial turf than on artificial turf in real-world environment, and 16% slower on Model 2 simulated carpet than real-world carpet. The speed on real-world artificial turf is 10% faster than on Model 2 simulated artificial turf, and is 20% faster on real-world carpet than on ergometer Model 2 simulated carpet.

4.5.6 Trunk Motion Angle

The mean and standard deviation of trunk motion angle for all treatment conditions are shown in Table 4-9. Details of pairwise comparisons between treatment conditions are also provided. The two factor ANOVA showed no significant main effect for environment, $F(1,22) = 2.30$, $p > 0.0125$, $r = 0.31$; no significant main effect for surface, $F(1,22) = 0.25$, $p > 0.0125$, $r = 0.11$; and no significant interaction between environment and surface, $F(1,22) = 0.067$, $p > 0.0125$, $r = 0.06$ for comparison between real-world and ergometer Model 1.

Table 4- 9 Descriptive output and pairwise comparison of trunk motion angle for each treatment condition in real-world and ergometer (Model 1 and 2).

Trunk Motion Angle (deg)		Independent Variable: Environment			Comparison Between Two Environments on the Same Surface	
		Real-world (a) Mean(SD)	Ergometer Model 1(b) Mean(SD)	Ergometer Model 2(c) Mean(SD)	Mean Difference (a-b)	Mean Difference (a-c)
Independent Variable: Surface	Artificial Turf (d) Mean(SD)	8.74(4.67)	10.72(7.47)	9.05(7.37)	-1.98 (-)	-0.61 (-)
	Carpet (e) Mean(SD)	8.62(3.80)	10.49 7.94)	7.12(5.12)	-1.87 (-)	0.84 (-)
Comparison Between Two Surfaces in the Same Environment	Mean Difference (d-e)	0.12 (-)	0.23 (-)	1.93 (-)		

NOTE. n=23 for real-world (a) and ergometer Model 1(b); n=12 for ergometer Model 2(c).

+ Significant difference within a comparison ($p \leq 0.025$).

- No significant difference.

The two factor ANOVA showed no significant main effect for environment, $F(1,10) = 0.02$, $p > 0.0125$, $r = 0.04$; no significant main effect for surface, $F(1,10) = 2.44$, $p > 0.0125$, $r = 0.44$; and no significant interaction between environment and surface, $F(1,10) = 8.98$, $p = 0.0128 > 0.0125$, $r = 0.69$ for comparison between real-world and ergometer Model 2. An interaction effect between environment and surface was significant and an interaction plot is provided in Appendix 3.

4.5.7 Maximum Peak Trunk Angular Velocity

The mean and standard deviation of maximum peak trunk angular velocity for all treatment conditions are shown in Table 4-10. Details of pairwise comparisons between treatment conditions are also provided. The two factor ANOVA showed no significant main effect for environment, $F(1,22) = 0.46$, $p > 0.0125$, $r = 0.14$; no significant main effect for surface, $F(1,22) = 2.71$, $p >$

0.0125, $r = 0.33$; and no significant interaction between environment and surface, $F(1,22) = 0.26$, $p > 0.0125$, $r = 0.11$ for comparison between real-world and ergometer Model 1.

For comparison between real-world and ergometer Model 2, the two factor ANOVA showed no significant main effect for environment, $F(1,10) = 3.40$, $p > 0.0125$, $r = 0.50$; a significant main effect for surface, $F(1,10) = 11.80$, $p = 0.006$, $r = 0.74$; and no significant interaction between environment and surface, $F(1,10) = 4.19$, $p > 0.0125$, $r = 0.54$.

Table 4- 10 Descriptive output and pairwise comparison of maximum peak trunk angular velocity for each treatment condition in real-world and ergometer (Model 1 and 2).

Maximum Peak Trunk Angular Velocity (deg. s ⁻¹)		Independent Variable: Environment			Comparison Between Two Environments on the Same Surface	
		Real-world (a) Mean(SD)	Ergometer Model 1(b) Mean(SD)	Ergometer Model 2(c) Mean(SD)	Mean Difference (a-b)	Mean Difference (a-c)
Independent Variable: Surface	Artificial Turf (d) Mean(SD)	33.98(13.34)	35.58(14.63)	33.50(15.00)	-1.60 (-)	0.71 (-)
	Carpet (e) Mean(SD)	32.24(12.04)	34.58(13.74)	25.13(8.63)	-2.34 (-)	0.13 (-)
Comparison Between Two Surfaces in the Same Environment	Mean Difference (d-e)	1.74 (-)	1.00 (-)	8.37 (+) (28.5%)		

NOTE. n=23 for real-world (a) and ergometer Model 1(b); n=12 for ergometer Model 2(c).

+ Significant difference within a comparison ($p \leq 0.025$).

- No significant difference.

4.7 Power Analysis

The Cohen's d value that is used to measure effect size for t tests and the partial eta squared η^2 that is used for ANOVA are both described as measuring a percentage of variance (standard deviation) [113]. Their evaluations are described in Table 4-11. The anticipated effect size and power for the study was one standard deviation and 90% respectively.

Table 4- 11 Evaluating effect size with Cohen's d and partial eta squared η^2 [113]

Magnitude of d or η^2	Mean Difference of Standard Deviation	Evaluation of Effect Size
d or $\eta^2 = 0.2$	0.2	Small effect
d or $\eta^2 = 0.5$	0.5	Medium effect
d or $\eta^2 = 0.8$	0.8	Large effect

In Table 4-11[113], the effect size and power for each performance parameter is calculated for both hypothesis 1 and 2. When there is no significant difference in a particular parameter comparison, an indication of number of participants that would have to be studied to adequately power (90%) a study is show.

Table 4- 11 Paired t test power analysis for hypothesis 1 and 2.

Parameters	Hypothesis 1: Real-world Surfaces			Hypothesis 2: Real-world Transitions		
	Estimated <i>d</i>	Observed Power	Significance or required number for participant	Estimate <i>d</i>	Observed Power	Significance or required number for participant
Peak Mz (<i>N · m</i>)	2.28	1.00	+	1.28	0.97	+
Peak Total Force (<i>N</i>)	2.42	1.00	+	1.15	0.88	+
Push Length (deg)	0.05	< 0.06	2102	0.18	0.09	526
Push Frequency (<i>s</i> ⁻¹)	0.50	0.33	85	0.48	0.33	85
Average Speed (<i>m · s</i> ⁻¹)	1.58	1.00	+	1.31	0.98	+
Trunk Motion Angle (deg)	0.10	0.06	2102	0.43	0.27	132
Maximum Peak Trunk Angular Velocity (deg · <i>s</i> ⁻¹)	0.48	0.33	85	NA	NA	NA

NOTE.

+ Significant difference within a comparison ($p \leq 0.025$ for hypothesis 1 and $p \leq 0.05$ for hypothesis 2).

Required number of participants is calculated according to a power of 90%, and two-tailed 0.05 because there was not enough sample size (23) in current study to show significant difference.

Results shown that participants pushed faster and applied less peak total force and peak M_z on carpet than on artificial turf in real-world. Absolute differences in self-selected average speed on two surfaces is 0.07m/s, equivalent to relative changes of 8% and Cohen' d effect sizes of 1.58 (Table 4-12). For peak M_z and peak total force, the absolute differences on two surfaces were 1.9 $N \cdot m$ and 9.06 N and Cohen' d effect sizes of 2.28 and 2.24 respectively, equivalent to relative changes of 14% for both.

Although the difference in push frequency and maximum peak trunk angular velocity on two surfaces were not found to be statistically significant, based on the significant p value (0.0125), their effect size were medium (Cohen' d value 0.50 and 0.48 respectively). The comparison of push length employed on the carpet and the artificial turf resulted in a p value of 0.037 and for maximum peak trunk angular velocity p value is 0.211, respectively. As power analysis suggests (Table 4-12), it might be possible to detect the difference between them with a larger sample size of 85. Then, we would be able to check whether the participants pushed more frequently and moved their trunk faster on rougher surfaces. The push length on both surfaces were similar.

Participants pushed faster and applied less peak M_z on the transition from high resistance surface to low resistance surface. Absolute difference in self-selected average velocity on the two different transitions is 0.06m/s, equivalent to relative changes of 7% and Cohen' d effect sizes of 1.31 (Table 4-12). For peak M_z the absolute differences on the two different surfaces were 1.17 $N \cdot m$, Cohen' d effect sizes of 1.28, equivalent to relative changes of 8%. Our results show when transitioning a wheelchair across different surfaces we found decreased velocity coupled with an increased peak M_z .

The comparison of peak total force on two transitions resulted in a p value of 0.019, which is slightly larger than our significance level 0.0125. The absolute differences on two transitions is 4.51N, Cohen' d effect sizes 1.15, equivalent to relative changes of 7%. It is likely participants pushed with less peak total force for transitions from high resistance surface to low resistance surface.

The effect size for peak total force was high, with a Cohen' d value of 1.15. The push frequency and trunk motions were medium (Cohen' d value: 0.48 and 0.43 respectively). The comparison of peak total force employed on transitions of different directions resulted in a p value of 0.019 and for push frequency and trunk motion angle, p value are 0.163, 0.427, respectively.

Table 4-13 and Table 4-14 shows the effect size and observed power for both environment and surface and the interaction between these two independent variables for hypothesis 3 Model 1 and Model 2 respectively. The significance of environment main effect is listed based on the interest of this study. A required sample size for 90% power is calculated if the main effect of environment is not significant.

Table 4- 12 ANOVA power analysis for hypothesis 3 (ergometer Model 1).

Parameters	Effect Size Estimation	Hypothesis 3: Part One Real-world and Ergometer Model 1			Significance of main effect from Environment or required number for participant
		Interaction	Main Effect		
		Environment * Surface	Environment	Surface	
Peak Mz ($N \cdot m$)	Eta Squared η^2	0.33	0.62	0.75	#
	Observed Power	0.88	1.00	1.00	
Peak Total Force (N)	Eta Squared η^2	0.45	0.38	0.67	#
	Observed Power	0.98	0.94	1.00	
Push Length (deg)	Eta Squared η^2	0.01	0.25	0.00	#
	Observed Power	0.06	0.73	0.05	
Push Frequency (s^{-1})	Eta Squared η^2	0.20	0.42	0.13	#
	Observed Power	0.60	0.97	0.42	
Average Speed ($m \cdot s^{-1}$)	Eta Squared η^2	0.38	0.69	0.72	#
	Observed Power	0.94	1.00	1.00	
Trunk Motion Angle (deg)	Eta Squared η^2	0.00	0.10	0.01	526
	Observed Power	0.06	0.31	0.08	
Maximum Peak Trunk Angular Velocity ($deg \cdot s^{-1}$)	Eta Squared η^2	0.01	0.02	0.11	2102
	Observed Power	0.08	0.10	0.35	

NOTE.

Significant main effect of environment ($p \leq 0.025$).

Required number of participants is calculated according to a power of 90%, because there was not enough participants (23) in this study to show significant main effect of environment.

Table 4- 13 ANOVA power analysis for hypothesis 3 (ergometer Model 2).

Parameters	Effect Size Estimation	Hypothesis 3: Part Two Real-world and Ergometer Model 2			Significance of main effect from Environment or required number for participant
		Interaction	Main Effect		
		Environment * Surface	Environment	Surface	
Peak Mz ($N \cdot m$)	Eta Squared η^2	0.20	0.54	0.83	#
	Observed Power	0.33	0.91	1.00	
Peak Total Force (N)	Eta Squared η^2	0.08	0.31	0.82	59
	Observed Power	0.15	0.53	1.00	
Push Length (deg)	Eta Squared η^2	0.21	0.03	0.19	2102
	Observed Power	0.34	0.08	0.32	
Push Frequency (s^{-1})	Eta Squared η^2	0.32	0.51	0.07	#
	Observed Power	0.55	0.87	0.14	
Average Speed ($m \cdot s^{-1}$)	Eta Squared η^2	0.35	0.56	0.72	#
	Observed Power	0.61	0.92	1.00	
Trunk Motion Angle (deg)	Eta Squared η^2	0.47	0.00	0.20	2102
	Observed Power	0.77	0.05	0.29	
Maximum Peak Trunk Angular Velocity ($deg \cdot s^{-1}$)	Eta Squared η^2	0.30	0.25	0.54	85
	Observed Power	0.46	0.39	0.87	

NOTE.

Significant main effect of environment ($p \leq 0.025$).

Required number of participants is calculated according to a power of 90%, because that there was enough participants (12) in this study to show significant main effect of environment.

Environment type has a substantial impact on peak M_z , peak total force, push frequency and average self-selected speed, with partial eta squared η^2 effect size of 0.62, 0.38, 0.42 and 0.69 respectively (Table 4-13) in the comparison between real-world and ergometer Model 1. When we compared real-world with ergometer Model 1, we found participants applied less peak total force and peak M_z and they pushed faster and more frequently.

Comparisons of real-world with ergometer Model 2 showed that the environment has a significant main effect on peak M_z , push frequency and average self-selected speed, with partial eta squared η^2 effect size of 0.54, 0.51 and 0.56 respectively (Table 4-14). Less peak M_z , faster average self-selected speed and more frequent strokes were applied in the real-world versus the ergometer Model 2.

Chapter 5 Discussion

5.1 Propulsion kinetics and trunk biomechanics on two surfaces of different rolling resistance existing in a real-world environment

The results for the first hypothesis are shown in Table 4-2. One of the findings is that the rolling resistance of the surface substantially affects peak M_z , peak total force and influences average self-selected speed. The higher the rolling resistance of the surface, the higher is the peak total force and peak M_z , and the lower is the wheelchair speed. This corresponds with the findings of Cowan et al. [23] who conducted a similar study with a population of minimal wheelchair experience, in their case older adults.

In the study of Koontz et al. [20], no differences in peak velocity or peak force on tile versus low-pile carpet versus high-pile carpet were reported for start-up pushes. The differences in their findings compared to those of our study might be attributed to the different populations of manual wheelchair users (SCI and able-bodied), and the fact that Koontz et al. measured start-up pushes rather than the steady-state pushes in the study reported here. The significant variations, particularly in the start-up pushes, may be attributable to the participants' style or level of "aggression" in pushing the wheelchair.

The type of surface less affects parameters like maximum peak trunk angular velocity, the trunk motion angle and the push length. These variables may be more responsive to the differences in the way people use their wheelchairs. It was found that there are large variances between subjects in trunk motion angle

and peak angular velocity but not between two different surfaces. It's possible that trunk movement related closely to individual technique rather than the biomechanics of the task. This is similar to the research results of Rodgers et al. [114], that large variance between subjects of trunk movements exist with experienced manual wheelchair users.

However, in Cowan et al. (2009) study, push frequency was sensitive in detecting the differences between low pile carpet, high pile carpet and ramp, but not for a difference between tile and low pile carpet. This may imply that the difference of resistance between artificial turf and carpet is too small and not sufficient enough to be distinguished from the push frequency parameter. The Push length parameter was not able to detect the difference between three types of level surfaces, only the difference between level surfaces and ramp (Cowan 2009). In my study, quantitative measurements of rolling resistance of both artificial turf and carpet are provided, which is absent from Cowan's study.

5.2 Propulsion kinetics and trunk biomechanics on transitions between two surfaces of different resistance in a real-world environment

If the direction of transition is from artificial turf to carpet, then we may conclude the transition is from high resistance surface to low resistance surface. A transition direction from carpet to artificial turf is from low to high resistance. It is found that the direction of transition substantially affects peak M_z , peak total force and average self-selected speed (Table 4-3). Participants pushed faster and

applied less peak M_z , peak total force on transition from high resistance surface to low resistance surface.

When participants encountered a sudden change of resistance from low to high at the transition, they applied more force to the wheelchair but resulted with a slower speed. However, when they transfer from a high resistance surface to a low resistance surface, the inertia effect assist the wheelchair propulsion and the participant can use less effort to cross the transition but resulted in a higher average speed.

As compared to speed and M_z , the push frequency, the trunk motion angle and the push length are less affected by the directions of transition. Although there are differences in the push frequency and the trunk motion angle on two transitions, they were found to be insignificant based on the significant p value (0.025). As the power analysis suggests (Table 4-19), it might be possible to detect the difference between them with a larger sample size of 85 for push frequency and 132 for trunk motion respectively. Then, we would be able to compare during transitioning whether push frequency is smaller and trunk motion angle is smaller on direction from high resistance to low resistance surface.

There was no similar studies done on the transitions between surfaces of different resistance. Data was also compared among steady-state pushes before, at, and after transition. It was found that participants applied higher M_z and total force, pushed the hand rim with a bigger contact angle and faster at the transitions

than on either surface. Participants were adjusting force at the transition to fit on the later surface.

It might be good to have transitions training for inexperienced wheelchair participants as adjustment in push patterns and force are required to accommodate sudden changes in requirement. For example, they have to slow down at the transition from a higher resistance surface to a lower resistance surface, or else the speed of the wheelchair might become too fast after the transition.

5.3 Comparisons of propulsion kinetics and trunk biomechanics between real-world and ergometer Model 1, and real-world and ergometer Model 2

New in this study is the inclusion of the inertia in the model of ergometer simulation for wheelchair study, so in that respect no comparison can be drawn with previous studies. No significant difference was found between the real-world and ergometer environments for parameters like push frequency, push length, trunk motion angle and maximum peak trunk angular velocity. These parameters were also not significantly different between the real-world surfaces, artificial turf and carpet. Three other biomechanical parameters studied here, namely peak M_z , peak total force, and average speed were found to differ significantly between the real-world and the Model 1 ergometer environments. Peak M_z was found similar in the comparison of real-world carpet and ergometer carpet with Model 2; peak total force was insignificant in the comparison of real-world and ergometer Model 2. The simulation of carpet in Model 2 can represent real-world carpet surface.

Hence, we may state that with more improvements of the present experimental design, ergometer might be able to represent the real-world environment.

5.3.1 Peak M_z

The difference of peak M_z between real-world surfaces and simulated surfaces (ergometer Model 1) is significant for both artificial turf and carpet. Participants applied more M_z on the ergometer than on the actual surfaces. However, the difference between artificial turf and carpet as simulated on the ergometer is not big enough to be related to the different rolling resistance of the two real-world surfaces.

A significant difference of peak M_z between real-world and on ergometer Model 2 does exist in the case of artificial turf, but not between simulated carpet and real-world carpet. The difference between simulated artificial turf and simulated carpet is close to the difference between real-world artificial turf and real-world carpet.

The lag in the response time of the ergometer system controlling program could be one reason for the significant difference in peak M_z . The acceleration or deceleration of two wheels is an important input for the resistance control, but the system takes some time to increase or decrease the resistance. Due to the delay, the resistance a participant experienced is somewhat different from what it actually should be in real time. Thus at the time of deceleration, a larger resistance acts on the wheels, decelerating the wheels even at faster rate. Hence, subjects had to push harder at the beginning of next push cycle in ergometer as compared to

the real-world environments. Also, the peak Mz value is sensitive to every push of the subjects as compared to an average value. However, with changes in the biomechanics model, the ergometer was shown to better simulate the real-world with Model 2 than Model 1, as there is no significant difference between the simulated carpet and the simulated artificial turf. Whatever significant difference exists between real-world and simulated conditions may stem from the fact that participants without any previous wheelchair experience have not yet learned to anticipate their own reaction as they move onto a different environment.

5.3.2 Peak total force

The differences in peak total force between real-world and ergometer Model 1 are significant for both artificial turf and carpet surfaces. The difference between simulated artificial turf and simulated carpet is not enough to distinguish these two surfaces on ergometer Model 1.

The difference in peak total force between real-world surfaces and simulated surfaces on ergometer Model 2 are insignificant for both artificial turf and carpet. The difference between simulated artificial turf and simulated carpet becomes similar to the difference between real-world artificial turf and real-world carpet.

The difference in the peak total force for different environments can be described by the same reason as explained for the peak Mz i.e. due to inexperienced subjects and lagging in the ergometer system response.

5.3.3 Push length

The difference in push length between real-world and ergometer Model 1 is significant for carpet surface but not for artificial turf. No significant difference was found in pair wise comparisons for real-world and ergometer environments in Model 2.

However, participants pushed the wheelchair with essentially identical push length (a minimal difference of 0.2% for both real-world and ergometer) in the same environment for two different surfaces. The larger push length in the ergometer environment may be due to the fact that in the real-world subjects need to adjust their direction all the time to maintain straight line motion while there is no such restriction in ergometer environment. A wheelchair stabilized on the ergometer, on the other hand, makes it easier for participants to reach the farther back and farther forward on the hand rim. Hence, they can cover more circumference of the rim and hence increased push length.

5.3.4 Push frequency

The differences in push frequency between real-world surfaces and simulated surfaces (ergometer Model 1) are significant for both artificial turf and carpet, but not for the comparison between real-world and ergometer Model 2. However, participants pushed a wheelchair with very similar push frequency in real-world for both artificial turf and carpet; and pushed with identical frequency on the ergometer for both surfaces.

One reason for the difference may be due to differences in wheelchair pushing technique in the two different environments. In the present study, subjects were required to follow a straight-line pushing on the real-world surface as much as possible. As they had no wheelchair experience, they frequently adjusted their direction during the experiment on the real-world surface, which may have caused them to push more frequently. While in the ergometer environment, subjects did not need to worry about the direction of the wheelchair. They just kept on pushing for the complete travelling distance. Hence, their push frequency was lower in the ergometer environment when compared to the real-world environment.

5.3.5 Average speed

The differences in average speed between the real-world surfaces and simulated surfaces (ergometer Model 1) are significant for both artificial turf and carpet. The difference between real-world and on the ergometer Model 2 is significant for the artificial turf surface but not for carpet.

The reason for the difference could be due to the lag of the ergometer system. The explanation is similar to what discussed in peak Mz. When the participants pushed the wheels, they encountered different resistance on ergometer from the real-world. When they finished pushing the rim and were recovering, both wheels decelerated at a faster rate as larger resistances were applied to both rollers. The next push would have been started at a much smaller velocity on ergometer than in real-world.

5.3.6 Trunk motion angle

There was no significant difference found between the real-world and ergometer environments on both artificial turf and carpet surfaces. It is likely because in the present study all able-bodied subjects were with no experience of wheelchair usage, and it contributed to a comparable large variation of data between subjects.

5.3.7 Maximum peak trunk angular velocity

Peak angular velocity describes the moment within a push when a participant move their trunk fastest. These values of several pushes were compared and the maximum value among them was recorded. No significant difference was found in the case of real-world and ergometer environments. It may be due to the inexperience of the participants influencing trunk motion angle. Another reason could be that only the maximum value among pushes during one trial was taken and not the average value, and it contributed to the big variation among data.

5.4 Others

5.4.1 Weight normalization

In some publications weight normalized peak Mz and weight normalized peak total force values were used for comparisons among different real-world surfaces or between real-world and simulated lab environments for repeated measures study [20, 22, 23, 34, 115, 116]. Weight normalization is a method to preprocess the data by dividing the actual peak Mz and peak total force values by

the weight of the participants. It is based on the assumption that there exists a correlation between the weight of the subjects and aforesaid values. The problem with weight normalization of M_z etc. is that it neglects to take into account that although mass affects the resistance to motion and therefore M_z so too does the acceleration generated by the users. Weight normalization assumes similar instantaneous acceleration for all participants on either surface. This is unlikely to be the case. Therefore, they wanted to mitigate the effect of weight of different participants to the data. However, in a study where the same participant experienced different experimental conditions and the data were paired and compared, the weight of the participant did not change between these treatment conditions. In the present study, same participant was studied in both real-world and ergometer environments. Hence, weight normalization should not be used for repeated measures study and is not required here.

The model used in the ergometer system to simulate real-world environment includes simulated inertial effects to simulate real-world wheelchair propulsion and incorporates the participants' weight consideration. Hence, no further modification/normalization of weight is required for our data.

5.4.2 Visual feedback

A state-of-the-art visual feedback system was developed in LabVIEW and implemented with ergometer so that participants can see the surface type, travel distance etc. on the computer screen. The visual feedback system helps in engaging participants in the pushing of the wheelchair on a lab simulator and

ensures their real-time reactions when encountering a change of resistance and makes them slow down and stop before reaching the end.

5.5 Study limitations

5.5.1 Selection of subjects

Participants of this study were on average young (age 26 ± 4 years) and with normal weight (62.82 ± 7.80 kg, body mass index 22.4 ± 2.4 $\text{kg} \cdot \text{m}^{-2}$). Able-bodied subjects with no or minimal experience of using a wheelchair were used to complete experiments. A study with daily manual wheelchair users could provide better comparisons.

5.5.2 Ergometer system

The friction in the bearings of the ergometer, although very low, creates resistance that is higher than that of tile and linoleum surfaces, which are so common in the real-world. We cannot accurately compare our results with any studies conducted on these two types of surface.

The lagging in our ergometer system contributed to the variation in measurements of peak Mz, peak total force and average speed.

5.5.3 Trunk motion measurement

In this thesis, we studied trunk excursion of wheelchair participants. However, the trunk excursion can be divided into extension and flexion. We did not distinguish these two movements.

5.5.4 Transition simulation in ergometer

In the present study, the transition between two surfaces with different resistance could only be studied on the real-world surfaces, because the comparison between real-world and ergometer environments was unexpectedly complicated and will need further study. The transition as simulated in the current study happens instantly, whereas when travelling on the actual surfaces, it took about one second for the rear wheel to cross the transition, and the rolling resistance during that second is difficult to measure.

5.5.5 Restriction of real-world surface travelled distance

In this study, 8 meters of carpet and 8 meters of artificial turf were used because of the length restriction of the hallway. In comparison, in Kwarciak et al.[29] a 50 meters tile surface was used as real-world environment to compare with treadmill simulation. For some participants in our study, they pushed at a very fast speed; as a result, data for fewer pushes were collected. This contributes to the variations in data within participants and also between participants because a very steady- state pushing had not been completely reached.

5.5.6. Wheelchair configuration

The only test wheelchair used in the study wasn't customized-configured for every participant. This limits the study in a way that it affects parameters such as push length. Wheelchair used in future study should be customized to individual participant according to their weight, arm length, etc.

5.6 Strength of the study

Simulation in rehabilitation is currently a fast developing field and our study will be able to provide useful information to them. Also, we included study of wheelchair propulsion at the time of transition between two surfaces with different resistances. The effect of different surface types before and after the transition, and their relationship with wheelchair participants' propulsion performance were investigated. We also developed a state-of-the-art visual feedback system. It helped in collecting real time response of the participants on ergometer.

5.7 Clinical interpretation

From this study, we find that participants push more frequently and with high peak force on surface with high rolling resistance and at the transition going from low resistance surface to high resistance. According to the clinical guidelines of upper limb function preservation[3], high peak force and high push frequency lead to injury in the median nerve and shoulder. Manual wheelchair users should limit or avoid the possibility of pushing on high resistance surface and on a transition with sudden change of resistance from low to high. When wheeling on a higher resistance surface or at the transition from low resistance to high resistance surface, forward leaning of the trunk would be helpful for the wheelchair user. There is at present no tool to evaluate wheelchair users' ability to negotiate surface transitions and it would be helpful to develop one.

By using a wheelchair simulator, newly injured wheelchair users can practice wheelchair skills in a safe environment. The wheelchair skill training program at

Dalhousie University [117, 118] has been conducted in a simulated environment. Significantly greater improvements were found when using a simulator than with standard occupational training. In a laboratory setting, realistic propulsion tasks that may contribute to over-use injuries during propulsion can be studied and better understanding and strategies can be made to prevent these injuries. In order to start using emerging technologies such as an immersion virtual reality to simulate wheelchair function, simulator has to be able to represent real-world. This is the first study to investigate it.

Tachyon and IMU used in this study is designed to be used to collect daily activity of wheelchair users. Combined with a GPS, the performance of a wheelchair user in a specific scenario, for example when pushing a wheelchair on a lawn or moving over a pedestrian crossing, can be monitored and studied by wireless in real time, which is useful for clinicians and researchers alike. This would allow no time and space limitation of wheelchair study and will provide greater understanding of what wheelchair users face in real life.

5.8 Suggestions to future studies

In future, active manual wheelchair users should be used as participants in the study. The analysis of wheelchair propulsion performance during transition associated with the pushes on surfaces before and after the transition should be investigated in the future. The transition between two surfaces should also be simulated in ergometer environment and can be compared with the real-world environment in future. A greater variety of surface types should be included in future studies. In order to reproduce direction control and balancing of a

wheelchair in real-world propulsion, different speed feedback from both wheels should be incorporated in the simulation model. To further investigate whether ergometers can represent real-world environment or not, motion capture systems should be used to improve accuracy of body segment movements. A 3-dimensional visual feedback system can provide better realization of real-world environment as compared to 2-dimentional feedback system. This should be considered in future studies.

Chapter 6 Conclusion

In daily life, wheelchair performance has to accommodate different types of surfaces. High resistance surfaces and sudden surface changes can be challenging. Ideally, those challenges should be studied in their real-world environments. However, in order to select a manageable set of variables, studies generally have to be conducted in a laboratory setting. The closer the laboratory simulation of a real-world environment, the more useful will be the results to be used in therapy and training. So far, there is a lack of studies comparing real-world with corresponding laboratory environments. The object of this study was to determine how closely a laboratory simulation can approximate real-world conditions and to explore ways to optimize the simulation.

The study was conducted with two commonly used real-world surfaces namely artificial turf and medium-pile carpet. Measurements of wheelchair propulsion and trunk biomechanics on the real-world surfaces were compared with the measurements obtained in the simulated environment on a wheelchair ergometer. The transition between these surfaces in real-world environment was also studied. For trunk biomechanics, an inertia measurement unit was used.

To simulate real-world environments, two different models, referred to as Model 1 and Model 2, were developed for use with the ergometer system. New in this study is the inclusion of the participant's and the wheelchair's inertia. A total of 23 able-bodied participants were used in the study. Participants were asked to push a test wheelchair on actual real-world surfaces, followed by propulsion on the ergometer system. Different biomechanical parameters, such as peak M_z ,

average speed, push frequency, push length, trunk motion angles etc. were used to compare each real-world with the corresponding simulated ergometer environment. Statistical software SPSS, paired t-test and repeated measures ANOVA methods were used to analyze study results.

In some of the biomechanical parameters, i.e. push length, trunk motion angle and maximum peak trunk angular velocity, no significant difference was found between real-world and ergometer environments. Neither was there any significant difference of these parameters when comparing actual artificial turf with carpet. For Model 1, the other parameters namely peak M_z , peak total force, and average speed showed significant differences between real-world and simulated environments. For Model 2, the similarity between actual carpet and simulated model was very close. For artificial turf, on the other hand, an additional calibration of the ergometer model was necessary to approximate the real-world setting. As for the transition between surfaces, the simulation was not successful. It will be necessary in future studies to accommodate such surface transitions in simulation models. Future studies should also extend research from able-bodied participants to the whole range of people who depend on wheelchair locomotion. It may eventually be possible, using GPS and wireless, to collect comprehensive data as wheelchair users go about their daily activities and imbed those data into improved simulation models.

Appendix 1 References

1. Armstrong, W., et al., Guidelines on the provision of manual wheelchairs in less resourced settings. Vol. 1. 2008: World Health Organization. 22.
2. Shields, M., Use of wheelchairs and other mobility support devices. Health Report, 2004. 15(3): p. 37-41.
3. Medicine', P.V.o.A.C.f.S.C., Preservation of upper limb function following spinal cord injury: a clinical practice guideline for health-care professionals. J Spinal Cord Med, 2005. 28(5): p. 434-70.
4. Sapey, B., Stewart, J., and Donaldson, G., The Social Implications of Increases in Wheelchair Use. 2004, Lancaster: Department of Applied Social Science, Lancaster University.
5. Finley, M.A. and Rodgers, M.M., Prevalence and identification of shoulder pathology in athletic and nonathletic wheelchair users with shoulder pain: A pilot study. Journal of Rehabilitation Research and Development, 2004. 41(3B): p. 395-402.
6. Rick Hansen Institute and Institute, U.F., The incidence and prevalence of Spinal Cord Injury in Canada overview and estimates based on current evidence. 2010, December 15.
7. Wolf, E., et al., Vibration exposure of individuals using wheelchairs over sidewalk surfaces. Disability and Rehabilitation, 2005. 27(23): p. 1443-9.
8. Wolf, E., et al., Longitudinal assessment of vibrations during manual and power wheelchair driving over select sidewalk surfaces. Journal of Rehabilitation Research and Development, 2007. 44(4): p. 573-80.
9. Pentland, W.E. and Twomey, L.T., The weight-bearing upper extremity in women with long term paraplegia. Paraplegia, 1991. 29(8): p. 521-30.
10. Curtis, K.A., et al., Shoulder pain in wheelchair users with tetraplegia and paraplegia. Archives of Physical Medicine and Rehabilitation, 1999. 80(4): p. 453-7.
11. Cooper, R.A., Heavy handed-repetitive strain injury among manual wheelchair users. 1998, Team Rehab Report.
12. Brose, S.W., et al., Shoulder ultrasound abnormalities, physical examination findings, and pain in manual wheelchair users with spinal cord injury. Archives of Physical Medicine and Rehabilitation, 2008. 89(11): p. 2086-93.
13. Paralyzed Veterans of America Consortium for Spinal Cord Medicine, Preservation of upper limb function following spinal cord injury: a clinical practice guideline for health-care professionals. Journal of Spinal Cord Medicine, 2005. 28(5): p. 434-70.

14. Meyers, A.R., et al., Barriers, facilitators, and access for wheelchair users: substantive and methodologic lessons from a pilot study of environmental effects. *Social Science and Medicine*, 2002. 55(8): p. 1435-46.
15. Hurd, W.J., et al., Influence of varying level terrain on wheelchair propulsion biomechanics. *American Journal of Physical Medicine & Rehabilitation*, 2008. 87(12): p. 984-91.
16. Hurd, W.J., et al., Wheelchair propulsion demands during outdoor community ambulation. *Journal of Electromyography and Kinesiology*, 2009. 19(5): p. 942-7.
17. Gao, C. and Abeysekera, J., A systems perspective of slip and fall accidents on icy and snowy surfaces. *Ergonomics*, 2004. 47(5): p. 573-98.
18. Cooper, R.A., et al., Manual wheeled mobility--current and future developments from the human engineering research laboratories. *Disability and Rehabilitation*, 2010. 32(26): p. 2210-21.
19. Lemaire, E.D., et al., Wheelchair ramp navigation in snow and ice-grit conditions. *Archives of Physical Medicine and Rehabilitation*, 2010. 91(10): p. 1516-23.
20. Koontz, A.M., et al., A kinetic analysis of manual wheelchair propulsion during start-up on select indoor and outdoor surfaces. *Journal of Rehabilitation Research and Development*, 2005. 42(4): p. 447-58.
21. Richter, W.M., et al., Stroke pattern and handrim biomechanics for level and uphill wheelchair propulsion at self-selected speeds. *Archives of Physical Medicine and Rehabilitation*, 2007. 88(1): p. 81-7.
22. Cowan, R.E., et al., Preliminary outcomes of the SmartWheel Users' Group database: a proposed framework for clinicians to objectively evaluate manual wheelchair propulsion. *Archives of Physical Medicine and Rehabilitation*, 2008. 89(2): p. 260-8.
23. Cowan, R.E., et al., Impact of surface type, wheelchair weight, and axle position on wheelchair propulsion by novice older adults. *Archives of Physical Medicine and Rehabilitation*, 2009. 90(7): p. 1076-83.
24. Veeger, H.E., van der Woude, L.H., and Rozendal, R.H., A computerized wheelchair ergometer. Results of a comparison study. *Scandinavian Journal of Rehabilitation Medicine*, 1992. 24(1): p. 17-23.
25. Robertson, R.N., et al., Pushrim forces and joint kinetics during wheelchair propulsion. *Archives of Physical Medicine and Rehabilitation*, 1996. 77(9): p. 856-64.
26. Vanlandewijck, Y.C., Spaepen, A.J., and Lysens, R.J., Wheelchair propulsion efficiency: movement pattern adaptations to speed changes. *Medicine and Science in Sports and Exercise*, 1994. 26(11): p. 1373-81.

27. DiGiovine, C.P., Cooper, R.A., and Boninger, M.L., Dynamic calibration of a wheelchair dynamometer. *Journal of Rehabilitation Research and Development*, 2001. 38(1): p. 41-55.
28. Chow, J.W., et al., Kinematic and electromyographic analysis of wheelchair propulsion on ramps of different slopes for young men with paraplegia. *Archives of Physical Medicine and Rehabilitation*, 2009. 90(2): p. 271-8.
29. Kwarciak, A.M., et al., Comparing handrim biomechanics for treadmill and overground wheelchair propulsion. *Spinal Cord*, 2011. 49(3): p. 457-62.
30. Newsam, C.J., et al., Temporal-spatial characteristics of wheelchair propulsion. Effects of level of spinal cord injury, terrain, and propulsion rate. *American Journal of Physical Medicine & Rehabilitation*, 1996. 75(4): p. 292-9.
31. Richter, W.M., The effect of seat position on manual wheelchair propulsion biomechanics: a quasi-static model-based approach. *Medical Engineering and Physics*, 2001. 23(10): p. 707-12.
32. Boninger, M.L., et al., Propulsion patterns and pushrim biomechanics in manual wheelchair propulsion. *Archives of Physical Medicine and Rehabilitation*, 2002. 83(5): p. 718-23.
33. Ambrosio, F., et al., Biomechanics and strength of manual wheelchair users. *Journal of Spinal Cord Medicine*, 2005. 28(5): p. 407-14.
34. Koontz, A.M., et al., Comparison between Overground and Dynamometer Manual Wheelchair Propulsion. *Journal of Applied Biomechanics*, 2011 In Press.
35. Rice, I., et al., Hand rim wheelchair propulsion training using biomechanical real-time visual feedback based on motor learning theory principles. *Journal of Spinal Cord Medicine*, 2010. 33(1): p. 33-42.
36. Bednarczyk, J.H. and Sanderson, D.J., Limitations of kinematics in the assessment of wheelchair propulsion in adults and children with spinal cord injury. *Physical Therapy*, 1995. 75(4): p. 281-9.
37. Chow, J.W., et al., Effect of resistance load on biomechanical characteristics of racing wheelchair propulsion over a roller system. *Journal of Biomechanics*, 2000. 33(5): p. 601-8.
38. Hwang, S., Lee, H., and Kim, Y. Upper limb dynamics during manual wheelchair propulsion with different resistances. in *International Federation for Medical and Biological Engineering* 31. 2010.
39. Rice, I., et al., Manual wheelchair stroke characteristics during an extended period of propulsion. *Spinal Cord*, 2009. 47(5): p. 413-7.
40. Worobey, L., Koontz, A., and Boninger, M. Role of trunk movement in manual wheelchair propulsion in various overground conditions. in *American Society of Biomechanics Conference*. 2010. Rhode Island, USA.

41. Koontz, A., et al. Trunk movement patterns and propulsion efficiency in wheelchair users with and without SCI. in American Society of Biomechanics Conference. 2004, September 8-11. Portland.
42. Subbarao, J.V., Klopstein, J., and Turpin, R., Prevalence and impact of wrist and shoulder pain in patients with spinal cord injury. *Journal of Spinal Cord Medicine*, 1995. 18(1): p. 9-13.
43. Lundqvist, C., et al., Spinal cord injuries. Clinical, functional, and emotional status. *Spine (Phila Pa 1976)*, 1991. 16(1): p. 78-83.
44. Sie, I.H., et al., Upper extremity pain in the postrehabilitation spinal cord injured patient. *Archives of Physical Medicine and Rehabilitation*, 1992. 73(1): p. 44-8.
45. Dalyan, M., Cardenas, D.D., and Gerard, B., Upper extremity pain after spinal cord injury. *Spinal Cord*, 1999. 37(3): p. 191-5.
46. Rose, L. and Ferguson-Pell, M. Prevalence of shoulder pain in people with spinal cord injury (SCI) less than 10 years post onset. International Posture and Mobility Group. 2010 June.
47. Davidoff, G., Werner, R., and Waring, W., Compressive mononeuropathies of the upper extremity in chronic paraplegia. *Paraplegia*, 1991. 29(1): p. 17-24.
48. Gellman, H., Sie, I., and Waters, R.L., Late complications of the weight-bearing upper extremity in the paraplegic patient. *Clinical Orthopaedics and Related Research*, 1988(233): p. 132-5.
49. Aljure, J., et al., Carpal tunnel syndrome in paraplegic patients. *Paraplegia*, 1985. 23(3): p. 182-6.
50. Tun, C.G. and Upton, J., The paraplegic hand: electrodiagnostic studies and clinical findings. *Journal of Hand Surgery (American Volume)*, 1988. 13(5): p. 716-9.
51. Nichols, P.J., Norman, P.A., and Ennis, J.R., Wheelchair user's shoulder? Shoulder pain in patients with spinal cord lesions. *Scandinavian Journal of Rehabilitation Medicine*, 1979. 11(1): p. 29-32.
52. Waring, W.P. and Karunas, R.S., Acute spinal cord injuries and the incidence of clinically occurring thromboembolic disease. *Paraplegia*, 1991. 29(1): p. 8-16.
53. Bussmann, J.B., et al., Effect of wearing an activity monitor on the amount of daily manual wheelchair propulsion in persons with spinal cord injury. *Spinal Cord*, 2010. 48(2): p. 128-33.
54. Warme, C.A., Whitney, J.D., and Belza, B., Measurement and description of physical activity in adult manual wheelchair users. *Disability and Health Journal*, 2008. 1(4): p. 236-44.

55. Wilson, S.K., et al., Objective assessment of mobility of the spinal cord injured in a free-living environment. *Spinal Cord*, 2008. 46(5): p. 352-7.
56. Rankin, J.W., Richter, W.M., and Neptune, R.R., Individual muscle contributions to push and recovery subtasks during wheelchair propulsion. *Journal of Biomechanics*, 2011. 44(7): p. 1246-52.
57. Qi, L., Use of wavelet analysis techniques with surface EMG and MMG to characterize motor unit recruitment patterns of shoulder muscles during wheelchair propulsion and voluntary contraction tasks. 2009 October, University College London: London.
58. Qi, L., et al., Changes in surface electromyography signals and kinetics associated with progression of fatigue at two speeds during wheelchair propulsion. *Journal of Rehabilitation Research and Development*, 2012. 49(1): p. 23-34.
59. Bayley, J.C., Cochran, T.P., and Sledge, C.B., The weight-bearing shoulder. The impingement syndrome in paraplegics. *Journal of Bone and Joint Surgery, American Volume*, 1987. 69(5): p. 676-8.
60. Burnham, R.S., et al., Shoulder pain in wheelchair athletes. The role of muscle imbalance. *American Journal of Sports Medicine*, 1993. 21(2): p. 238-42.
61. Pentland, W.E. and Twomey, L.T., Upper limb function in persons with long term paraplegia and implications for independence: Part II. *Paraplegia*, 1994. 32(4): p. 219-24.
62. Pentland, W.E. and Twomey, L.T., Upper limb function in persons with long term paraplegia and implications for independence: Part I. *Paraplegia*, 1994. 32(4): p. 211-8.
63. Riek, L.M., Ludewig, P.M., and Nawoczenski, D.A., Comparative shoulder kinematics during free standing, standing depression lifts and daily functional activities in persons with paraplegia: considerations for shoulder health. *Spinal Cord*, 2008. 46(5): p. 335-43.
64. Nawoczenski, D.A., et al., Clinical trial of exercise for shoulder pain in chronic spinal injury. *Physical Therapy*, 2006. 86(12): p. 1604-18.
65. Forslund, E.B., et al., Transfer from table to wheelchair in men and women with spinal cord injury: coordination of body movement and arm forces. *Spinal Cord*, 2007. 45(1): p. 41-8.
66. Davis, J.L., et al., Three-dimensional kinematics of the shoulder complex during wheelchair propulsion: a technical report. *Journal of Rehabilitation Research and Development*, 1998. 35(1): p. 61-72.
67. Boninger, M.L., et al., Pushrim biomechanics and injury prevention in spinal cord injury: recommendations based on CULP-SCI investigations. *Journal of Rehabilitation Research and Development*, 2005. 42(3 Suppl 1): p. 9-19.

68. Koontz, A.M., et al., Investigation of the performance of an ergonomic handrim as a pain-relieving intervention for manual wheelchair users. *Assistive Technology*, 2006. 18(2): p. 123-43; quiz 45.
69. Brose, S.W., et al., Shoulder ultrasound abnormalities, physical examination findings, and pain in manual wheelchair users with spinal cord injury. *Arch Phys Med Rehabil*, 2008. 89(11): p. 2086-93.
70. Collinger, J.L., et al., Shoulder biomechanics during the push phase of wheelchair propulsion: a multisite study of persons with paraplegia. *Archives of Physical Medicine and Rehabilitation*, 2008. 89(4): p. 667-76.
71. Troy, B.S., et al., An analysis of work postures of manual wheelchair users in the office environment. *Journal of Rehabilitation Research and Development*, 1997. 34(2): p. 151-61.
72. Reid, D., et al., Home is where their wheels are: Experiences of women wheelchair users. *American Journal of Occupational Therapy*, 2003. 57(2): p. 186-95.
73. Winter, D., *Biomechanics and motor control of human movement*. Fourth ed. 2009: John Wiley & Sons, Inc. United States. 45-7, 107, 85-8.
74. Vanlandewijck, Y., Theisen, D., and Daly, D., Wheelchair propulsion biomechanics: implications for wheelchair sports. *Sports Medicine*, 2001. 31(5): p. 339-67.
75. De Groot, S., et al., Wheelchair propulsion technique and mechanical efficiency after 3 wk of practice. *Medicine and Science in Sports and Exercise*, 2002. 34(5): p. 756-66.
76. de Groot, S., et al., Effect of wheelchair stroke pattern on mechanical efficiency. *American Journal of Physical Medicine & Rehabilitation*, 2004. 83(8): p. 640-9.
77. Veeger, H.E., van der Woude, L.H., and Rozendal, R.H., Effect of handrim velocity on mechanical efficiency in wheelchair propulsion. *Medicine and Science in Sports and Exercise*, 1992. 24(1): p. 100-7.
78. Boninger, M.L., et al., Three-dimensional pushrim forces during two speeds of wheelchair propulsion. *American Journal of Physical Medicine & Rehabilitation*, 1997. 76(5): p. 420-6.
79. Hills, L., 'Every push matters'. 2010, University College London.
80. Hoxie, R.E. and Rubenstein, L.Z., Are older pedestrians allowed enough time to cross intersections safely? *Journal of the American Geriatrics Society*, 1994. 42(3): p. 241-4.
81. Somers, M.F., *Spinal Cord Injury: Functional Rehabilitation* Second ed. 2001: Prentice Hall. 458.

82. Gagnon, D., et al., Effects of trunk impairments on manual wheelchair propulsion among individuals with a spinal cord injury : a brief overview and future challenges. *Topics in Spinal Cord Injury Rehabilitation*, 2009 Fall: p. 59-70.
83. Boninger, M.L., et al., Shoulder and elbow motion during two speeds of wheelchair propulsion: a description using a local coordinate system. *Spinal Cord*, 1998. 36(6): p. 418-26.
84. City of Toronto Accessibility Plan (CTAP), City of Toronto Accessibility Design Guidelines. 2003.
85. Shirado, O., et al., Outdoor winter activities of spinal cord-injured patients. With special reference to outdoor mobility. *American Journal of Physical Medicine & Rehabilitation*, 1995. 74(6): p. 408-14.
86. Chesney, D.A. and Axelson, P.W., Preliminary test method for the determination of surface firmness. *IEEE Transactions on Biomedical Engineering*, 1996. 4(3): p. 182-7.
87. Kauzlarich, J.J. and Thacker, J.G., Wheelchair tire rolling resistance and fatigue. *Journal of Rehabilitation Research and Development*, 1985. 22(3): p. 25-41.
88. Kwarciak, A.M., et al., Redefining the manual wheelchair stroke cycle: identification and impact of nonpropulsive pushrim contact. *Archives of Physical Medicine and Rehabilitation*, 2009. 90(1): p. 20-6.
89. Sawatzky, B.J., Kim, W.O., and Denison, I., The ergonomics of different tyres and tyre pressure during wheelchair propulsion. *Ergonomics*, 2004. 47(14): p. 1475-83.
90. Koontz, A.M., et al., Manual wheelchair propulsion patterns on natural surfaces during start-up propulsion. *Archives of Physical Medicine and Rehabilitation*, 2009. 90(11): p. 1916-23.
91. City of Edmonton Advisory Board on Services for Persons with Disabilities (ABSPD), Checklist for Accessibility and Universal Design in Architecture 2008.
92. Archambault, P.S., et al., Driving performance in a power wheelchair simulator. *Disability and Rehabilitation: Assistive Technology*, 2012. 7(3): p. 226-33.
93. Shechtman, O., et al., Comparison of driving errors between on-the-road and simulated driving assessment: a validation study. *Traffic Injury Prevention*, 2009. 10(4): p. 379-85.
94. Langbein, W., et al., Calibration of a new wheelchair ergometer: the wheelchair aerobic fitness trainer. *IEEE Transactions on Rehabilitation Engineering*, 1993. 1: p. 49-58.

95. Gil-Agudo, A., et al., Shoulder joint kinetics during wheelchair propulsion on a treadmill at two different speeds in spinal cord injury patients. *Spinal Cord*, 2010. 48(4): p. 290-6.
96. Richter, W., et al., Stroke pattern and handrim biomechanics for level and uphill wheelchair propulsion at self-selected speeds. *Archives of Physical Medicine and Rehabilitation*, 2007. 88: p. **81-7**.
97. Veeger, H.E., et al., Differences in performance between trained and untrained subjects during a 30-s sprint test in a wheelchair ergometer. *European Journal of Applied Physiology and Occupational Physiology*, 1992. 64(2): p. 158-64.
98. Veeger, H.E., van der Woude, L.H., and Rozendal, R.H., Within-cycle characteristics of the wheelchair push in sprinting on a wheelchair ergometer. *Medicine and Science in Sports and Exercise*, 1991. 23(2): p. 264-71.
99. Niesing, R., et al., Computer-controlled wheelchair ergometer. *Medical and Biological Engineering and Computing*, 1990. 28(4): p. 329-38.
100. Newsam, C.J., et al., Three dimensional upper extremity motion during manual wheelchair propulsion in men with different levels of spinal cord injury. *Gait Posture*, 1999. 10(3): p. 223-32.
101. Tordi, N., et al., Interval training program on a wheelchair ergometer for paraplegic subjects. *Spinal Cord*, 2001. 39(10): p. 532-7.
102. Yim, S.Y., et al., Effect of wheelchair ergometer training on spinal cord-injured paraplegics. *Yonsei Medical Journal*, 1993. 34(3): p. 278-86.
103. Goosey-Tolfrey, V.L., et al., A kinetic analysis of trained wheelchair racers during two speeds of propulsion. *Medical Engineering and Physics*, 2001. 23(4): p. 259-66.
104. The Advisory Group on Computer Graphics (AGOCG), *Advising UK Higher Education on Computer Graphics, Visualization, Multimedia and Virtual Environments*. 1999
105. Richter, W.M., et al., Effects of single-variable biofeedback on wheelchair handrim biomechanics. *Archives of Physical Medicine and Rehabilitation*, 2011. 92(4): p. 572-7.
106. Goosey-Tolfrey, V.L., et al., Influence of varied tempo music on wheelchair mechanical efficiency following 3-week practice. *International Journal of Sports Medicine*, 2011. 32(2): p. 126-31.
107. Stephens, C.L. and Engsberg, J.R., Comparison of overground and treadmill propulsion patterns of manual wheelchair users with tetraplegia. *Disability and Rehabilitation: Assistive Technology*, 2010. 5(6): p. 420-7.
108. Kirkwood, B.R. and Sterne, J.A.C., *Essential medical statistics*. Second ed. 2003: Blackwell Science Publishing.

109. Hamaluik K., W.J., Ferguson-Pell M. Development of a long-term wheelchair propulsion instrumentation device for use in evaluating community ambulation parameters. in 2011 Spotlight on Research Breakfast and Symposium. 2011. Edmonton, AB, Canada.
110. Ionescu, H., 6 degrees of freedom. 2010, Wikipedia.
111. Sauret, C., et al., Assessment of field rolling resistance of manual wheelchairs. *Journal of Rehabilitation Research and Development*, 2012. 49(1): p. 63-74.
112. Hoffman, M.D., et al., Assessment of wheelchair drag resistance using a coasting deceleration technique. *American Journal of Physical Medicine & Rehabilitation*, 2003. 82(11): p. 880-9; quiz 90-2.
113. Portney, L.G. and Watkins, M.P., *Foundations of Clinical Research*. 3rd ed. 2009: Pearson Hall Health.
114. Rodgers, M.M., et al., Influence of training on biomechanics of wheelchair propulsion. *Journal of Rehabilitation Research and Development*, 2001. 38(5): p. 505-11.
115. Koontz, A.M., et al., Multisite comparison of wheelchair propulsion kinetics in persons with paraplegia. *Journal of Rehabilitation Research and Development*, 2007. 44(3): p. 449-58.
116. Boninger, M.L., et al., Shoulder magnetic resonance imaging abnormalities, wheelchair propulsion, and gender. *Archives of Physical Medicine and Rehabilitation*, 2003. 84(11): p. 1615-20.
117. Kirby, R.L., et al., The Wheelchair Skills Test: a pilot study of a new outcome measure. *Archives of Physical Medicine and Rehabilitation*, 2002. 83(1): p. 10-8.
118. MacPhee, A.H., et al., Wheelchair skills training program: A randomized clinical trial of wheelchair users undergoing initial rehabilitation. *Archives of Physical Medicine and Rehabilitation*, 2004. 85(1): p. 41-50.

Appendix 2 Real-world and Roller Calibration

Table Appendix 2- 1 Deceleration α of real-world surfaces and weight of participants

Subject No.	Body Mass (Kg)	α on Artificial turf (m/s ²)	α on Carpet (m/s ²)
1	54	-2.21	-2.02
2	77	-2.71	-2.22
3	64.7	-2.30	-2.04
4	74	-2.39	-2.32
5	53	-2.82	-1.95
6	57.3	-2.54	-2.18
7	61.3	-2.72	-2.47
8	54.3	-2.98	-2.29
9	60.5	-2.37	-2.06
10	77.8	-2.97	-2.34
11	56.4	-2.43	-2.17
12	70.3	-2.73	-2.07
13	59.2	-2.27	-1.94
14	75	-2.74	-2.08
15	59.9	-2.32	-2.20
16	61.8	-2.23	-2.19
18	63.1	-2.91	-2.41
20	60.7	-2.07	-1.59
21	48.5	-2.68	-2.03
22	63.9	-2.39	-2.23
23	65.8	-2.27	-2.24
24	61	-2.31	-1.97
25	65.4	-2.35	-2.00
Mean±SD	62.82±7.80	-2.51±0.26	-2.13±0.18

Table Appendix 2- 2 Linear equations of individual participant for pressure used by actuators and the deceleration of both rollers. (a and b are the gradient and intercept values of equation respectively)

Subject No.	Mass (Kg)	Left Roller a	Left Roller b	Right Roller a	Right Roller b
1	54	-1.67	-0.60	-2.20	-0.47
2	77	-2.17	-0.51	-2.50	-0.90
3	64.7	-1.93	-0.54	-2.63	0.07
4	74	-1.90	-0.80	-2.34	-0.63
5	53	-2.07	-0.35	-2.36	-0.25
6	57.3	-2.46	0.27	-2.76	0.12
7	61.3	-2.43	0.24	-2.34	-0.46
8	54.3	-2.05	-0.19	-2.57	-0.10
9	60.5	-2.07	-0.42	-2.42	-0.35
10	77.8	-2.12	-0.34	-2.39	-0.55
11	56.4	-2.14	-0.04	-2.48	-0.28
12	70.3	-2.26	-0.10	-2.69	-0.26
13	59.2	-2.04	-0.14	-2.60	-0.29
14	75	-1.79	-0.88	-2.61	-0.54
15	59.9	-2.46	-0.25	-2.44	-0.50
16	61.8	-2.46	0.27	-2.50	-0.33
18	63.1	-2.32	0.05	-2.54	-0.28
20	60.7	-2.09	-0.09	-2.57	-0.34
21	48.5	-2.09	0.07	-2.69	-0.11
22	63.9	-2.14	-0.16	-2.51	-0.48
23	65.8	-2.36	-0.04	-2.72	-0.34
24	61	-2.03	-0.07	-2.37	-0.62
25	65.4	-1.86	-0.40	-2.44	-0.24

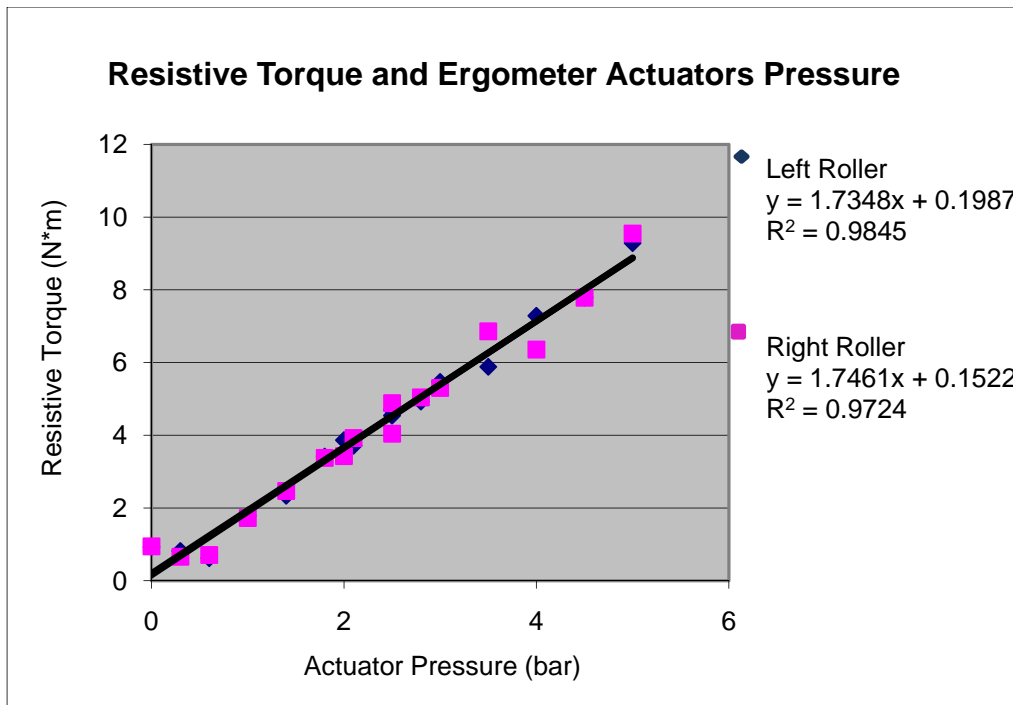


Figure Appendix 2- 1 Resistive Torque and Ergometer Actuator Pressure

Appendix 3 Interaction Plots for Hypothesis 3

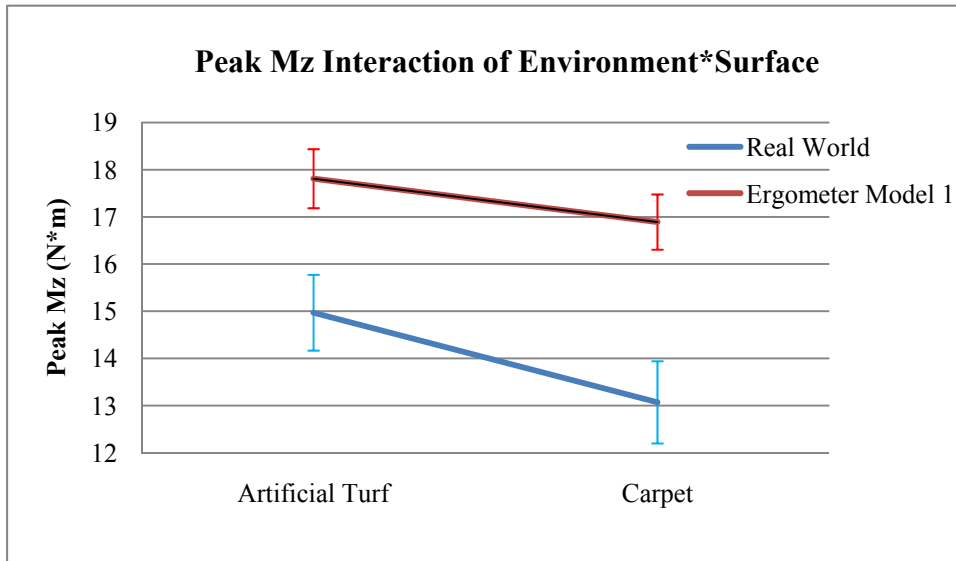


Figure Appendix 3- 1 Interaction plot for parameter peak M_z (comparing real-world and ergometer Model 1) of two independent variables: Environment and Surface (with mean and standard error)

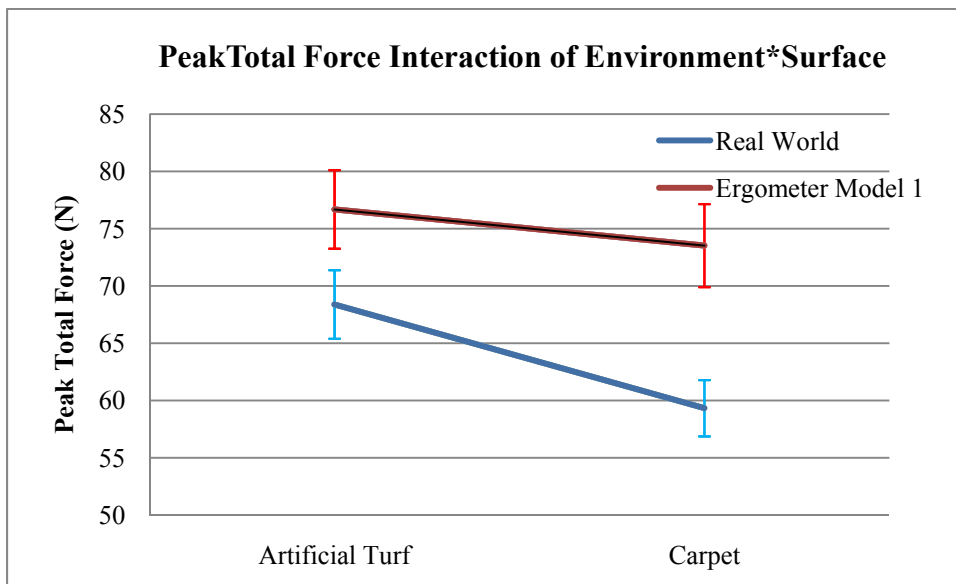


Figure Appendix 3- 2 Interaction plot for parameter peak total force (comparing real-world and ergometer Model 1) of two independent variables: Environment and Surface (with mean and standard error)

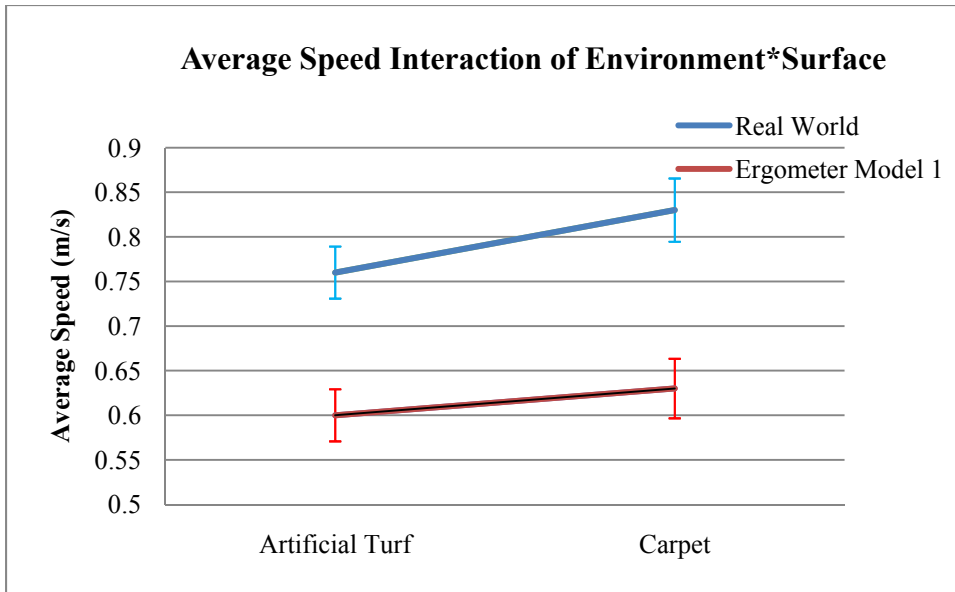


Figure Appendix 3- 3 Interaction plot for parameter average speed (comparing real-world and ergometer Model 1) of two independent variables: Environment and Surface (with mean and standard error)

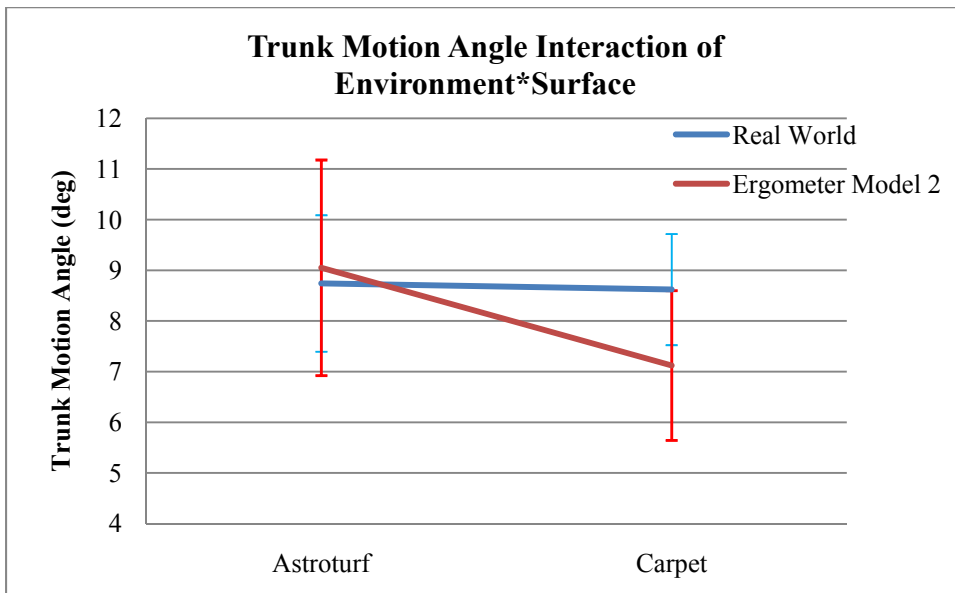


Figure Appendix 3- 4 Interaction plot for parameter trunk motion angle (comparing real-world and ergometer Model 2) of two independent variables: Environment and Surface (with mean and standard error)